



NORSAR Scientific Report No. 1-2003

Semiannual Technical Summary

1 July - 31 December 2002

Frode Ringdal (ed.)

Kjeller, February 2003

REPORT DOCUMENTATION PAGE

Form Approved
OMB No. 0704-0188

1a. REPORT SECURITY CLASSIFICATION Unclassified			1b. RESTRICTIVE MARKINGS Not applicable	
2a. SECURITY CLASSIFICATION AUTHORITY Not Applicable			3. DISTRIBUTION / AVAILABILITY OF REPORT Approved for public release; distribution unlimited	
2b. DECLASSIFICATION / DOWNGRADING SCHEDULE				
4. PERFORMING ORGANIZATION REPORT NUMBER(S) Scientific Rep. 1-2003			5. MONITORING ORGANIZATION REPORT NUMBER(S) Scientific Rep. 1-2003	
6a. NAME OF PERFORMING ORGANIZATION NORSAR		6b. OFFICE SYMBOL (if applicable)	7a. NAME OF MONITORING ORGANIZATION HQ/AFTAC/TTS	
6c. ADDRESS (City, State, and ZIP Code) Post Box 53 NO-2027 Kjeller, Norway			7b. ADDRESS (City, State, and ZIP Code) Patrick AFB, FL 32925-6001	
8a. NAME OF FUNDING / SPONSORING ORGANIZATION Defense Threat Reduction Agency/NTPO		8b. OFFICE SYMBOL (if applicable) DTRA/NTPO	9. PROCUREMENT INSTRUMENT IDENTIFICATION NUMBER Contract No. F08650-01-C-0055	
8c. ADDRESS (City, State, and ZIP Code) 1515 Wilson Blvd., Suite 720 Arlington, VA 22209			10. SOURCE OF FUNDING NUMBERS	
			PROGRAM ELEMENT NO. R&D	PROJECT NONORSAR Phase 3
			TASK NOSOW Task 5.0	WORK UNIT ACQUISITION NO. No. 004A2
11. TITLE (Include Security Classification) Semiannual Technical Summary, 1 July - 31 December 2002 (Unclassified)				
12. PERSONAL AUTHOR(S)				
13a. TYPE OF REPORT Scientific Summary		13b. TIME COVERED FROM 1 Jul 02 TO 31 Dec 02	14. DATE OF REPORT (Year, Month, Day) 2003 Feb	15. PAGE COUNT 88
16. SUPPLEMENTARY NOTATION				
17. COSATI CODES			18. SUBJECT TERMS (Continue on reverse if necessary and identify by block number) NORSAR, Norwegian Seismic Array	
FIELD	GROUP	SUB-GROUP		
8	11			
19. ABSTRACT (Continue on reverse if necessary and identify by block number) This report describes the research activities carried out at NORSAR under Contract No. F08650-01-C-0055 for the period 1 July - 31 December 2002. In addition, it provides summary information on operation and maintenance (O&M) activities at the Norwegian National Data Center (NDC) during the same period. Research activities described in this report, as well as transmission of selected data to the United States NDC, are funded by the United States Department of Defense. The O&M activities, including operation of transmission links within Norway and to Vienna, Austria, are being funded jointly by the CTBTO/PTS and the Norwegian Government, with the understanding that the funding of IMS-related activities will gradually be transferred to the CTBTO/PTS. The O&M statistics presented in this report are included for the purpose of completeness, and in order to maintain consistency with earlier reporting practice. (cont.)				
20. DISTRIBUTION / AVAILABILITY OF ABSTRACT <input type="checkbox"/> UNCLASSIFIED/UNLIMITED <input type="checkbox"/> SAME AS RPT. <input type="checkbox"/> DTIC USERS			21. ABSTRACT SECURITY CLASSIFICATION	
22a. NAME OF RESPONSIBLE INDIVIDUAL Lt. Col. William S. Jones		22b. TELEPHONE (Include Area Code) (407) 494-7985	22c. OFFICE SYMBOL AFAC/TTS	

Abstract (cont.)

The NOA Detection Processing system has been operated throughout the period with an average uptime of 100.00%. A total of 2221 seismic events have been reported in the NOA monthly seismic bulletin from July through December 2002. On-line detection processing and data recording at the NDC of NORES, ARCES and FINES data have been conducted throughout the period. Data from two small-aperture arrays at sites in Spitsbergen and Apatity, Kola Peninsula, as well as the Hagfors array in Sweden, have also been recorded and processed. Processing statistics for the arrays for the reporting period are given.

A summary of the activities related to the GSETT-3 experiment and experience gained at the Norwegian NDC during the reporting period is provided in Section 4. Norway is now contributing primary station data from two seismic arrays: ARCES and NOA and one auxiliary array (SPITS). These data are being provided to the IDC via the global communications infrastructure (GCI). Continuous data from all three arrays are in addition being transmitted to the US NDC. The performance of the data transmission to the US NDC has been satisfactory during the reporting period.

A new alert system for large seismic events has been implemented at the NORSAR data center, and is described in Section 4.4s: NORSAR's Event Warning System (NEWS). The results are made available on the NORSAR Web pages and distributed by e-mail.

Summaries of five scientific and technical contributions are presented in Chapter 6 of this report.

Section 6.1 contains a description of a new detector recipe that has been implemented for the ARCES array. The new beam set and data processing recipes were installed for NORSAR's on-line processing of ARCES data from 21 November 2002.

Section 6.2 describes work to use a single regional seismic array (ARCES) to characterize seismic signals resulting from explosions that are known to have occurred at the Kovdor open cast mine in Russia and use these observations to determine whether other events recorded at ARCES are the result of operations at this mine. Our single-array location procedure, with adjustment for systematic bias, provided locations for 38 events with detected P and S phases with a median error of only 5.8 km. This is significantly better than the median error (12.1 km) obtained in our regular analyst-reviewed network bulletin for the same event set.

Section 6.3 is a study of experimental Site-Specific Generalized Beamforming (SSGBF) applied to the Novaya Zemlya former nuclear test site. The combination of the Site-Specific Threshold Monitoring (SSTM) and the SSGBF methods is shown to provide a very convenient tool for day-to-day monitoring of the Novaya Zemlya test site. The SSTM technique has as its main strength the ability to display the real seismic field, regardless of "station detector performance". On the other hand, the SSGBF technique takes advantage of the individual station detector outputs, and uses this combined information to narrow down the number of possible candidates for events in the target area.

Section 6.4 is a study of infrasound data recorded at the Apatity seismic/infrasound array. This array is equipped with three infrasound sensors in the inner ring, which has a diameter of 500m. We have analyzed a number of infrasonic recordings of selected events in the Kola Peninsula and adjacent regions. The analysis includes frequency-wavenumber analysis of the array recordings, estimation of phase velocity and azimuth, and estimation of group velocity based on travel time calculations. We find that the azimuth estimates are quite stable, typically within

a range of 5 degrees or less for events from the same location. This is very satisfactory taking into account the small array aperture.

Section 6.5 is a study of the threshold monitoring technique applied to a target area at local and near-regional distances from the monitoring stations. Using data from the ARCES and Apatity arrays, we have implemented a regional threshold monitoring scheme for northern Fennoscandia, including the Kola Peninsula. For the most active mining areas in this region (Khibiny, Olenegorsk, Zapoljarny and Kovdor), the magnitude thresholds during “normal” noise conditions vary between 0.7 and 1.0 magnitude units. This demonstrates that the TM technique has the potential to provide reliable monitoring at very low magnitude levels in the case of local and near-regional monitoring.

AFTAC Project Authorization : T/0155/PKO
ARPA Order No. : 4138 AMD # 53
Program Code No. : 0F10
Name of Contractor : Stiftelsen NORSAR
Effective Date of Contract : 1 Feb 2001 (T/0155/PKO)
Contract Expiration Date : 31 December 2005
Project Manager : Frode Ringdal +47 63 80 59 00
Title of Work : The Norwegian Seismic Array
(NORSAR) Phase 3
Amount of Contract : \$ 3,383,445
Period Covered by Report : 1 July - 31 December 2002

The views and conclusions contained in this document are those of the authors and should not be interpreted as necessarily representing the official policies, either expressed or implied, of the U.S. Government.

The research presented in this report was supported by the Defense Threat Reduction Agency and was monitored by AFTAC, Patrick AFB, FL32925, under contract no. F08650-01-C-0055.

The operational activities of the seismic field systems and the Norwegian National Data Center (NDC) are currently jointly funded by the Norwegian Government and the CTBTO/PTS, with the understanding that the funding of IMS-related activities will gradually be transferred to the CTBTO/PTS.

NORSAR Contribution No. 796

Table of Contents

		Page
1	Summary	1
2	Operation of International Monitoring System (IMS) Stations in Norway	5
2.1	PS27 — Primary Seismic Station NOA	5
2.2	PS28 — Primary Seismic Station ARCES	7
2.3	AS72 — Auxiliary Seismic Station Spitsbergen	8
2.4	AS73 — Auxiliary Seismic Station at Jan Mayen.....	9
2.5	IS37 — Infrasound Station at Karasjok.....	9
2.6	RN49 — Radionuclide Station on Spitsbergen	10
3	Contributing Regional Seismic Arrays.....	11
3.1	NORES	11
3.2	Hagfors (IMS Station AS101)	11
3.3	FINES (IMS station PS17)	12
3.4	Apatity	13
3.5	Regional Monitoring System Operation and Analysis	15
4	NDC and Field Activities	17
4.1	NDC Activities	17
4.2	Status Report: Norway's Participation in GSETT-3	18
4.3	Field Activities.....	26
4.4	NORSAR's Event Warning System (NEWS).....	27
5	Documentation Developed	47
6	Summary of Technical Reports / Papers Published.....	33
6.1	Upgrading the ARCES (PS 28) on-line data processing system	33
6.2	Single array analysis and processing of events from the Kovdor mine, Kola, NW Russia	44
6.3	Site-specific GBF monitoring of the Novaya Zemlya test site	56
6.4	Analysis of infrasound data recorded at the Apatity array	68
6.5	Threshold Monitoring of the Mines in the Kola Region.....	78

1 Summary

This report describes the research activities carried out at NORSAR under Contract No. F08650-01-C-0055 for the period 1 July - 31 December 2002. In addition, it provides summary information on operation and maintenance (O&M) activities at the Norwegian National Data Center (NDC) during the same period. Research activities described in this report, as well as transmission of selected data to the United States NDC, are funded by the United States Department of Defense. The O&M activities, including operation of transmission links within Norway and to Vienna, Austria are being funded jointly by the CTBTO/PTS and the Norwegian Government, with the understanding that the funding of all IMS-related activities will gradually be transferred to the CTBTO/PTS. The O&M statistics presented in this report are included for the purpose of completeness, and in order to maintain consistency with earlier reporting practice.

The seismic arrays operated by the Norwegian NDC comprise the Norwegian Seismic Array (NOA), the Norwegian Regional Seismic Array (NORES), the Arctic Regional Seismic Array (ARCES) and the Spitsbergen Regional Array (SPITS). This report also presents statistics for additional seismic stations which through cooperative agreements with institutions in the host countries provide continuous data to the NORSAR Data Processing Center (NDPC). These stations comprise the Finnish Regional Seismic Array (FINES), the Hagfors array in Sweden and the regional seismic array in Apatity, Russia.

The NOA Detection Processing system has been operated throughout the period with an average uptime of 100.00%. A total of 2221 seismic events have been reported in the NOA monthly seismic bulletin from July through December 2002. On-line detection processing and data recording at the NDC of NORES, ARCES and FINES data have been conducted throughout the period. Data from two small-aperture arrays at sites in Spitsbergen and Apatity, Kola Peninsula, as well as the Hagfors array in Sweden, have also been recorded and processed. Processing statistics for the arrays for the reporting period are given.

A summary of the activities related to the GSETT-3 experiment and experience gained at the Norwegian NDC during the reporting period is provided in Section 4. Norway is now contributing primary station data from two seismic arrays: ARCES and NOA and one auxiliary array (SPITS). These data are being provided to the IDC via the global communications infrastructure (GCI). Continuous data from all three arrays are in addition being transmitted to the US NDC. The performance of the data transmission to the US NDC has been satisfactory during the reporting period.

The PrepCom has encouraged states that operate IMS-designated stations to continue to do so on a voluntary basis and in the framework of the GSETT-3 experiment until the stations have been certified for formal inclusion in IMS. So far among the Norwegian stations, the NOA and the ARCES array (PS27 and PS28 respectively) have been certified. We envisage continuing the provision of data from these and other Norwegian IMS-designated stations in accordance with current procedures.

A new alert system for large seismic events has been implemented at the NORSAR data center, and is described in Section 4.4. Today, data from the highly sensitive regional arrays ARCES, FINES, HFS, SPITS, and NORES, and the teleseismic NORSAR array (NOA) are automatically processed in on-line mode. However, the routine data processing of single arrays can be delayed due to data transfer problems. Therefore, the full automatic regional and local event

location process GBF can be delayed by hours or even days because this process waits for the results of all arrays. In addition, GBF does not use automatic analysis results from the teleseismic NORSAR array although this may help to locate local or regional events. Therefore, during the last two years, a new extra event location system has been developed to provide quick but reliable solutions for strong events: NORSAR's Event Warning System (NEWS). The results are made available on the NORSAR Web pages and distributed by e-mail.

Summaries of five scientific and technical contributions are presented in Chapter 6 of this report.

Section 6.1 contains a description of a new detector recipe that has been implemented for the ARCES array. The analysis of the ARCES processing results based on this new recipe clearly shows a better adjustment to the observed seismic onsets at the array site. The number of detections increases and on average the seismic phases are detected with a higher SNR. The number of single array event locations is higher and a relative increase in spurious events is not observed. Comparing the GBF results shows that the number of more reliably defined events increases. This is eventually connected with a slight increase of erroneous defined events. The latter happened in particular in connection with observations of the SPITS array. This point has to be observed and a change of the GBF processing scheme in the case of two-station event locations may be considered in the future. Because of these overall positive results the new beam set and data processing recipes were installed for NORSAR's on-line processing of ARCES data from 21 November 2002.

Section 6.2 is entitled "Single array analysis and processing of events from the Kovdor mine, Kola, NW Russia". The goal of this work is to use a single regional seismic array (ARCES) to characterize seismic signals resulting from explosions that are known to have occurred at the Kovdor open cast mine in Russia (67.557° N, 30.425° E) and use these observations to determine whether other events recorded at ARCES are the result of operations at this mine. Wherever possible, events which are deemed to be likely candidates for Kovdor events are located to the best possible accuracy. We have developed a stepwise, fully automatic algorithm for identifying, processing, and locating events from the Kovdor mine, using only data from the ARCES array. Using results from the analysis of confirmed Kovdor events, we have developed a set of criteria to help determine whether or not detections from ARCES result from events at Kovdor. A total of 38 events were located in this way and the location error was compared with that of the manually reviewed network locations.

The results of the Kovdor study are quite encouraging. We started out with the ARCES automatic detection lists for a processing period of 208 days. During this period, we identified 6176 ARCES detections that potentially corresponded to events from Kovdor. By sophisticated automatic processing, we were able to reduce this number to 50 event candidates, out of which 47 were correct and only 3 were false alarms. The 47 events included all of the 28 Kovdor mining explosions originally reported by KRSC during the time period, plus a number of secondary events in "double" explosions. Our single-array location procedure, with adjustment for systematic bias, provided locations for the 38 events with detected P and S phases with a median error of only 5.8 km. This is significantly better than the median error (12.1 km) obtained in our regular analyst-reviewed network bulletin for the same event set.

Section 6.3 is a study of experimental Site-Specific Generalized Beamforming (SSGBF) applied to the Novaya Zemlya former nuclear test site. The SSGBF approach supplements the SSTM system described in preceding NORSAR Semiannual Technical Summaries. We also

comment briefly on the relative merits of the two approaches (SSTM and SSGBF), and the extent to which they complement each other in this particular case study.

In the present study we have used data from the regional arrays ARCES, SPITS, FINES and NORES, with calibration based on available data for the Novaya Zemlya region. We present some preliminary results in applying site-specific generalized beamforming to the Novaya Zemlya test site, using two data sets for performance testing. The first data set covers the day 23 February 2002, when a seismic event near the test site occurred. The second data set covers the day 11 January 2002, which was a typical “quiet” day. Examples of the data analysis for these data sets are presented.

The combination of the SSTM and the SSGBF methods are shown to provide a very convenient tool for day-to-day monitoring of the Novaya Zemlya test site. The SSTM technique has as its main strength the ability to display the real seismic field, regardless of “station detector performance”. On the other hand, the SSGBF technique takes advantage of the individual station detector outputs, and uses this combined information to narrow down the number of possible candidates for events in the target area.

Section 6.4 is a study of infrasound data recorded at the Apatity seismic/infrasound array. This array is equipped with three infrasound sensors in the inner ring, which has a diameter of 500m. We have analyzed a number of infrasonic recordings of selected events in the Kola Peninsula and adjacent regions. Several large mines in this region generate explosions that are routinely detected by the seismic systems installed in northern Fennoscandia and NW Russia. Some of these explosions are also recorded by the infrasound sensors. We present analysis results from 19 such mining explosions, with a distance range from 38 to 220 km. The analysis includes frequency-wavenumber analysis of the array recordings, estimation of phase velocity and azimuth, and estimation of group velocity based on travel time calculations. We have analyzed 3-6 events from each of the following mining areas: Khibiny, Zapolarnyi, Kovdor and Olenegorsk. We find that the azimuth estimates are quite stable, typically within a range of 5 degrees or less for events from the same mine. This is very satisfactory taking into account the small array aperture.

Another source of data has been a set of ammunition demolition explosions in Northern Finland, at a distance of 300 km from the array. In these cases, we have been able to identify three separate phase arrivals for each of the five analyzed events. Following the phase conventions used at the prototype IDC, these phases are identified as the tropospheric arrival (Iw), the stratospheric arrival (Is) and the thermospheric arrival (It). Again, we find that the azimuth estimates from the (in this case) 15 total phases are very consistent, ranging from 278 to 288 degrees (true azimuth is 284 degrees). The observed group velocities (average travel velocities) range between 326-336 m/s for the Iw arrival, 300-305 m/s for the Is arrival and 244-254 m/s for the It arrival. The phase velocities (apparent velocities) range between 330-400 m/s, with the lowest values for the Iw phases and the highest values for the It phases. However, with this very small array the estimates of phase velocity are not quite stable enough to provide a confident indication of the phase type.

We note that the detection of infrasonic phases is very dependent on the background atmospheric conditions, and that such phases are usually observed only during relatively quiet wind conditions. Our future plans include the installation of additional noise-reducing porous hoses to improve the detectability during windy conditions. After the projected infrasonic array in Karasjok, northern Norway, is installed, we plan to carry out joint processing of data from

these two arrays. Further perspectives include cooperation with colleagues in Sweden, the Netherlands and Germany for more extensive joint processing.

Section 6.5 is a study of the threshold monitoring technique applied to mines in the Kola Peninsula. We have access to ground truth information, and explosion and rockburst observations for these mines. Such information is regularly collected from the mine operators by Kola Regional Seismological Center (KRSC), and serves a reference set for our studies. The mining areas comprise Khibiny, Olenegorsk, Kovdor and Zapolyarnyi.

We note that the mines of the Khibiny Massif provide a natural laboratory for examining and contrasting the signals generated by different types of mining explosions and rockbursts. Of the five mines in the Massif, three have both underground operations and surface pits. Shots underground range in size from very small (~2 tons) with only a few delays and durations on the order of a few hundred milliseconds, to very large (400 tons) with many delays and durations approaching a half second. Shots above ground range from 0.5 tons to 400 tons with a wide range of delays and durations. Induced seismicity is frequent and triggered rockbursts accompany a significant fraction of the underground explosions.

Using data from the ARCES and Apatity arrays, we have implemented a regional threshold monitoring scheme for northern Fennoscandia, including the Kola Peninsula. For the most active mining areas in this region (Khibiny, Olenegorsk, Zapolyarny and Kovdor), the magnitude thresholds during “normal” noise conditions vary between 0.7 and 1.0 magnitude units. During the studied time interval (12 April 2002), 10 out of 18 peaks exceeding threshold magnitude 1.2 at any of the mining areas were caused by events in the actual mining areas. However, the spatial resolution of the threshold magnitudes when using the ARCES and Apatity arrays is quite low, such that the mining events also created significant threshold peaks for the other mining areas.

We conclude that for a regional threshold monitoring scheme for the Kola Peninsula it will be sufficient to deploy a set of targets for the most active mining areas. When a threshold peak is found at any of these targets, the peaks have to be associated to seismic events by correlating the threshold plots to seismic detection lists or bulletins.

Frode Ringdal

2 Operation of International Monitoring System (IMS) Stations in Norway

2.1 PS27 — Primary Seismic Station NOA

The average recording time was 100%, the same as for the previous reporting period.

There were no outages of all subarrays at the same time.

Monthly uptimes for the NORSAR on-line data recording task, taking into account all factors (field installations, transmissions line, data center operation) affecting this task were as follows:

July	:	100%
August	:	100%
September	:	100%
October	:	100%
November	:	100%
December	:	100%

J. Torstveit

NOA Event Detection Operation

In Table 2.1.1 some monthly statistics of the Detection and Event Processor operation are given. The table lists the total number of detections (DPX) triggered by the on-line detector, the total number of detections processed by the automatic event processor (EPX) and the total number of events accepted after analyst review (teleseismic phases, core phases and total).

	Total DPX	Total EPX	Accepted Events		Sum	Daily
			P-phases	Core Phases		
Jul	6,080	745	226	48	274	8.8
Aug	7,728	1,046	343	116	459	14.8
Sep	8,513	824	256	71	327	10.9
Oct	10,815	922	303	54	357	11.5
Nov	10,940	1,081	428	65	493	16.4
Dec	11,418	881	244	67	311	10.0
	55,494	5,499	1,800	421	2,221	12.1

Table 2.1.1. *Detection and Event Processor statistics, 1 July - 31 December 2002.*

NOA detections

The number of detections (phases) reported by the NORSAR detector during day 182, 2002, through day 365, 2002, was 55,494, giving an average of 302 detections per processed day (184 days processed).

B. Paulsen

U. Baadshaug

2.2 PS28 — Primary Seismic Station ARCES

The average recording time was 100% as compared to 99.16% for the previous period.

There was one outage of 20 seconds in the period.

Monthly uptimes for the ARCES on-line data recording task, taking into account all factors (field installations, transmission lines, data center operation) affecting this task were as follows:

July	:	100%
August	:	100%
September	:	100%
October	:	100%
November	:	100%
December	:	100%

J. Torstveit

Event Detection Operation

ARCES detections

The number of detections (phases) reported during day 182, 2002, through day 365, 2002, was 162,614, giving an average of 884 detections per processed day (184 days processed).

Events automatically located by ARCES

During days 182, 2002, through 365, 2002, 8,084 local and regional events were located by ARCES, based on automatic association of P- and S-type arrivals. This gives an average of 43.9 events per processed day (184 days processed). 56% of these events are within 300 km, and 83% of these events are within 1000 km.

U. Baadshaug

2.3 AS72 — Auxiliary Seismic Station Spitsbergen

The average recording time was 99.96% as compared to 97.60% for the previous reporting period.

Table 2.2.1 lists the reasons for and time periods of the main downtimes in the reporting period.

	Date	Time
	26 Sep	1035 - 1109
	21 Nov	1112 - 1120
	29 Nov	0700 - 0707
	29 Nov	0813 - 0817
	29 Nov	2017 - 2025
	29 Nov	2104 - 2112
	30 Nov	1218 - 1222
	30 Nov	2015 - 2023
	30 Nov	2216 - 2223
	01 Dec	0123 - 0127

Table 2.2.1. *The main interruptions in recording of Spitsbergen data at NDPC, 1 July - 31 December 2002.*

Monthly uptimes for the Spitsbergen on-line data recording task, taking into account all factors (field installations, transmissions line, data center operation) affecting this task were as follows:

July	:	100%
August	:	100%
September	:	99.92%
October	:	100%
November	:	99.87%
December	:	99.99%

J. Torstveit

Event Detection Operation

Spitsbergen array detections

The number of detections (phases) reported from day 182, 2002, through day 365, 2002, was 473,050, giving an average of 2571 detections per processed day (184 days processed).

Events automatically located by the Spitsbergen array

During days 182, 2002, through 365, 2002, 55,866 local and regional events were located by the Spitsbergen array, based on automatic association of P- and S-type arrivals. This gives an average of 303.6 events per processed day (184 days processed). 62% of these events are within 300 km, and 84% of these events are within 1000 km.

U. Baadshaug

2.4 AS73 — Auxiliary Seismic Station at Jan Mayen

The IMS auxiliary seismic network will include a three-component station on the Norwegian island of Jan Mayen. The station location given in the protocol to the Comprehensive Nuclear-Test-Ban Treaty is 70.9°N, 8.7°W.

The University of Bergen has operated a seismic station at this location since 1970. An investment in the new station at Jan Mayen will be made in due course and in accordance with Prep-Com program and budget decisions. A so-called Parent Network Station Assessment for AS73 was completed in April 2002. Work is now underway to prepare for the installation of a vault at a new location (71.0°N, 8.5°W) recently approved by the PrepCom. In the meantime, data from the existing seismic station on Jan Mayen are being transmitted to the NDC at Kjeller and to the University of Bergen via a VSAT link installed in April 2000.

J. Fyen

2.5 IS37 — Infrasound Station at Karasjok

The IMS infrasound network will include a station at Karasjok in northern Norway. The coordinates given for this station are 69.5°N, 25.5°E. These coordinates coincide with those of the primary seismic station PS28.

A site survey for this station was carried out during June/July 1998 as a cooperative effort between the Provisional Technical Secretariat of the CTBTO and NORSAR. Analysis of the data collected at several potential locations for this station in and around Karasjok has been completed. The results of this analysis have led to a recommendation on the exact location of the infrasound station. This location needs to be surveyed in detail. The next step will be to approach the local authorities to obtain the permission necessary to establish the station. Station installation is now expected to take place in the year 2004.

S. Mykkeltveit

2.6 RN49 — Radionuclide Station on Spitsbergen

The IMS radionuclide network will include a station at Longyearbyen on the island of Spitsbergen, with location 78.2°N, 16.4°E, as given in the protocol to the Comprehensive Nuclear-Test-

Ban Treaty. These coordinates coincide with those of the auxiliary seismic station AS72. According to PrepCom decision, this station will also be among those IMS radionuclide stations that will have a capability of monitoring for the presence of relevant noble gases upon entry into force of the CTBT.

A site survey for this station was carried out in August of 1999 by NORSAR, in cooperation with the Norwegian Radiation Protection Authority. The site survey report to the PTS contained a recommendation to establish this station at Platåberget, some 20 km away from the Treaty location. The PrepCom approved the corresponding coordinate change in its meeting in May 2000. The station installation was part of PrepCom's work program and budget for the year 2000. The infrastructure for housing the station equipment has been established, and a noble gas detection system, based on the Swedish "SAUNA" design, was installed at this site in May 2001, as part of PrepCom's noble gas experiment. A particulate station ("ARAME" design) was installed at the same location in September 2001. Currently, the two systems are undergoing testing and evaluation. A certification visit to the station took place in October 2002. It is expected that the particulate station will be certified in mid-2003.

S. Mykkeltveit

3 Contributing Regional Seismic Arrays

3.1 NORES

NORES has been out of operation since a thunderstorm destroyed the station electronics on 11 June 2002.

J. Torstveit

3.2 Hagfors (IMS Station AS101)

The average recording time was 100% as compared to 99.97% for the previous reporting period.

Monthly uptimes for the Hagfors on-line data recording task, taking into account all factors (field installations, transmissions line, data center operation) affecting this task were as follows:

July	:	100%
August	:	100%
September	:	100%
October	:	100%
November	:	99.99%
December	:	100%

J. Torstveit

Hagfors Event Detection Operation

Hagfors array detections

The number of detections (phases) reported from day 182, 2002, through day 365, 2002, was 94,929, giving an average of 516 detections per processed day (184 days processed).

Events automatically located by the Hagfors array

During days 182, 2002, through 365, 2002, 2637 local and regional events were located by the Hagfors array, based on automatic association of P- and S-type arrivals. This gives an average of 14.3 events per processed day (184 days processed). 58% of these events are within 300 km, and 83% of these events are within 1000 km.

U. Baadshaug

3.3 FINES (IMS station PS17)

The average recording time was 100% as it was for the previous reporting period.

Monthly uptimes for the FINES on-line data recording task, taking into account all factors (field installations, transmissions line, data center operation) affecting this task were as follows:

July	:	99.99%
August	:	100%
September	:	100%
October	:	100%
November	:	100%
December	:	100%

J. Torstveit

FINES Event Detection Operation

FINES detections

The number of detections (phases) reported during day 182, 2002, through day 365, 2002, was 55,417, giving an average of 303 detections per processed day (184 days processed).

Events automatically located by FINES

During days 182, 2002, through 365, 2002, 2493 local and regional events were located by FINES, based on automatic association of P- and S-type arrivals. This gives an average of 13.6 events per processed day (181 days processed). 73% of these events are within 300 km, and 88% of these events are within 1000 km.

U. Baadshaug

3.4 Apatity

The average recording time was 99.32% in the reporting period compared to 99.94% during the previous period.

The main outages in the period are given in Table 3.4.1.

08 Aug 02	09.45.23	-	09.51.25
14 Aug	18.35.30	-	18.42.34
14 Aug	18.55.48	-	19.02.02
26 Aug	09.54.42	-	10.01.16
28 Aug	13.11.31	-	13.17.36
29 Aug	12.03.57	-	12.11.16
12 Sep	12.04.13	-	12.11.18
26 Sep	12.05.52	-	12.11.57
29 Sep	00.06.19	-	00.12.01
29 Sep	00.45.46	-	00.51.51
29 Sep	01.25.11	-	01.31.22
29 Sep	02.04.33	-	02.11.23
29 Sep	02.44.27	-	02.51.24
29 Sep	03.22.42	-	03.29.31
03 Oct	15.58.21	-	16.06.20
10 Oct	12.06.07	-	12.12.12
17 Oct	10.21.51	-	
18 Oct		-	07.42.45
18 Oct	13.05.21	-	13.21.47
20 Oct	04.35.12	-	04.41.22
24 Oct	01.08.02	-	01.19.45
24 Oct	12.07.22	-	12.19.04
25 Oct	06.02.12	-	06.08.19
26 Oct	02.16.34	-	02.22.40
29 Oct	13.30.52	-	13.36.56
29 Oct	14.44.04	-	19.52.40
30 Oct	12.32.22	-	12.44.04
07 Nov	12.08.42	-	12.16.24
21 Nov	11.44.48	-	11.51.26
21 Nov	12.09.42	-	12.16.26
30 Nov	03.04.48	-	03.21.27
30 Nov	09.33.04	-	09.38.46
05 Dec	12.10.51	-	12.16.57
09 Dec	11.30.53	-	11.36.59

09 Dec	12.00.09 -	12.06.27
18 Dec	11.22.12 -	11.28.18
19 Dec	12.11.33 -	12.17.37

Table 3.4.1. *The main interruptions in recording of Apatity data at NDPC, 1 July - 31 December 2002.*

Monthly uptimes for the Apatity on-line data recording task, taking into account all factors (field installations, transmissions line, data center operation) affecting this task were as follows:

July	:	100%
August	:	99.91%
September	:	99.88%
October	:	96.24%
November	:	99.90%
December	:	99.91%

J. Torstveit

Apatity Event Detection Operation

Apatity array detections

The number of detections (phases) reported from day 182, 2002, through day 365, 2002, was 206,366, giving an average of 1122 detections per processed day (184 days processed).

As described in earlier reports, the data from the Apatity array is transferred by one-way (simplex) radio links to Apatity city. The transmission suffers from radio disturbances that occasionally result in a large number of small data gaps and spikes in the data. In order for the communication protocol to correct such errors by requesting retransmission of data, a two-way radio link would be needed (duplex radio). However, it should be noted that noise from cultural activities and from the nearby lakes cause most of the unwanted detections. These unwanted detections are “filtered” in the signal processing, as they give seismic velocities that are outside accepted limits for regional and teleseismic phase velocities.

Events automatically located by the Apatity array

During days 182, 2002, through 365, 2002, 2526 local and regional events were located by the Apatity array, based on automatic association of P- and S-type arrivals. This gives an average of 13.7 events per processed day (184 days processed). 35% of these events are within 300 km, and 70% of these events are within 1000 km.

U. Baadshaug

3.5 Regional Monitoring System Operation and Analysis

The Regional Monitoring System (RMS) was installed at NORSAR in December 1989 and has been operated at NORSAR from 1 January 1990 for automatic processing of data from ARCES and NORES. A second version of RMS that accepts data from an arbitrary number of arrays and single 3-component

stations was installed at NORSAR in October 1991, and regular operation of the system comprising analysis of data from the 4 arrays ARCES, NORES, FINES and GERES started on 15 October 1991. As opposed to the first version of RMS, the one in current operation also has the capability of locating events at teleseismic distances.

Data from the Apatity array was included on 14 December 1992, and from the Spitsbergen array on 12 January 1994. Detections from the Hagfors array were available to the analysts and could be added manually during analysis from 6 December 1994. After 2 February 1995, Hagfors detections were also used in the automatic phase association.

Since 24 April 1999, RMS has processed data from all the seven regional arrays ARCES, NORES, FINES, GERES (until January 2000), Apatity, Spitsbergen, and Hagfors. Starting 19 September 1999, waveforms and detections from the NORSAR array have also been available to the analyst.

Phase and event statistics

Table 3.5.1 gives a summary of phase detections and events declared by RMS. From top to bottom the table gives the total number of detections by the RMS, the number of detections that are associated with events automatically declared by the RMS, the number of detections that are not associated with any events, the number of events automatically declared by the RMS, and finally the total number of events worked on interactively (in accordance with criteria that vary over time; see below) and defined by the analyst.

New criteria for interactive event analysis were introduced from 1 January 1994. Since that date, only regional events in areas of special interest (e.g, Spitsbergen, since it is necessary to acquire new knowledge in this region) or other significant events (e.g, felt earthquakes and large industrial explosions) were thoroughly analyzed. Teleseismic events of special interest are also analyzed.

To further reduce the workload on the analysts and to focus on regional events in preparation for Gamma-data submission during GSETT-3, a new processing scheme was introduced on 2 February 1995. The GBF (Generalized Beamforming) program is used as a pre-processor to RMS, and only phases associated with selected events in northern Europe are considered in the automatic RMS phase association. All detections, however, are still available to the analysts and can be added manually during analysis.

	Jul 02	Aug 02	Sep 02	Oct 02	Nov 02	Dec 02	Total
Phase detections	171290	174227	209691	197836	193039	185678	1131761
- Associated phases	4244	5044	6823	6289	4236	5280	31916
- Unassociated phases	167046	169183	202868	191547	188803	180398	1099845
Events automatically declared by RMS	922	1160	1647	1445	931	1109	7214
No. of events defined by the analyst	72	62	77	83	79	81	454

Table 3.5.1. *RMS phase detections and event summary.*

U. Baadshaug

B. Paulsen

4 NDC and Field Activities

4.1 NDC Activities

NORSAR functions as the Norwegian National Data Center (NDC) for CTBT verification. Six monitoring stations, comprising altogether 119 field instruments, will be located on Norwegian territory as part of the future IMS as described elsewhere in this report. The four seismic IMS stations are all in operation today, and three of them are currently providing data to the IDC. The radionuclide station at Spitsbergen is currently operating in a testing mode, whereas the infrasound station in northern Norway will need to be established within the next few years. Data recorded by the Norwegian stations is being transmitted in real time to the Norwegian NDC, and provided to the IDC through the Global Communications Infrastructure (GCI). Norway is connected to the GCI with a frame relay link to Vienna.

Operating the Norwegian IMS stations continues to require increased resources and additional personnel both at the NDC and in the field. The PTS has established new and strictly defined procedures as well as increased emphasis on regularity of data recording and timely data transmission to the IDC in Vienna. This has led to increased reporting activities and implementation of new procedures for the NDC operators. The NDC carries out all the technical tasks required in support of Norway's treaty obligations. NORSAR will also carry out assessments of events of special interest, and advise the Norwegian authorities in technical matters relating to treaty compliance.

Verification functions; information received from the IDC

After the CTBT enters into force, the IDC will provide data for a large number of events each day, but will not assess whether any of them are likely to be nuclear explosions. Such assessments will be the task of the States Parties, and it is important to develop the necessary national expertise in the participating countries. An important task for the Norwegian NDC will thus be to make independent assessments of events of particular interest to Norway, and to communicate the results of these analyses to the Norwegian Ministry of Foreign Affairs.

Monitoring the Arctic region

Norway will have monitoring stations of key importance for covering the Arctic, including Novaya Zemlya, and Norwegian experts have a unique competence in assessing events in this region. On several occasions in the past, seismic events near Novaya Zemlya have caused political concern, and NORSAR specialists have contributed to clarifying these issues.

International cooperation

After entry into force of the treaty, a number of countries are expected to establish national expertise to contribute to the treaty verification on a global basis. Norwegian experts have been in contact with experts from several countries with the aim of establishing bilateral or multi-lateral cooperation in this field. One interesting possibility for the future is to establish NORSAR as a regional center for European cooperation in the CTBT verification activities.

NORSAR event processing

The automatic routine processing of NORSAR events as described in NORSAR Sci. Rep. No. 2-93/94, has been running satisfactorily. The analyst tools for reviewing and updating the solutions have been continually modified to simplify operations and improve results. NORSAR is currently applying teleseismic detection and event processing using the large-aperture NORSAR array as well as regional monitoring using the network of small-aperture arrays in Fennoscandia and adjacent areas.

Certification of PS28

On 8 November 2001 the IMS station PS28-ARCES was formally certified. PTS personnel visited the station during the winter of 2000 and carried out a detailed technical evaluation. As a result of this inspection and subsequent discussions between NORSAR and the PTS, it was concluded that PS28 needed only one enhancement in order to be certified: to install a centralized authentication process at the central array recording facility. After this was done during the fall of 2001 and the subsequent verification by the PTS, station certification was granted.

Communication topology

Norway has implemented an independent subnetwork, which connects the IMS stations AS72, AS73, PS28, and RN49 operated by NORSAR to the GCI at NOR_NDC. A contract has been concluded and VSAT antennas have been installed at each station in the network. Under the same contract, VSAT antennas for 6 of the PS27 subarrays have been installed for intra-array communication. The seventh subarray is connected to the central recording facility via a leased land line. The central recording facility for PS27 is connected directly to the GCI (Basic Topology). All the VSAT communication is functioning satisfactorily.

The Norwegian NDC has been cooperating with institutions in other countries for transmission of IMS data to the Prototype IDC during GSETT-3. Details on this can be found in Section 4.2.

Jan Fyen

4.2 Status Report: Norway's Participation in GSETT-3

Introduction

This contribution is a report for the period July - December 2002 on activities associated with Norway's participation in the GSETT-3 experiment, which provides data to the International Data Centre (IDC) in Vienna on an experimental basis until the participating stations have been commissioned as part of the International Monitoring System (IMS) network defined in the protocol to the Comprehensive Nuclear-Test-Ban Treaty. This report represents an update of contributions that can be found in previous editions of NORSAR's Semiannual Technical Summary. It is noted that as of 31 December 2002, two out of the three Norwegian seismic stations providing data to the IDC have been formally certified and thus commissioned as part of the IMS network.

Norwegian GSETT-3 stations and communications arrangements

During the reporting interval 1 July - 31 December 2002, Norway has provided data to the GSETT-3 experiment from the three seismic stations shown in Fig. 4.2.1. The NORSAR array

(PS27, station code NOA) is a 60 km aperture teleseismic array, comprised of 7 subarrays, each containing six vertical short period sensors and a three-component broadband instrument. ARCES is a 25-element regional array with an aperture of 3 km, whereas the Spitsbergen array (station code SPITS) has 9 elements within a 1-km aperture. ARCES and SPITS both have a broadband three-component seismometer at the array center.

The intra-array communication for NOA utilizes a land line for subarray NC6 and VSAT links based on TDMA technology for the other 6 subarrays. The central recording facility for NOA is at NOR_NDC.

Continuous ARCES data has been transmitted from the ARCES site to NOR_NDC using a 64 kbits/s VSAT satellite link, based on BOD technology.

Continuous SPITS data has been transmitted to NOR_NDC via a VSAT terminal located at Platåberget in Longyearbyen (which is the site of the IMS radionuclide monitoring station RN49 installed during 2001).

Seven-day station buffers have been established at the ARCES and SPITS sites and at all NOA subarray sites, as well as at NOR_NDC for ARCES, SPITS and NOA.

The NOA and ARCES arrays are primary stations in the GSETT-3 network and the IMS, which implies that data from these stations is transmitted continuously to the receiving international data center. Since October 1999, this data has been transmitted (from NOR_NDC) via the Global Communications Infrastructure (GCI) to the IDC in Vienna. The SPITS array is an auxiliary station in GSETT-3 and the IMS, and the SPITS data have been available to the IDC throughout the reporting period on a request basis via use of the AutoDRM protocol (Kradolfer, 1993; Kradolfer, 1996). The Norwegian stations are thus participating in GSETT-3 with the same status (primary/auxiliary seismic stations) they have in the IMS defined in the protocol to the Comprehensive Nuclear-Test-Ban Treaty. In addition, continuous data from all three arrays is transmitted to the US NDC.

Uptimes and data availability

Figs. 4.2.2 - 4.2.3 show the monthly uptimes for the Norwegian GSETT-3 primary stations ARCES and NOA, respectively, for the period 1 July - 31 December 2002, given as the hatched (taller) bars in these figures. These barplots reflect the percentage of the waveform data that are available in the NOR_NDC tape archives for these two arrays. The downtimes inferred from these figures thus represent the cumulative effect of field equipment outages, station site to NOR_NDC communication outage, and NOR_NDC data acquisition outages.

Figs. 4.2.2-4.2.3 also give the data availability for these two stations as reported by the IDC in the IDC Station Status reports. The main reason for the discrepancies between the NOR_NDC and IDC data availabilities as observed from these figures is the difference in the ways the two data centers report data availability for arrays: Whereas NOR_NDC reports an array station to be up and available if at least one channel produces useful data, the IDC uses weights where the reported availability (capability) is based on the number of actually operating channels.

Use of the AutoDRM protocol

NOR_NDC's AutoDRM has been operational since November 1995 (Mykkeltveit & Baadshaug, 1996). The monthly number of requests by the IDC for SPITS data for the period July - December 2002 is shown in Fig. 4.2.4.

NDC automatic processing and data analysis

These tasks have proceeded in accordance with the descriptions given in Mykkeltveit and Baadshaug (1996). For the period January - June 2002, NOR_NDC derived information on 456 supplementary events in northern Europe and submitted this information to the Finnish NDC as the NOR_NDC contribution to the joint Nordic Supplementary (Gamma) Bulletin, which in turn is forwarded to the IDC. These events are plotted in Fig. 4.2.5.

Data forwarding for GSETT-3 stations in other countries

NOR_NDC continued to provide communications for the GSETT-3 auxiliary station at Nilore, Pakistan, through a VSAT satellite link between NOR_NDC and Pakistan's NDC in Nilore. The IDC obtains data from the Hagfors array (HFS) in Sweden through requests to the Auto-DRM server at NOR_NDC (in the same way requests for Spitsbergen array data are handled, see above). No requests for Hagfors data were received in the reporting period..

Current developments and future plans

NOR_NDC is continuing the efforts towards improving and hardening all critical data acquisition and data forwarding hardware and software components, so as to meet future requirements related to operation of IMS stations to the maximum extent possible.

The PrepCom has tasked its Working Group B with overseeing, coordinating, and evaluating the GSETT-3 experiment. The PrepCom has also encouraged states that operate IMS-designated stations to continue to do so on a voluntary basis and in the framework of the GSETT-experiment until such time that the stations have been certified for formal inclusion in IMS. The NOA array was formally certified by the PTS on 28 July 2000, and a contract with the PTS in Vienna currently provides partial funding for operation and maintenance of this station. The ARCES array was formally certified by the PTS on 8 November 2001. A contract has also been signed with the PTS for operation and maintenance of this station. Provided that adequate funding continues to be made available (from the PTS and the Norwegian Ministry of Foreign Affairs), we envisage continuing the provision of data from all Norwegian IMS-designated seismic stations without interruption to the IDC in Vienna.

U. Baadshaug
S. Mykkeltveit
J. Fyen

References

- Kradolfer, U. (1993): Automating the exchange of earthquake information. *EOS, Trans., AGU*, 74, 442.
- Kradolfer, U. (1996): AutoDRM — The first five years, *Seism. Res. Lett.*, 67, 4, 30-33.
- Mykkeltveit, S. & U. Baadshaug (1996): Norway's NDC: Experience from the first eighteen months of the full-scale phase of GSETT-3. *Semiann. Tech. Summ.*, 1 October 1995 - 31 March 1996, NORSAR Sci. Rep. No. 2-95/96, Kjeller, Norway.

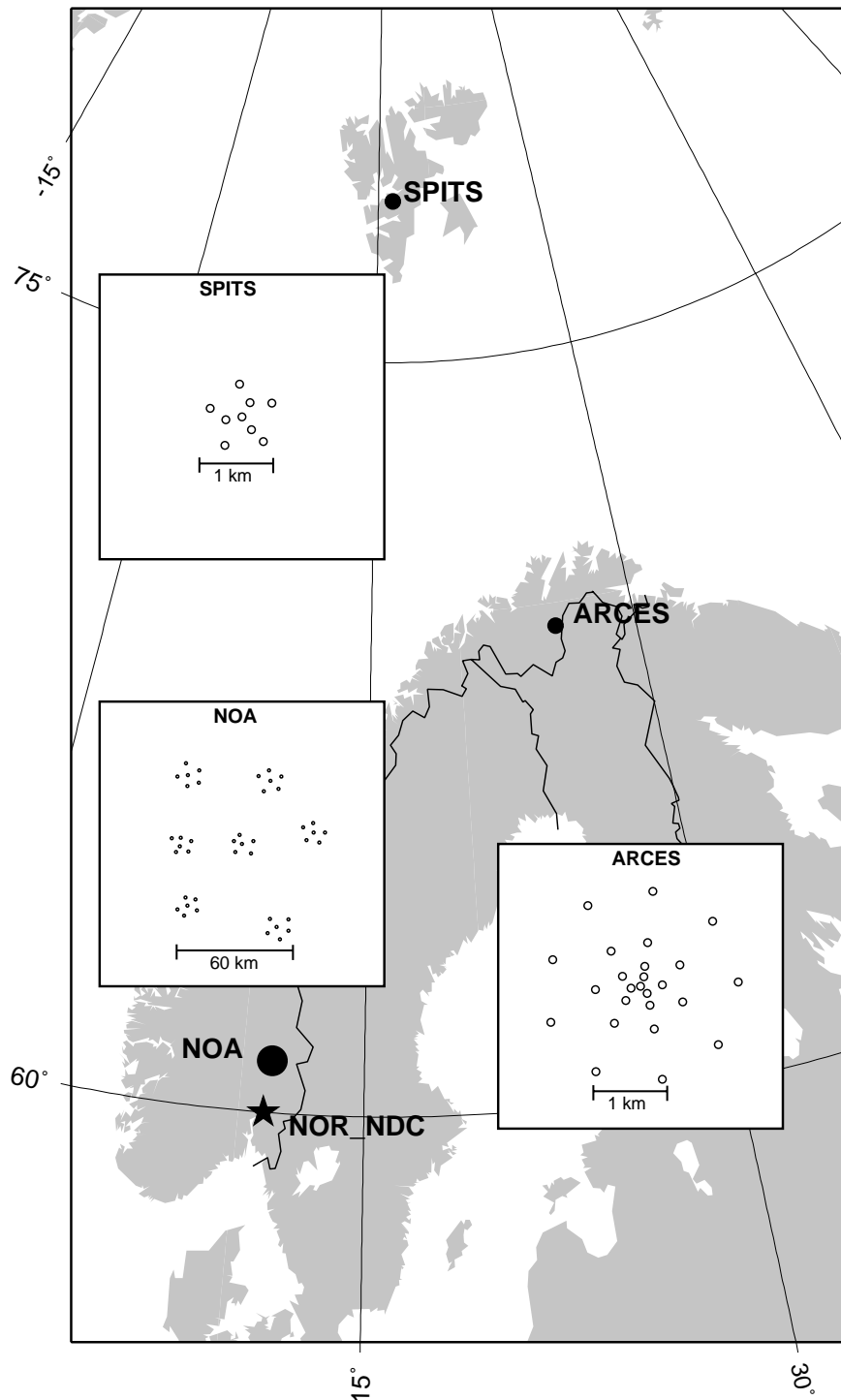


Fig. 4.2.1. The figure shows the locations and configurations of the three Norwegian seismic array stations that have provided data to the GSETT-3 experiment during the period 1 January - 30 June 2003. The data from these stations are transmitted continuously and in real time to the Norwegian NDC (NOR_NDC). The stations NOA and ARCES have participated in GSETT-3 as primary stations, whereas SPITS has contributed as an auxiliary station.

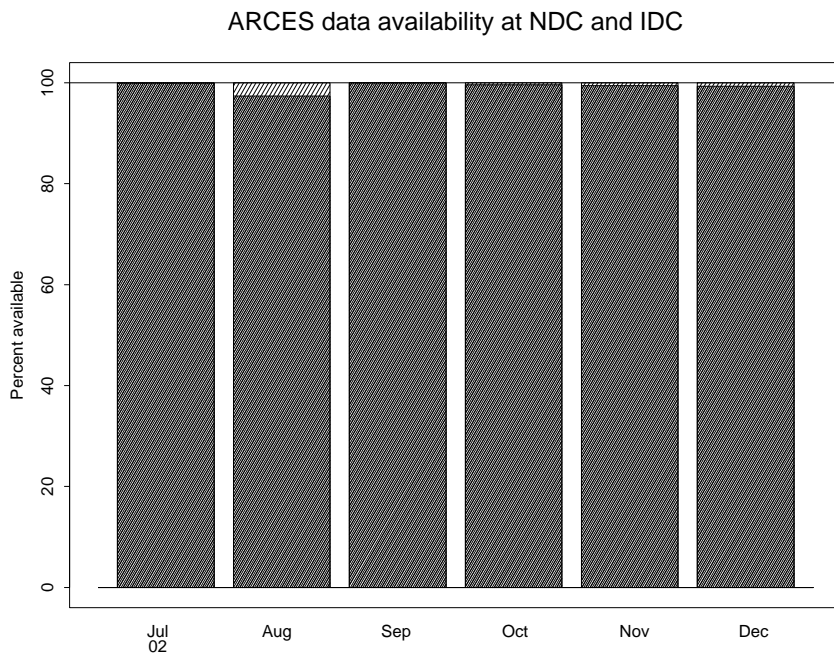


Fig. 4.2.2. The figure shows the monthly availability of ARCES array data for the period January - June 2003 at NOR_NDC and the IDC. See the text for explanation of differences in definition of the term “data availability” between the two centers. The higher values (hatched bars) represent the NOR_NDC data availability.

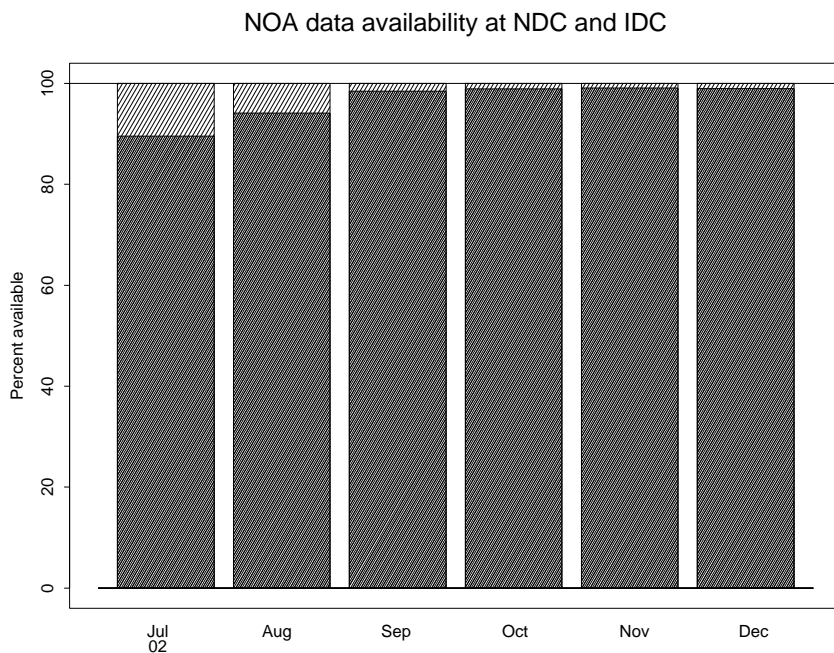


Fig. 4.2.3. The figure shows the monthly availability of NORSAR array data for the period January - June 2003 at NOR_NDC and the IDC. See the text for explanation of differences in definition of the term “data availability” between the two centers. The higher values (hatched bars) represent the NOR_NDC data availability.

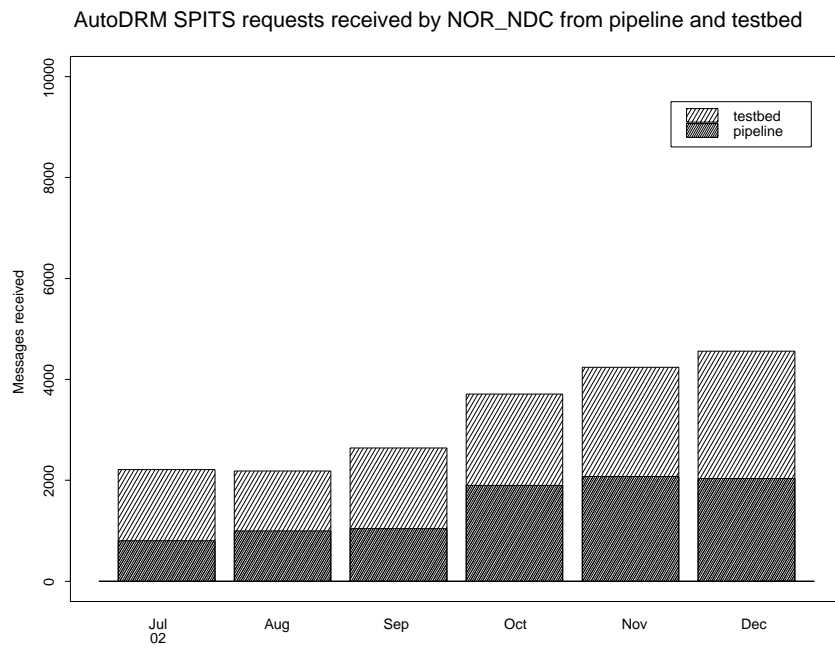


Fig. 4.2.4. The figure shows the monthly number of requests received by NOR_NDC from the IDC for SPITS waveform segments during January - June 2003.

Reviewed Supplementary events

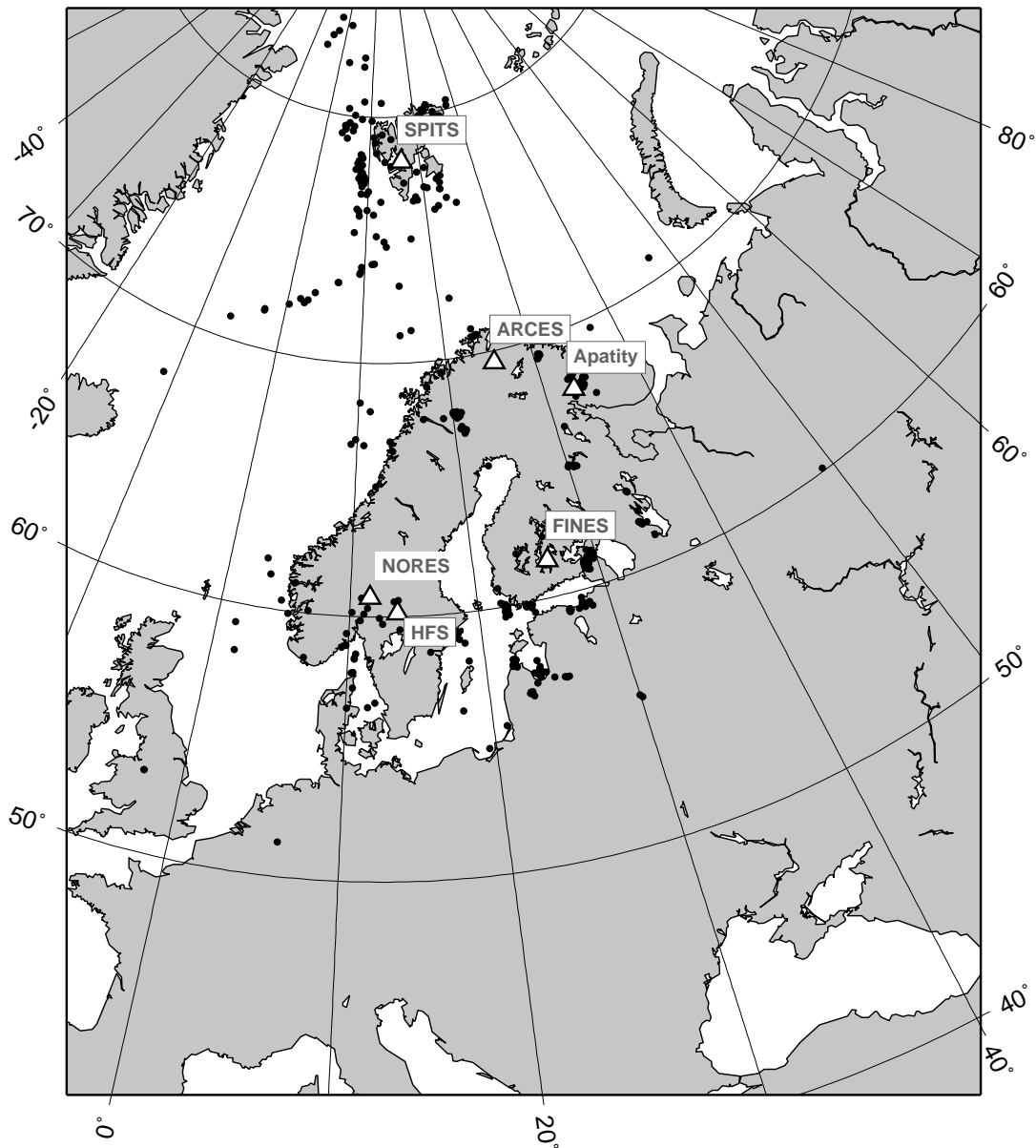


Fig. 4.2.5. The map shows the 447 events in and around Norway contributed by NOR_NDC during January - June 2003 as supplementary (Gamma) events to the IDC, as part of the Nordic supplementary data compiled by the Finnish NDC. The map also shows the seismic stations used in the data analysis to define these events.

4.3 Field Activities

The activities at the NORSAR Maintenance Center (NMC) at Hamar currently include work related to operation and maintenance of the following IMS seismic stations: the NOA teleseismic array (PS27), the ARCES array (PS28) and the Spitsbergen array (AS72). Some preparatory work has also been carried out in connection with the seismic station on Jan Mayen (AS73), the infrasound station at Karasjok (IS37) and the radionuclide station at Spitsbergen (RN49). NORSAR also acts as a consultant for the operation and maintenance of the Hagfors array in Sweden (AS101).

In addition to the above activities, which are directly related to the International Monitoring System, NORSAR's field staff are continuing, within available resources, to maintain the small-aperture NORES array, which is co-located with NOA subarray 06C. These efforts are given low priority, since there is no requirement for specific uptimes at NORES.

NORSAR carries out the field activities relating to IMS stations in a manner generally consistent with the requirements specified in the appropriate IMS Operational Manuals, which are currently being developed by Working Group B of the Preparatory Commission. For seismic stations these specifications are contained in the Operational Manual for Seismological Monitoring and the International Exchange of Seismological Data (CTBT/WGB/TL-1 1/2), currently available in a draft version.

All regular maintenance on the NORSAR field systems is conducted on a one-shift-per-day, five-day-per-week basis. The maintenance tasks include:

- Operating and maintaining the seismic sensors and the associated digitizers, authentication devices and other electronics components.
- Maintaining the power supply to the field sites as well as backup power supplies.
- Operating and maintaining the VSATs, the data acquisition systems and the intra-array data transmission systems.
- Assisting the NDC in evaluating the data quality and making the necessary changes in gain settings, frequency response and other operating characteristics as required.
- Carrying out preventive, routine and emergency maintenance to ensure that all field systems operate properly.
- Maintaining a computerized record of the utilization, status, and maintenance history of all site equipment.
- Providing appropriate security measures to protect against incidents such as intrusion, theft and vandalism at the field installations.

Details of the daily maintenance activities are kept locally. As part of its contract with CTBTO/PTS NORSAR submits, when applicable, problem reports, outage notification reports and equipment status reports. The contents of these reports and the circumstances under which they will be submitted are specified in the draft Operational Manual.

P.W. Larsen

K.A. Løken

4.4 NORSAR's Event Warning System (NEWS)

4.4.1 Introduction

Data from the highly sensitive regional arrays ARCES, FINES, HFS, SPITS, and NORES, and the teleseismic NORSAR array (NOA) are automatically processed in on-line mode. However, the routine data processing of single arrays can be delayed due to data transfer problems. Therefore, the full automatic regional and local event location process GBF (Ringdal and K v rna, 1989) can also be delayed by hours or even days because this process waits for the results of all arrays. In some cases of felt seismic events the GBF system is not fast enough to deliver event locations, which could be used to inform the public calling NORSAR directly after the events occur. In addition, GBF does not use automatic analysis results from the teleseismic NORSAR array although this may help to locate local or regional events. Therefore, during the last two years, a new extra event location system was developed to provide quick but reliable solutions for strong events: NORSAR's Event Warning System (NEWS).

4.4.2 Triggering NEWS

The whole NEWS system is based on high signal-to-noise ratio (SNR) detections, which usually correspond to large amplitudes. Whenever one of the regional arrays observes a P-type onset with an SNR larger than 50, the NEWS process is started. The SNR threshold of 50 is used to avoid too many false alarms by larger man-made events, which can easily reach SNR values of 20 or 30. Seismic events which are felt in Fennoscandia on the other hand usually have first-P onsets with SNR values of around 100 or larger for the closest array. In the case of larger teleseismic onsets at the small aperture arrays, the threshold of 50 gives for example, a trigger level for events in the Japanese area of station magnitudes between mb 4 and 5.

The automatic data processing of NOA also starts the NEWS process whenever the automatic NOA data analysis locates an event after detecting a teleseismic P-type onset (i.e., apparent velocity larger than 10 km/s), with an SNR larger than 8.5 for this onset, and an estimated event body-wave magnitude of larger than 4.9.

Once triggered, the NEWS process searches the automatic result lists of all other arrays for corresponding onsets. Corresponding in this context means that the other onsets have to come from a backazimuth, and with an apparent velocity, which is consistent with the triggering onset. For example, any triggering P onset reaching HFS from the south will not be associated with any P-type onset reaching ARCES from the North. To formulate robust rules for which onsets can eventually be associated with the same event took some time. As implemented today, these rules build on the travel-time differences between the onset times at the different stations, measured backazimuth and apparent velocity of the signals, and the SNR of the onset. If the triggering onset has a large SNR, all corresponding onsets at the other arrays should also have an SNR of greater than 8 apart from a higher SNR threshold of 30 for SPITS and a lower threshold of 6 for NOA. This was implemented to reduce spurious associations due to the numerous high SNR P-type onsets at SPITS from local events and because measured parameters on NOA onsets are reliable enough also with lower SNRs due to the larger aperture of this array. In the case of local or regional events, NEWS also searches for S-type onsets in the onset lists for the small aperture arrays. Corresponding S-type onsets must have at least an SNR of 10 to be accepted for NEWS.

4.4.3 Locating the event

After all available lists are searched; the NEWS process locates the seismic event. To make this automatic event location as robust as possible, only onsets times and apparent velocity values from first P and S arrivals are used. From all other onsets in compliance with the selection rules only measured backazimuth values are used to locate the event. Depending on the mean apparent velocity of the P onsets, the program defines the event as probably regional, or as near, far or very far teleseismic. Then, together with the mean backazimuth observation, an initial source region is chosen. Depending on this initial solution, either a regional or a global velocity model is used to locate the event. In the case of a far-regional or teleseismic event, all observed P amplitudes are used to calculate an event magnitude.

For the determination of the source parameters NORSAR's location program HYPOSAT (Schweitzer, 2001) is used. An automatic phase association and event location can only be a preliminary source parameter determination. With the limited amount of data available for localizing the event, the event's depth cannot be resolved and is therefore fixed. However, during the last two years, such preliminary locations have been sufficient for preliminary information to the public in the case of local / regional events.

Although the network of seismic arrays used has an aperture of ca. 18 deg in north-south direction, teleseismic events are usually observed over only a very small azimuth range. Therefore, the small number of available observations produces solutions with limited accuracy and large error bars. Some events are even not locatable and the inversion for an epicenter becomes unstable. This is in particular true for events in the South Pacific for which only PKP-type onsets can be observed.

4.4.4 NEWS results

The earliest versions of the NEWS system was implemented at NORSAR during winter / spring 2000 / 2001. In the following months the results were systematically followed up and the system tuned for more stable solutions and fewer false alarms. On average, NEWS solutions are available between a few and up to about 10 minutes after the first P onset with high SNR have been recorded at the seismic station. From 16 January 2001, a listing of the 30 most recent NEWS solutions has been available on the web (<http://www.norsar.no/bulletins/alert/>). For some events, NEWS reports more than one solution. This is due to the fact that in particular for stronger events several of the arrays have P onsets above the SNR threshold of 50. In addition, sometimes the data analysis of single arrays is significantly delayed. In all these cases, the NEWS system is constructed such that it only reports again events with significantly different epicenter solutions, more defining parameters and/or smaller error bars. In summer 2002, NORSAR started to send the NEWS solutions to interested data centers, which also work on quick epicenter solutions in Europe. Since 16 June 2002, the European data center for broadband data ORFEUS in De Bilt and, since 16 July 2002, the European-Mediterranean Seismological Centre (EMSC/CSEM) in Paris have received NEWS solutions in IMS1.0 format. However, the solutions sent by E-mail are only subsets of the events published on NORSAR's web page since these data centers are not interested in all the small events in Fennoscandia or the European Arctic; only events located with at least three P-type onsets are reported.

In the case of teleseismic events, the NEWS reports are often listed together with only one or two of the many alert-messages from distributing institutes on the Real Time Seismicity Page

of the EMSC (<http://www.emsc-csem.org/Welcome.html>) and thereby help the EMSC to locate such events more accurate.

NEWS reported 1406 events in the period between 16 June and 31 December 2002, which is approximately 7 events per day. However, 186 of these reports were multiple events. Fig. 6.1.1 shows only the 1220 events without the 186 multiples as red dots. In addition, the global seismicity as seen by the REBs is shown as light gray dots. Obviously, the array network sees mainly seismic events from the Eurasian continent and the European Arctic. Other source regions in similar epicentral distance as the Mid-Atlantic Ridge System, the Caribbean Sea, or North and Central America do not produce sufficiently large P onsets at the arrays to trigger NEWS. It also seems that the array network is not very sensitive to the high seismicity in far-regional distances such as for example the whole Mediterranean Region.

4.4.5 The 8 September 2002 event - a case study

On 8 September 2002 the Russian authorities destroyed with an underwater explosion the last remains of the submarine Kursk. This event with a GBF network magnitude of 2.75 was strong enough to be observed at many seismic stations. The P onsets at ARCES and at FINES were recorded with an SNR large enough to trigger the NEWS system (ARCES 362.6, FINES 196.9). Five P onsets of the automatic data-processing lists at ARCES (3), FINES (1) and HFS (1) were retrieved and the event was located. The first P onset at ARCES was recorded at 17:17:32.4 and, 8 minutes later, at 17:25:31 NEWS had send out an alert E-mail. Fig. 6.1.2 shows a map of the different locations related to this event; the NEWS solution using only five P onsets from three stations, a single array solution using two P and two S onsets at ARCES (<http://www.norsar.no/bulletins/dpep/2002/251/ARC/ARC02251.html>), the GBF solution using ten P and S onsets from five arrays (<http://www.norsar.no/bulletins/gbf/2002/GBF02251.html>), the REB solution with 9 defining P and S onsets from 5 stations, and the known Kursk location (e.g., Schweitzer, 2002). NEWS reports and REB bulletins also contain error ellipses, which are plotted in addition on the map. The map clearly demonstrates how helpful the quick NEWS solutions can be in responding to public requests regarding large seismic events at local or regional distances; the distance between the know explosion site and the NEWS location is only about 79 km.

Johannes Schweitzer

References

- Ringdal, F. and T. Kväerna (1989): A multi-channel processing approach to real time network detection, phase association, and threshold monitoring. *Bull. Seism. Soc. Am.* 79, 1927-1940.
- Schweitzer, J. (2001): HYPOSAT - an enhanced routine to locate seismic events. *Pure appl. geophys.* 158, 277-289.
- Schweitzer, J. (2002): Some results derived from the seismic signals of the accident of the Russian submarine Kursk. *Semiannual Technical Summary, 1 July 2001 - 31 December 2002, NORSAR Scientific Report 1-2002*, 115-121.

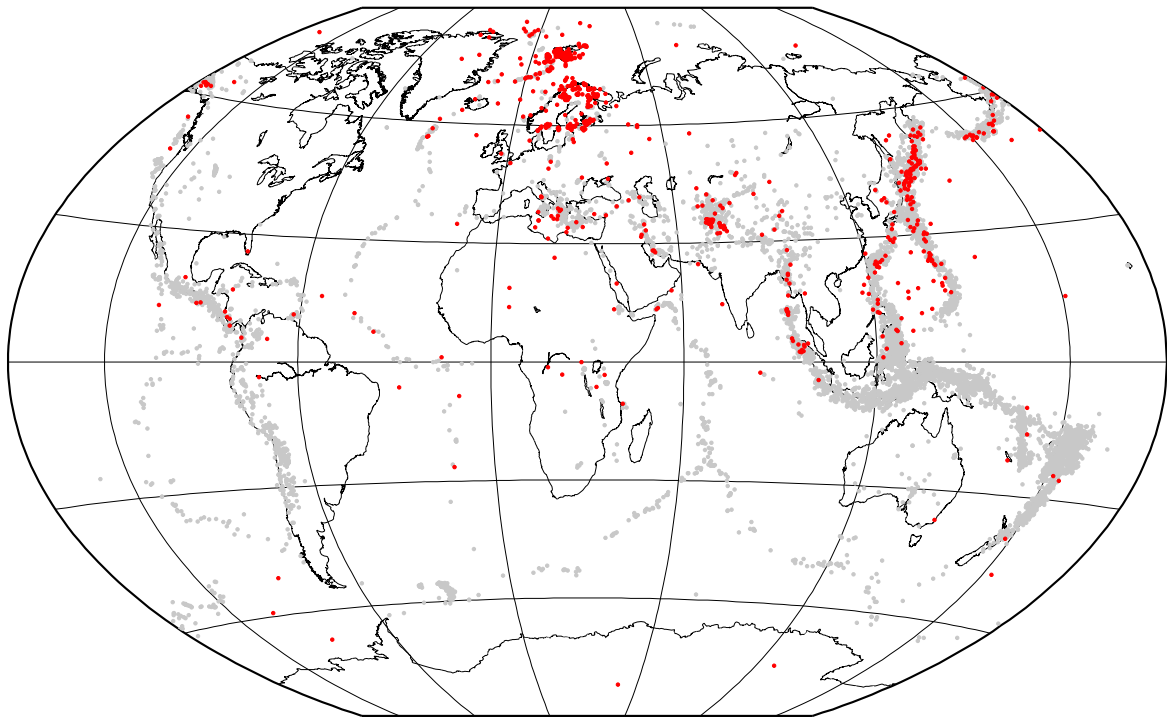


Fig. 4.4.1. Map with all 1220 NEWS locations (red) between 16 June and 31 December 2002 on top of all 10796 events (grey) as listed in the REBs of the same period.

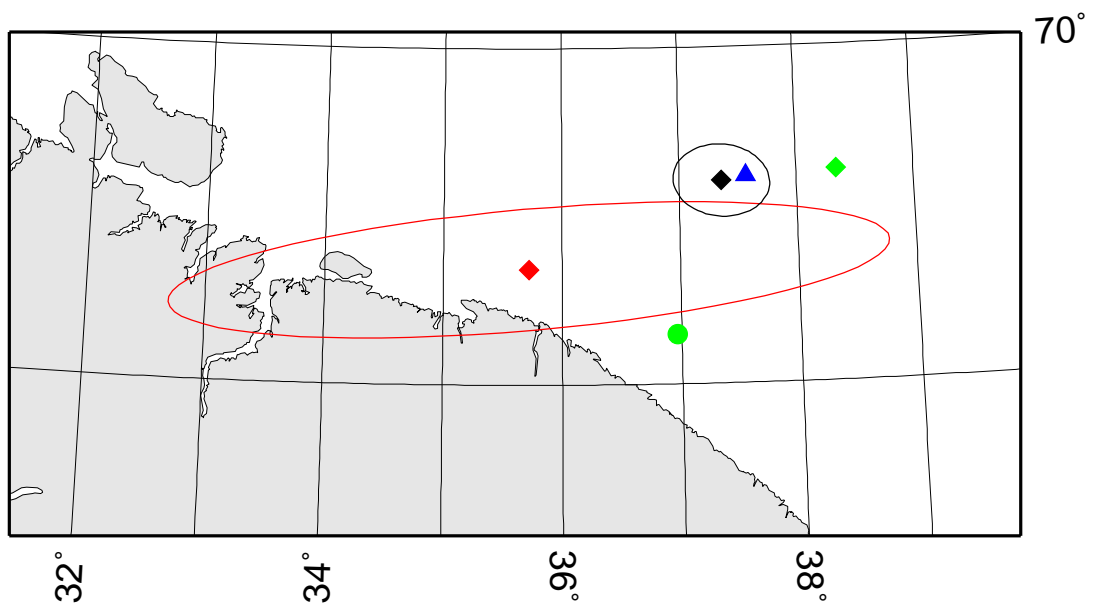


Fig. 4.4.2. Different locations of the Kursk explosion on 08 September 2002 as reported by: NEWS in red with 95% error ellipses, ARCES as a green circle, GBF as a green diamond, REB with 90% error ellipses in black, and the known Kursk position as blue triangle.

5 Documentation Developed

- Dahlman, O., J. Mackby, S. Mykkeltveit & H. Haak (2002): Cheaters beware. *Bull. Atomic Scientists*, 58, 28-35.
- Gibbons, S., T. Kværna & F. Ringdal (2003): Single array analysis and processing of events from the Kovdor mine, Kola, NW Russia, **In:** NORSAR Sci. Rep. 1-2002, 1 July - 31 December 2002, Kjeller, Norway.
- Harris, D., F. Ringdal, E. Kremenetskaya, S. Mykkeltveit, D.W. Rock & J. Schweitzer (2002): Ground truth collection for mining explosions in northern Fennoscandia and Russia, 24th Seism. Res. Review, Ponte Vedra Beach FL., Proc. Vol. 1, 54-60.
- Kværna, T., E. Hicks & F. Ringdal (2003): Site-Specific GBF monitoring of the Novaya Zemlya test site, **In:** NORSAR Sci. Rep. 1-2002, 1 July - 31 December 2002, Kjeller, Norway.
- Kværna, T. (2003): Threshold Monitoring of the mines in the Kola region, **In:** NORSAR Sci. Rep. 1-2002, 1 July - 31 December 2002, Kjeller, Norway.
- Kværna, T., E. Hicks, J. Schweitzer & F. Ringdal (2002): Regional seismic Threshold Monitoring, 24th Seism. Res. Review, Ponte Vedra, FL., Proc. Vol 2, 859-860.
- Ringdal, F., T. Kværna, E. Kremenetskaya, V. Asming, C. Lindholm & J. Schweitzer (2002): Research in regional seismic monitoring, 24th Seism. Res. Review, Ponte Vedra Beach, FL., Proc. Vol. 1, 385-393.
- Schweitzer, J. (2003): Upgrading the ARCES (PS28) on-line data processing system, **In:** NORSAR Sci. Rep. 1-2002, 1 July - 31 December 2002, Kjeller, Norway.
- Schweitzer, J. (2002): Simultaneous inversion of steep-angle observations of PcP and ScP in Europe — what can we learn about the core-mantle boundary?, *Geophys. J. Int.*, 151, 209-220.
- Schweitzer, J. (2002): HYPOSAT Vers. 4.4 (including HYPOMOD 1.1), User Manual, NORSAR, Kjeller, 15 pp.
- Vinogradov, Y. & F. Ringdal (2003): Analysis of infrasound data recorded at the Apatity array, **In:** NORSAR Sci. Rep. 1-2002, 1 July - 31 December 2002, Kjeller, Norway.

6 Summary of Technical Reports / Papers Published

6.1 Upgrading the ARCES (PS 28) on-line data processing system

6.1.1 Introduction

The main part of the detector recipe for the ARCES array has not been modified since its installation in 1989 (Fyen, 1989). The only major change was an extension with the inclusion of more horizontal beams in 1999 (Kværna et al., 1999) after the sensitivity of these beams for local and regional S phases had been demonstrated in an earlier study (Schweitzer, 1994). However, the detector recipe, as installed in 1989, was restricted by the limited computer capabilities of at that time. It consisted of 76 beams; 66 coherent beams with slowness parameters for regional P onsets, and 10 incoherent beams of narrow-band pre-filtered data for vertical (6) and horizontal (4) components. The change in April 1999 was the addition of 108 new beams; 36 beams of rotated transverse components, 36 beams of rotated radial components, and 36 incoherent beams of horizontal components for an apparent velocity of 4 km/s and various backazimuths. Fig. 6.1.1 shows the slowness distribution of this ARCES beam set. The distribution of red points represent the slowness values used to calculate the different beams as function of ray parameter in [s/deg] and backazimuth in [deg]. Many of the shown slowness values were used several times but for different bandpass filters. All incoherent beams using the vertical components were calculated with an infinite apparent velocity, which places them all in the center of the slowness space. The radii of the blue circles are at 4.4, 13.9, 18.5, and 27.8 s/deg, which corresponds with apparent velocities of P waves from the core-mantle boundary, Pn waves of 8, Pg waves of 6, and regional S waves of 4 km/s, respectively.

However, these detection beams do not cover all interesting parts of the slowness space and after some P onsets, for analysts clearly visible, were not detected by this automatic detector recipe, a principle restructuring of the detector recipe for ARCES data was considered.

6.1.2 The new beam table for ARCES

Since computer capabilities have increased dramatically during the last decade, the first decision for a new ARCES detector recipe was to increase the total number of beams to 573, of which only 13 are incoherent beams. Table 6.1.1 lists the whole new beam set for ARCES. The number of incoherent beams, in particular of horizontal components, was reduced because the small number of only four 3C sites results in a relatively high sensitivity of such beams to disturbances and noise at only one site. This reduction is compensated for by a new set of coherent vertical beams using S-phase typical apparent velocities. Fig. 6.1.2 shows the slowness distribution (ray parameters and backazimuths) of the new beam set. Note that beams are now calculated down to an apparent velocity of 2.5 km/s (or 44.5 s/deg), which resolves much better the numerous Rg-type onsets from local events. In addition, the beams for detecting P onsets are much more evenly distributed in the ray-parameter space of regional and teleseismic P phases up to apparent velocities of lower most-mantle P waves (~20 km/s). To detect PKP onsets, still only beams with an infinite apparent velocity are used. Since the installation of ARCES in 1987, some events had been observed from the Novaya Zemlya area. Therefore, mean observed backazimuth and apparent velocity values could be calculated for this source region. In the new

ARCES beam table, these values are used to calculate five Pn beams and 15 Sn beams in particular sensitive for this source region of interest.

6.1.3 Performance of the new ARCES detector recipe

Because of the larger number of beams and the better coverage of the slowness space, the new detector recipe led to a dramatic increase in the number of detections. The new detector recipe was tested over several months in parallel with the original on-line data processing at NORSAR. In the period between 8 August (DOY 220) and 31 October 2002 (DOY 304), the number of detections increased by about 42.3% from 54488 to 77519 detections. In particular, the number of S and Rg onsets increased. As for other arrays, the array-transfer function of the ARCES array is not perfect (see for example, Schweitzer et al., 2002) and a seismic signal will trigger on many different beams. In such cases, the detector processor as developed at NORSAR (Fyen 1989; 2001) chooses the beam which has the best relative signal-to-noise ratio (SNR) that means the highest ratio SNR to predefined detection threshold of the beam. In the detector-result lists the beam names are reported and thereby all beam parameters.

For the 54488 detections with the old detection recipe, 152 of the 184 implemented beams were reported as detecting, of which 70.8% (38571) of the detections were made with coherent and 29.2% (15917) with incoherent beams. The distribution for the new beam deployment is different; during the 84 days test period, 564 of the 573 defined detecting beams (or 98.4%) were the defining beam with best SNR on at least one occasion and only the small number of 2717 (or 3.5%) of all detections were found with incoherent beams. That detection-time estimates on coherent beams are more reliable than on incoherent beams is obvious, consequently the whole automatic parameter extraction by fk-analysis will be more stable for such detected onsets.

From former studies (Schweitzer, 1994; 1997; 1998), it is known how important it is to choose an optimum time-window definition for the automatic fk-analysis. After changing the detector recipe for ARCES, the positioning and length of the time window for the automatic fk-analysis was also modified. For the new ARCES processing, up to eight different time windows are tested for each detection and the one chosen is that which gives the best quality value (i.e., the highest signal coherence) for the fk-analysis. In cases where the original detection was made on one of the horizontal component beams, the fk-analysis is initially performed on the vertical components. A subsequent fk-result is performed on the horizontal components only in cases where the vertical component fk-analysis result displays very low coherence. The later fk-result will then of course be less reliable (note; ARCES has only four 3C sites!) and will only be accepted in the case of measured apparent velocities belonging to S- or Rg-type onsets.

All phase identifications are based on these slowness measurements done during the automatic data processing. Table 6.1.2 gives some additional information about the differences between the old and the new beam recipes with respect to the different phase types. The number of detected phases increases for all types of detections apart from a small decrease in P- and PKP-type detections. This reduction is understandable given the better coverage of the slowness space (compare Fig. 6.1.1 with Fig. 6.1.2); slower phases are much less often detected and wrongly interpreted as teleseismic onsets and many regional P onsets are now much better detected by the Pn- and Pg-type beams and consequently also more robustly analyzed.

6.1.4 Event locations

The results for the automatic measurement of onset times, apparent velocities, backazimuths, amplitudes and dominant signal frequencies are used in a later step of NORSAR's automatic data processing for single array (RONAPP, Mykkeltveit and Bungum, 1984) and multi array (GBF, Ringdal and Kværna, 1989) locations. The described modifications to the recipes for detector and fk-analysis should also improve these location results.

Between 8 August (DOY 220) and 31 October 2002 (DOY 304), the number of located events using the RONAPP algorithm increased by about 23.9% from 3072 to 3806 located events. The geographical distribution of the two event sets is shown in Fig. 6.1.3 and Fig. 6.1.4. For orientation on both maps, circles of 500 km and 1000 km distance around ARCES are shown. It is known that single array locations from small aperture regional arrays show some scatter. To show only the most robust solutions, the located events were binned on both figures in 1000 km² large areas and the number of events per bin is shown in a color coded scale. No bin containing only one event is shown. The number of bins is 213 for the old and 255 for the new processing results. However, the number of bins containing only one event also increased from 820 to 1011; i.e., in both cases about 75% of all bins were hit only once. Most of the events occur inside the 500 km radius around ARCES. The differences between the two maps are not very large. However, the known source areas of mining activities in Kiruna, Malmberg, Khibiny, and in Finland show more events for the new data processing results. This is also true for events on the Mid Atlantic Ridge southwest of Spitsbergen.

The next step in evaluating the new ARCES data processing was in comparing the GBF bulletins produced with the old and new ARCES fk-results. For a period of 58 days (8 August - 5 October 2002), GBF was reprocessed using the new automatic ARCES results. The total number of events located by GBF using the old and the new ARCES data processing is only slightly changed. However, comparing the single locations, some differences become evident. Because not only the fk-results but also the onset time estimations and the total number of ARCES observations changed, the whole GBF bulletin shows many differences, some of them being listed in Table 6.1.3. To compare two such different bulletins, one has to define the criterion that two event locations represent identical seismic events. Because most locations in the GBF bulletins are based on a relatively small number of defining parameters, changing, adding, or removing one of these defining parameters can drastically change the epicenter determination. Therefore, in this study two events were defined as common if the horizontal distance between them is not more than 150 km and if the origin-time difference between these two events is not more than 25 s. Using these rules, both GBF bulletins have 17222 or more than 80% common events. The new GBF results show a systematic shift of locations to better defined events; as also shown in Table 6.1.3, the number of single array solutions decreased by 4.6% from 17145 to 16375 events, and the number of events observed by more than two stations increases by 18.9% from 797 to 948 events.

Events located with observations from at least two stations with a defining P onset and at one of these two stations in addition with a defining S onset are assumed to be relatively well located GBF events. The number of such events increased by 16%. However, 88 of the events from the GBF bulletins created using the old ARCES results do not appear in the GBF bulletins created with the new ARCES results. This can have two reasons; for some events the new ARCES contribution moved the event outside the 150 km and/or 25 s limit or the new ARCES results no longer contribute with observations that the event is just no longer definable. Fig. 6.1.5 shows a

map with all 88 events, which are not longer defined in the GBF bulletins using the new ARCES results. Most of the events are scattered in or around the Barents Sea region.

The same is true for the 186 events Fig. 6.1.6 which are only in the GBF bulletin using the new ARCES results; many of these new events lay in the vicinity of either the ARCES or the SPITS arrays, both arrays with a high number of detections and local or regional events nearby. In these cases, onsets from the other array can by chance easily erroneously be associated to such a one array solution.

6.1.5 Conclusions

The analysis of the new ARCES processing results clearly shows a better adjustment to the observed seismic onsets at the array site. The number of detections increases and on average the seismic phases are detected with a higher SNR. The number of single array event locations is higher and a relative increase in spurious events is not be observed. Comparing the GBF results shows that the number of more reliably defined events increases. This is eventually connected with a slight increase of erroneous defined events (see Fig. 6.1.6). The latter happened in particular in connection with observations of the SPITS array. This point has to be observed and a change of the GBF processing scheme in the case of two-station event locations may be considered in the future.

Because of these overall positive results the new beam set and data processing recipes were installed for NORSAR' s on-line processing of ARCES data from 21 November 2002 (DOY 325) on.

Johannes Schweitzer

References

- Fyen, J. (1989): Improvements and modifications. Semiannual Technical Summary, 1 April 1988 - 30 September 1988, NORSAR Scientific Report **1-89/90**, 30-38.
- Fyen, J. (2001): NORSAR seismic data processing - user guide and command reference. NORSAR (contribution 731), Kjeller, Norway.
- Kværna, T., J. Schweitzer, L. Taylor and F. Ringdal (1999): Monitoring of the European Arctic Using Regional Generalized Beamforming. Semiannual Technical Summary, 1 October 1998 - 31 March 1999, NORSAR Scientific Report **2-98/99**, 78-94.
- Mykkeltveit, S. and H. Bungum (1984): Processing of regional seismic events using data from small-aperture arrays. *Bull. Seism. Soc. Am.* **74**, 2313-2333.
- Ringdal, F. and T. Kværna (1989): A multi-channel processing approach to real time network detection, phase association, and threshold monitoring. *Bull. Seism. Soc. Am.* **79**, 1927-1940.
- Schweitzer, J. (1994): Some improvements of the detector / SigPro-system at NORSAR. Semiannual Technical Summary, 1 October 1993 - 31 March 1994, NORSAR Scientific Report **2-93/94**, 128-139.
- Schweitzer, J. (1997): Recommendations for improvements in the PIDC processing of Matsushiro (MJAR) array data. Semiannual Technical Summary, 1 April - 30 September 1997, NORSAR Scientific Report **1-97/98**, 128-141.
- Schweitzer, J. (1998): Tuning the automatic data processing for the Spitsbergen array (SPITS). Semiannual Technical Summary, 1 April - 30 September 1998, NORSAR Scientific Report **1-98/99**, 110-125.
- Schweitzer, J., J. Fyen, S. Mykkeltveit and T. Kværna (2002): Seismic Arrays. **In:** P. Bormann (ed.) (2002): *New Manual of Seismological Observatory Practice (NMSOP)*, Chapter 9, 52 pp.

Table 6.1.1. Definition of all beams used in the new configuration of the on-line detector for ARCES. Listed are beam names, applied apparent velocities (VEL), backazimuths (BAZ), bandpass and order (ord) of the Butterworth filters, the detection thresholds (THR), and the beam configurations (CONFIG).

BEAM NAME	VEL [km/s]	BAZ [°]	FILTER		THR	CONFIG
			bandpass [Hz]	ord		
FA01	99999.9	0.0	0.8 – 2.0	4	3.8	ALL
FA02	99999.9	0.0	0.8 – 2.0	4	3.8	DRING
FA03	99999.9	0.0	0.8 – 2.0	4	3.8	TELEV
FA04	99999.9	0.0	0.8 – 2.0	4	3.8	CRING
FA05	99999.9	0.0	1.0 – 2.5	3	3.8	ALL
FA06	99999.9	0.0	1.0 – 2.5	3	3.8	DRING
FA07	99999.9	0.0	1.0 – 2.5	3	3.8	TELEV
FA08	99999.9	0.0	1.0 – 2.5	3	3.8	CRING
FA09	99999.9	0.0	3.0 – 5.0	3	3.8	ALL
FA10	99999.9	0.0	3.0 – 5.0	3	3.8	DRING
FA11	99999.9	0.0	3.0 – 5.0	3	3.8	TELEV
FA12	99999.9	0.0	3.0 – 5.0	3	3.8	CRING
FB01 – FB06	18.0	0 60 120 180 240 300	1.0 – 2.5	3	3.8	TELE
FB07 – FB12	18.0	0 60 120 180 240 300	2.5 – 4.0	3	3.8	TELE
FB09 – FB18	18.0	0 60 120 180 240 300	3.5 – 5.5	3	3.8	TELE
FB19 – FB24	20.0	30 90 150 210 270 330	0.8 – 2.0	4	3.8	ALL
FB25 – FB30	20.0	30 90 150 210 270 330	1.0 – 2.0	3	3.8	ALL
FB31 – FB36	20.0	30 90 150 210 270 330	3.0 – 5.0	3	3.8	ALL
FC01 – FC06	16.0	0 60 120 180 240 300	0.8 – 2.0	4	3.8	ALL
FC07 – FC12	16.0	0 60 120 180 240 300	1.0 – 2.5	3	3.8	ALL
FC13 – FC18	16.0	0 60 120 180 240 300	3.0 – 5.0	3	3.8	ALL
FC19 – FC24	14.0	30 90 150 210 270 330	1.0 – 2.5	3	3.8	DRING
FC25 – FC30	14.0	30 90 150 210 270 330	2.5 – 4.0	3	3.8	DRING
FC31 – FC36	14.0	30 90 150 210 270 330	3.5 – 5.5	3	3.8	DRING
FD01 – FD08	13.0	0 45 90 135 180 225 270 315	1.5 – 3.0	3	3.8	ALL
FD13 – FD20	13.0	0 45 90 135 180 225 270 315	3.0 – 5.0	3	3.8	ALL
FD25 – FD32	13.0	0 45 90 135 180 225 270 315	4.0 – 8.0	3	3.8	ALL
FD37 – FD44	11.0	22.5 67.5 112.5 202.5 247.5 292.5 337.5	2.0 – 3.5	3	3.8	INTER
FD49 – FD56	11.0	22.5 67.5 112.5 202.5 247.5 292.5 337.5	3.5 – 5.5	3	3.8	INTER
FD61 – FD68	11.0	22.5 67.5 112.5 202.5 247.5 292.5 337.5	5.0 – 10.0	3	3.8	INTER
FE01 – FE12	10.0	0 30 60 90 120 150 180 210 240 270 300 330	2.0 – 3.5	3	3.8	ALL
FE13 – FE24	10.0	0 30 60 90 120 150 180 210 240 270 300 330	3.0 – 5.0	3	3.8	ALL
FE25 – FE36	10.0	0 30 60 90 120 150 180 210 240 270 300 330	4.0 – 8.0	3	3.8	ALL
FE37 – FE48	9.0	0 30 60 90 120 150 180 210 240 270 300 330	2.5 – 4.0	3	3.8	CRING
FE49 – FE60	9.0	0 30 60 90 120 150 180 210 240 270 300 330	3.5 – 5.5	3	3.8	CRING
FE61 – FE72	9.0	0 30 60 90 120 150 180 210 240 270 300 330	5.0 – 10.0	3	3.8	CRING
FF01 – FF12	8.5	0 30 60 90 120 150 180 210 240 270 300 330	2.0 – 3.5	3	3.8	ALL
FF13 – FF24	8.5	0 30 60 90 120 150 180 210 240 270 300 330	3.0 – 5.0	3	3.8	ALL
FF25 – FF36	8.5	0 30 60 90 120 150 180 210 240 270 300 330	4.0 – 8.0	3	3.8	ALL
FF37 – FF48	7.5	0 30 60 90 120 150 180 210 240 270 300 330	2.5 – 4.0	3	3.8	CRING
FF49 – FF60	7.5	0 30 60 90 120 150 180 210 240 270 300 330	3.5 – 5.5	3	3.8	CRING
FF61 – FF72	7.5	0 30 60 90 120 150 180 210 240 270 300 330	5.0 – 10.0	3	3.8	CRING
FG01 – FG12	6.5	0 30 60 90 120 150 180 210 240 270 300 330	2.0 – 3.5	3	3.8	ALL
FG13 – FG24	6.5	0 30 60 90 120 150 180 210 240 270 300 330	3.0 – 5.0	3	3.8	ALL
FG25 – FG36	6.5	0 30 60 90 120 150 180 210 240 270 300 330	4.0 – 8.0	3	3.8	ALL
FG37 – FG48	6.0	0 30 60 90 120 150 180 210 240 270 300 330	2.5 – 4.0	3	3.8	CRING
FG49 – FG60	6.0	0 30 60 90 120 150 180 210 240 270 300 330	3.5 – 5.5	3	3.8	CRING
FG61 – FG72	6.0	0 30 60 90 120 150 180 210 240 270 300 330	5.0 – 10.0	3	3.8	CRING
FI01 – FI12	4.5	0 30 60 90 120 150 180 210 240 270 300 330	1.5 – 3.0	3	3.8	ALL
FI13 – FI24	4.5	0 30 60 90 120 150 180 210 240 270 300 330	2.5 – 4.0	3	3.8	ALL
FI25 – FI36	4.5	0 30 60 90 120 150 180 210 240 270 300 330	4.0 – 8.0	3	3.8	ALL
FJ01 – FJ12	3.5	0 30 60 90 120 150 180 210 240 270 300 330	1.5 – 3.0	3	3.8	ALL
FJ13 – FJ24	3.5	0 30 60 90 120 150 180 210 240 270 300 330	2.5 – 4.0	3	3.8	ALL
FJ25 – FJ36	3.5	0 30 60 90 120 150 180 210 240 270 300 330	4.0 – 8.0	3	3.8	ALL
FK01 – FK12	2.5	0 30 60 90 120 150 180 210 240 270 300 330	1.0 – 2.5	3	3.8	ALL
FK13 – FK24	2.5	0 30 60 90 120 150 180 210 240 270 300 330	3.0 – 5.0	3	3.8	ALL

FK25 – FK36	2.5	0 30 60 90 120 150 180 210 240 270 300 330	4.0 – 8.0	3	3.8	ALL
FK37 – FK48	2.5	0 30 60 90 120 150 180 210 240 270 300 330	5.0 – 10.0	3	3.8	BRING
FN01	10.0	64.	1.5 – 3.0	3	3.5	ALL *
FN02	10.0	64	2.5 – 4.0	3	3.5	ALL *
FN03	10.0	64	3.5 – 5.5	3	3.5	ALL *
FN04	10.0	64	5.0 – 10.0	3	3.5	CRING *
FN05	10.0	64	6.0 – 12.0	3	3.5	CRING *
FN06	5.0	58	1.5 – 3.0	3	3.5	ALL *
FN07	5.0	58	2.0 – 3.5	3	3.5	ALL *
FN08	5.0	58	2.5 – 4.0	3	3.5	ALL *
FN09	5.0	58	3.0 – 5.0	3	3.5	ALL *
FN10	5.0	58	4.0 – 8.0	3	3.5	ALL *
FR01 – FR12	4.0	0 30 60 90 120 150 180 210 240 270 300 330	1.0 – 2.0	3	3.8	HR
FR13 – FR24	4.0	0 30 60 90 120 150 180 210 240 270 300 330	3.5 – 5.5	3	3.5	HR
FR25 – FR36	4.0	0 30 60 90 120 150 180 210 240 270 300 330	2.0 – 3.5	3	3.5	HR
FH01 – FH12	4.0	0 30 60 90 120 150 180 210 240 270 300 330	1.0 – 2.0	3	3.8	HT
FH13 – FH24	4.0	0 30 60 90 120 150 180 210 240 270 300 330	3.5 – 5.5	3	3.5	HT
FH25 – FH36	4.0	0 30 60 90 120 150 180 210 240 270 300 330	2.0 – 3.5	3	3.5	HT
FNR1	5.0	58	1.5 – 3.0	3	3.5	HR *
FNR2	5.0	58	2.0 – 3.5	3	3.5	HR *
FNR3	5.0	58	2.5 – 4.5	3	3.5	HR *
FNR4	5.0	58	3.0 – 5.0	3	3.5	HR *
FNR5	5.0	58	4.0 – 8.0	3	3.5	HR *
FNT1	5.0	58	1.5 – 3.0	3	3.5	HT *
FNT2	5.0	58	2.0 – 3.5	3	3.5	HT *
FNT3	5.0	58	2.5 – 4.5	3	3.5	HT *
FNT4	5.0	58	3.0 – 5.0	3	3.5	HT *
FNT5	5.0	58	4.0 – 8.0	3	3.5	HT *
FS13 – FS24	4.0	0 30 60 90 120 150 180 210 240 270 300 330.	1.0 – 2.5	3	3.0	HINC
FV01	99999.9	0.	6.0 – 12.0	3	2.4	VINC

Explanation for the codes used in the column CONFIG:

ALL means all vertical instruments of the ARCES array.

BRING means vertical instruments at the ARCES sites A0, A1, A2, A3, B1, B2, B3, B4, and B5.

CRING means vertical instruments at the ARCES sites A0, B1, B2, B3, B4, B5, C1, C2, C3, C4, C5, C6, and C7

DRING means vertical instruments at the ARCES sites A0, D1, D2, D3, D4, D5, D6, D7, D8, and D9.

HINC means incoherent beam using both horizontal components at the ARCES sites A0, C2, C4, and C7.

HR means radial components rotated from the original horizontal components at the ARCES sites A0, C2, C4, and C7. The rotation angle is identical with the beam azimuth.

HT means transverse components rotated from the original horizontal components at the ARCES sites A0, C2, C4, and C7. The rotation angle is identical with the beam azimuth.

INTER means vertical instruments at the ARCES sites A0, B1, B2, B3, B4, B5, C1, C2, C3, C4, C5, C6, C7, D1, D2, D3, D4, D5, D6, D7, D8, and D9.

TELEV means vertical instruments at the ARCES sites A0, C1, C2, C3, C4, C5, C6, C7, D1, D2, D3, D4, D5, D6, D7, D8, and D9.

VINC means incoherent beam using the vertical components at the ARCES sites A0, C1, C2, C3, C4, C5, C6, and C7.

All beam configurations marked with an star (*) are beams using the apparent velocities and backazimuths for Pn and Sn phases as observed at ARCES for events in the Novaya Zemlya area.

Table 6.1.2. Results of the old and new ARCES beam deployment. # gives the number of detections, the percent value is with respect to the total number of detections, $\overline{\text{SNR}}$ is the mean value of the measured SNR values, 'sum' are all accepted detections after automatic fk-analysis.

Phase	OLD			NEW		
	#	%	$\overline{\text{SNR}}$	#	%	$\overline{\text{SNR}}$
P / PKP	4176	7.8	12.52	3767	4.9	13.66
Pn / Pg	10563	19.4	9.11	14399	18.6	8.53
S / Sn	8487	15.6	5.08	10906	14.1	5.34
Sg / Lg	14290	26.2	4.64	15488	20.0	5.58
Rg	15003	27.5	6.19	29639	38.2	6.32
sum	52519	96.4	6.68	74199	95.7	6.83
noise/error	1969	3.6	-	3320	4.3	-

Table 6.1.3. Evaluation of the GBF results one time using the OLD and one time using the NEW automatic fk-results for ARCES. The locations of the events of the table cells with gray background are plotted in Fig. 6.1.5 and Fig. 6.1.6, respectively.

	Number of events		events occurring	
	OLD	NEW	only in OLD	only in NEW
all events	21433	21462	4211	4240
single station	17145	16374	2790	2231
2 st, 1 st with P + S	789	915	88	186

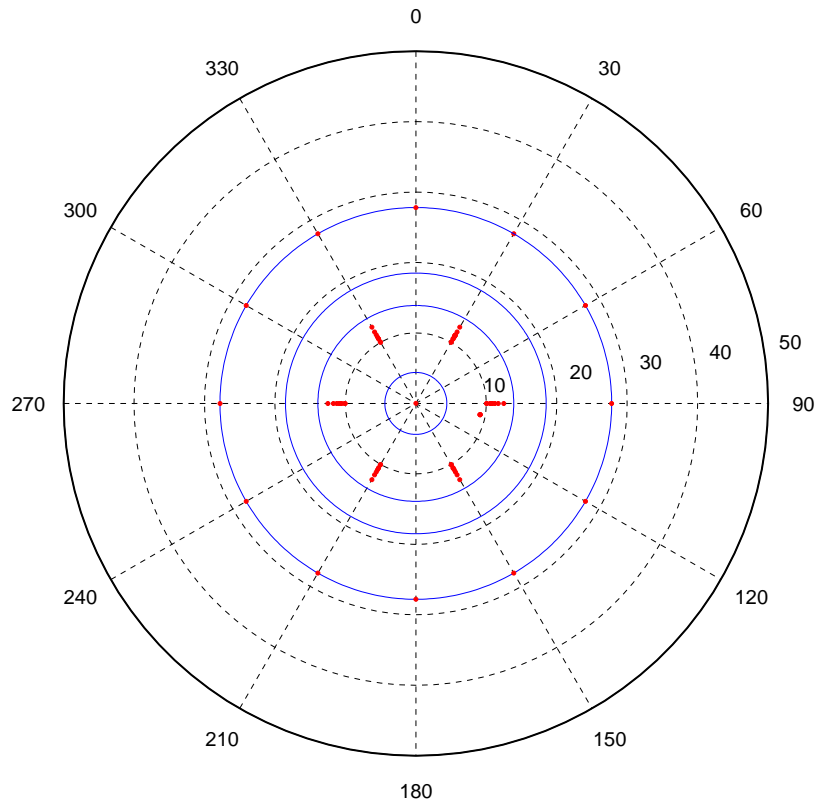


Fig. 6.1.1. Coverage of the slowness space by the old ARCES beam deployment (details see text).

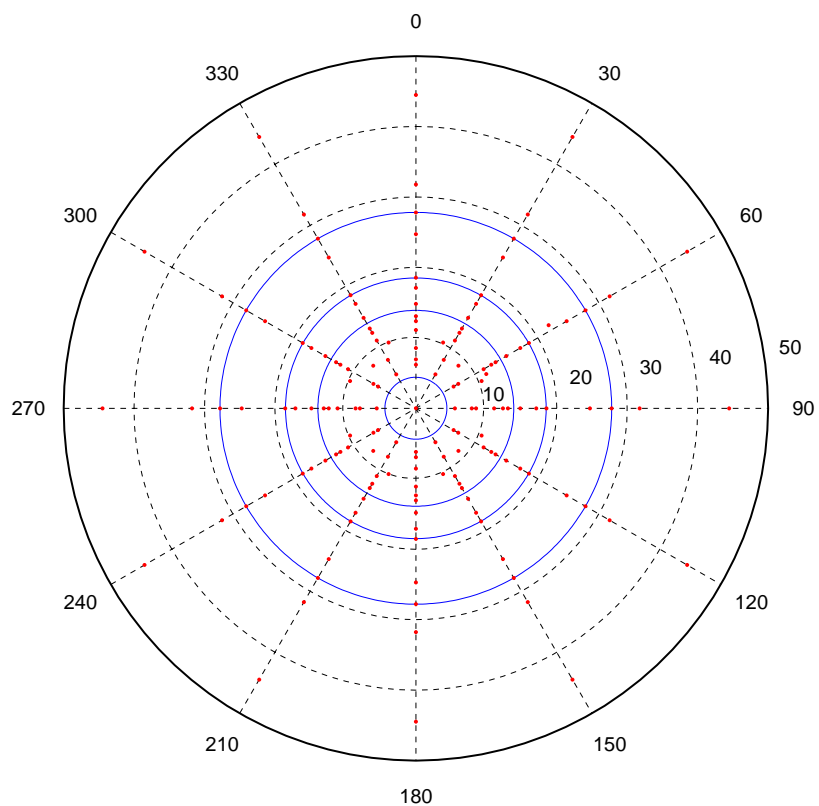


Fig. 6.1.2. As Fig. 6.1.1, now for the new ARCES beam deployment.

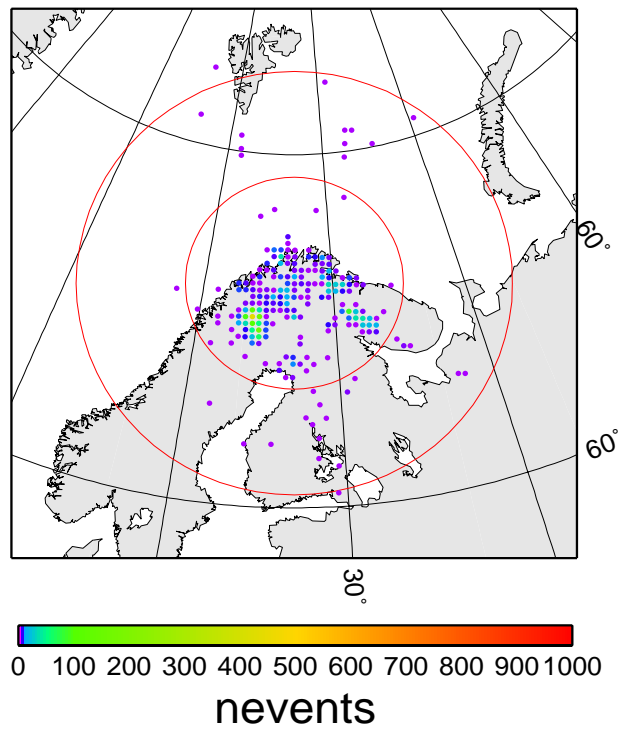


Fig. 6.1.3. Seismic events as located by the RONAPP algorithm using the *fk*-results from the old ARCES beam table. Shown are only bins (size 1000 km²) with at least 2 events.

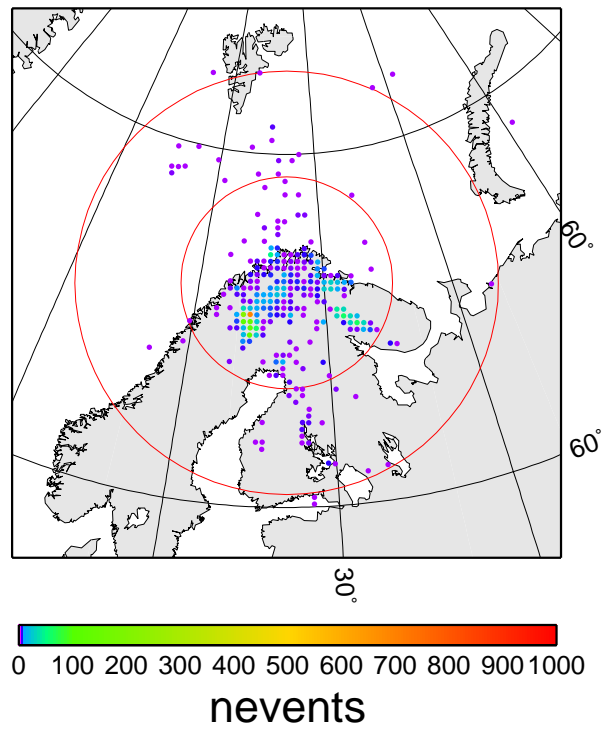


Fig. 6.1.4. As Fig. 6.1.3, but the events using the *fk*-results from the new ARCES beam table.

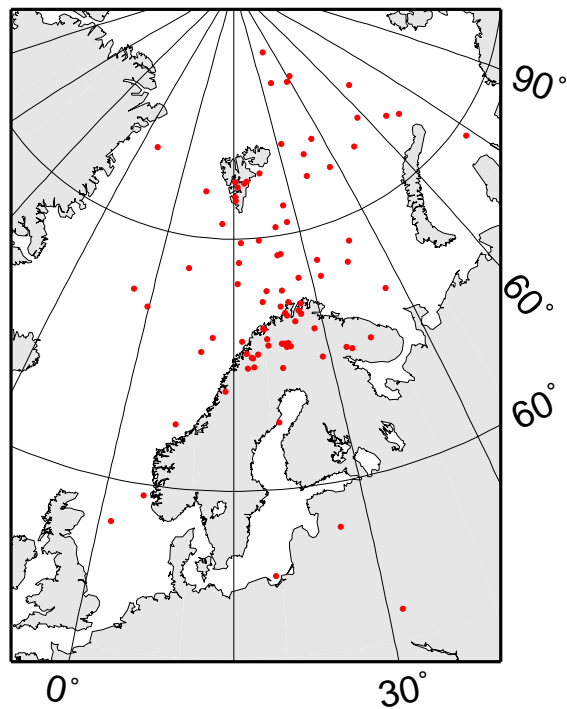


Fig. 6.1.5. Events located by GBF with at least 2 *P* onsets at 2 different stations and 1 *P* + 1 *S* onsets as defining observation at one station using the old ARCES processing results; here are only shown the 88 events, which were not in the GBF bulletins using the new ARCES recipes (see Table 6.1.3).

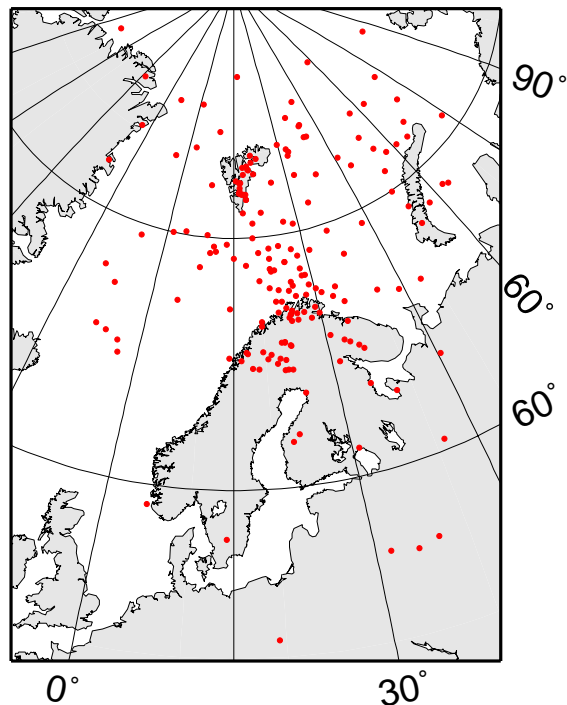


Fig. 6.1.6. As Fig. 6.1.5, now showing the 186 events located by the GBF system applying the new ARCES recipes but not located by the old recipes (see Table 6.1.3).

6.2 Single array analysis and processing of events from the Kovdor mine, Kola, NW Russia

6.2.1 Introduction

In several regions of the world, the majority of observed seismic events are the result of mining activities. For example, on the Kola Peninsula in north-western Russia, there are several concentrations of mines where explosions are routinely carried out with varying frequency. The yield of explosives used varies from explosion to explosion as does the nature of the blasts; for example, whether they are underground or surface detonations, compact or ripple-fired.

Within the context of monitoring nuclear explosions, it is important to be able to identify such events and associate them with a specific source. In an automated monitoring process, the identification of events which can be attributed to activities at a given mine with a high level of confidence can free analytical resources to investigate events which cannot, with confidence, be ascribed to a known source.

In the monitoring context, situations will arise where an interesting event is only detected by a single array. It is therefore essential to quantify how accurately such events can be located.

The goal of this work is to use a single regional seismic array (ARCES) to characterize seismic signals resulting from explosions that are known to have occurred at the Kovdor open cast mine in Russia (67.557° N, 30.425° E) and use these observations to determine whether other events recorded at ARCES are the result of operations at this mine. Wherever possible, events which are deemed to be likely candidates for Kovdor events are located to the best possible accuracy.

Figure 6.2.1 shows the location of the Kovdor mine relative to ARCES together with the Zapoljarny, Olenegorsk and Khibiny mining regions on the Kola Peninsula. The distance between ARA0, the central seismometer of the ARCESS array, and Kovdor is 298 kilometers with a receiver to source backazimuth of 135° .

Ground Truth information for events at the mines indicated in Figure 6.2.1 has been provided by the Kola Regional Seismological Centre (KRSC) in Apatity on the Kola peninsula. Table 6.2.1 gives the reported yield information and approximate origin times for explosions at the Kovdor mine between October 6, 2001, and July 13, 2002.

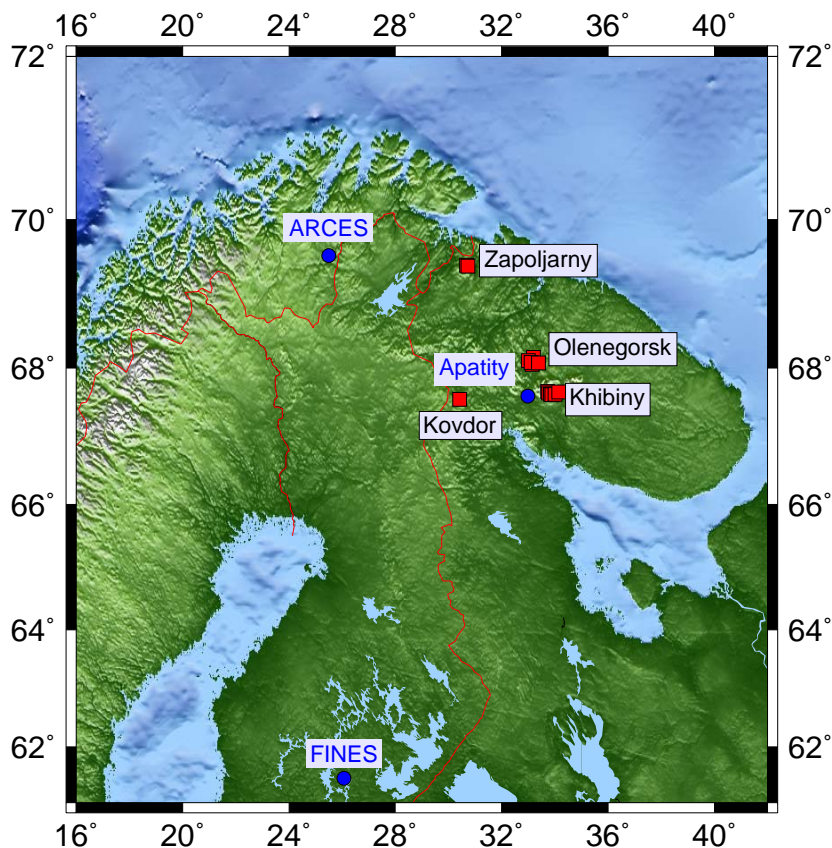


Fig. 6.2.1. Locations of the mining regions in NW Russia for which ground truth information is provided by KRSC. Also shown are the locations of the seismic arrays in the region (ARCÉS, Apatity and FINES).

A daily list of phase detections for the ARCÉS array is created by NORSAR's DP/EP processing system (Fyen, 1989, 2001). These detection lists (referred to as FKX lists) are used in two ways. Firstly, for the initial P-arrival (P_n phase) for each confirmed Kovdor event, the detection time from the ARCESS FKX lists is used as an initial estimate in determining accurate arrival times. In addition, the detection lists are also scanned for the presence of signals from further events which may originate at Kovdor.

The work described in this report is performed in two stages.

1. Firstly, using the origin information reported by KRSC, we study a set of events which are known to result from explosions at the Kovdor mine. The characteristics of the signals are described in section 6.2.2.
2. The FKX automatic detection lists for the ARCÉS array are used to obtain a list of events which could originate from Kovdor, irrespective of whether or not they were reported by KRSC. Based upon the properties observed for the known events in Step 1, a series of tests (described in section 6.2.3) is carried out on ARCÉS data in order to estimate the likelihood that such an event is a genuine Kovdor event.

Date	Origin time	Yield (tons)	Date	Origin time	Yield (tons)
Sat, Oct 6, 2001	2001-279:10.28.15	307	Sat, Feb 16, 2002	2002-047:11.47.17	406
Sat, Oct 13, 2001	2001-286:10.28.51	284	Fri, Feb 22, 2002	2002-053:11.24.45	292
Sat, Oct 20, 2001	2001-293:10.35.50	255	Sat, Mar 2, 2002	2002-061:11.16.08	216
Sat, Oct 27, 2001	2001-300:10.24.45	293	Thu, Mar 7, 2002	2002-066:11.27.43	179
Sat, Nov 3, 2001	2001-307:11.27.15	281	Sat, Mar 23, 2002	2002-082:11.29.21	226
Sat, Nov 10, 2001	2001-314:11.20.39	213	Sat, Mar 30, 2002	2002-089:11.10.43	196
Sat, Nov 17, 2001	2001-321:11.44.34	304	Sat, Apr 6, 2002	2002-096:10.13.27	244
Sat, Nov 24, 2001	2001-328:11.20.42	148	Sat, Apr 13, 2002	2002-103:10.23.52	195
Wed, Nov 28, 2001	2001-332:12.04.48	112	Sat, Apr 20, 2002	2002-110:10.22.50	315
Sat, Dec 1, 2001	2001-335:11.20.18	155	Sun, Apr 28, 2002	2002-118:10.12.49	365
Sat, Dec 8, 2001	2001-342:11.39.15	308	Sat, May 4, 2002	2002-124:10.13.19	108
Sat, Dec 15, 2001	2001-349:11.17.23	220	Wed, May 8, 2002	2002-128:10.19.54	98
Sat, Dec 22, 2001	2001-356:11.21.12	244	Sat, May 18, 2002	2002-138:10.29.47	221
Sat, Dec 29, 2001	2001-363:10.55.19	293	Sat, May 25, 2002	2002-145:10.16.45	185
Sat, Jan 5, 2002	2002-005:11.15.48	185	Sat, Jun 1, 2002	2002-152:10.16.45	203
Sat, Jan 12, 2002	2002-012:11.12.55	181	Sat, Jun 8, 2002	2002-159:10.22.29	405
Sat, Jan 19, 2002	2002-019:11.33.25	368	Sat, Jun 15, 2002	2002-166:10.16.17	240
Sat, Jan 26, 2002	2002-026:11.20.54	291	Sat, Jun 22, 2002	2002-173:10.21.37	312
Sat, Feb 2, 2002 ^a	2002-033:11.17.12	212	Sat, Jun 29, 2002	2002-180:10.20.18	247
Sat, Feb 9, 2002	2002-040:11.31.27	198	Sat, Jul 6, 2002	2002-187:10.31.01	256
			Sat, Jul 13, 2002	2002-194:10.32.30	256

a. Note that there is no ARCES data available for this event.

Table 6.2.1. List of events reported by KRSC from the Kovdor mine between October 6, 2001 and July 13, 2002.

6.2.2 A study of events confirmed to have originated at the Kovdor mine

Based upon the origin times listed in Table 6.2.1, the ARCYES detection lists were searched for the first (Pn phase) arrivals resulting from each of these events. The *barey* velocity model is derived from the Barents model of Kremenetskaya *et al.* (2001) and provides a good representation of paths from the Kara Sea to Fennoscandia (see Schweitzer and Kennett, 2002). According to *barey*, an event at a distance of 298 km is followed by Pn, Sn, and Lg phase arrivals at 44.1, 77.2, and 83.3 seconds respectively.

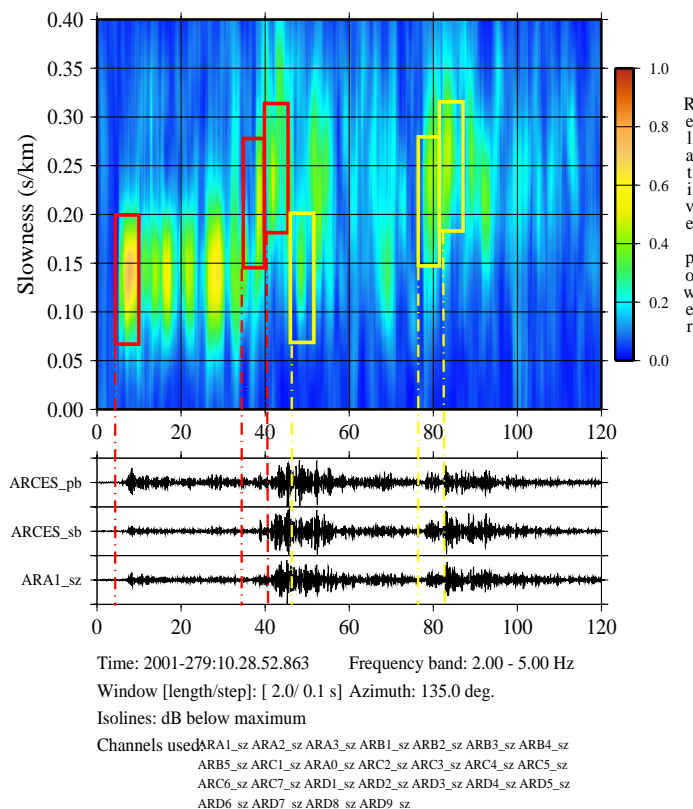


Fig. 6.2.2. Vesogram of the 2001-279 event for the frequency band 2.0-5.0 Hz and constant azimuth 135°. ARCES_pb and ARCES_sb are beams with azimuth 135° and apparent velocity 8.0 kms⁻¹ and 4.0 kms⁻¹ respectively.

The ARCYES recording of one such confirmed event is illustrated in Figure 6.2.2. Red boxes have been drawn around the Pn (slowness 0.14 skm⁻¹), Sn (slowness 0.21 skm⁻¹), and Lg (slowness 0.24 kms⁻¹) phases. Phases corresponding to a secondary event occurring approximately 40 seconds after the first are highlighted by yellow boxes. Such secondary events are very characteristic of blasts at the Kovdor mine.

On identification of the automatic ARCYES detection corresponding to the first Pn-arrival from a confirmed event, the following process was initiated:-

1. A beam was formed from the sz (short period, vertical) component traces from the ARCYES array with a velocity 7.25 kms⁻¹ and azimuth 135.0°, and then filtered in an “optimal frequency band”, calculated to maximize a combination of band-width and signal to noise ratio (SNR). This filtered trace was used to calculate an accurate time for

- the Pn arrival, t_p using the AR-AIC onset picker (Akaike, 1974, GSE/JAPAN/40, 1992, Kværna, 1995).
2. Azimuth and slowness for the Pn-phase were calculated using fk-analysis in three fixed frequency bands; 2-5 Hz, 3-8 Hz, and 8-16 Hz. All the ARCES sz instruments were used for the first two frequency bands and all but the D-ring for the third, given the decrease in coherency which occurs at these higher frequencies. The time window used was $(t_p-0.5, t_p+2.5)$ seconds.
 3. Fk-analysis was performed in two fixed time windows: $(t_p+32.5, t_p+35.5)$ for the Sn phase and $(t_p+36.5, t_p+39.5)$ for the Lg phase. For both of these phases, all sz traces were filtered in the single frequency band 2-5 Hz.
 4. AR-AIC onset times for the Sn- and Lg- phases were determined from beams filtered in the 2-5 Hz frequency band. In addition to the sz beam, the transverse beam from the rotated ARA0, ARC2, ARC4, and ARC7 horizontal components was used, the onset time taken being that from the beam giving the greatest SNR value. Irrespective of the results of the fk-analysis, the Sn and Lg beams had apparent velocity 4.5 and 4.0 kms^{-1} respectively and azimuth 135° . The initial guesses of 33.0 and 37.0 seconds after t_p for Sn and Lg respectively were decided upon following the manual inspection of many seismograms and vespagrams.

The time windows for the Pn, Sn, and Lg phase fk-analysis are shown together with the filtered beams and AR-AIC onset picks in Figure 6.2.3.

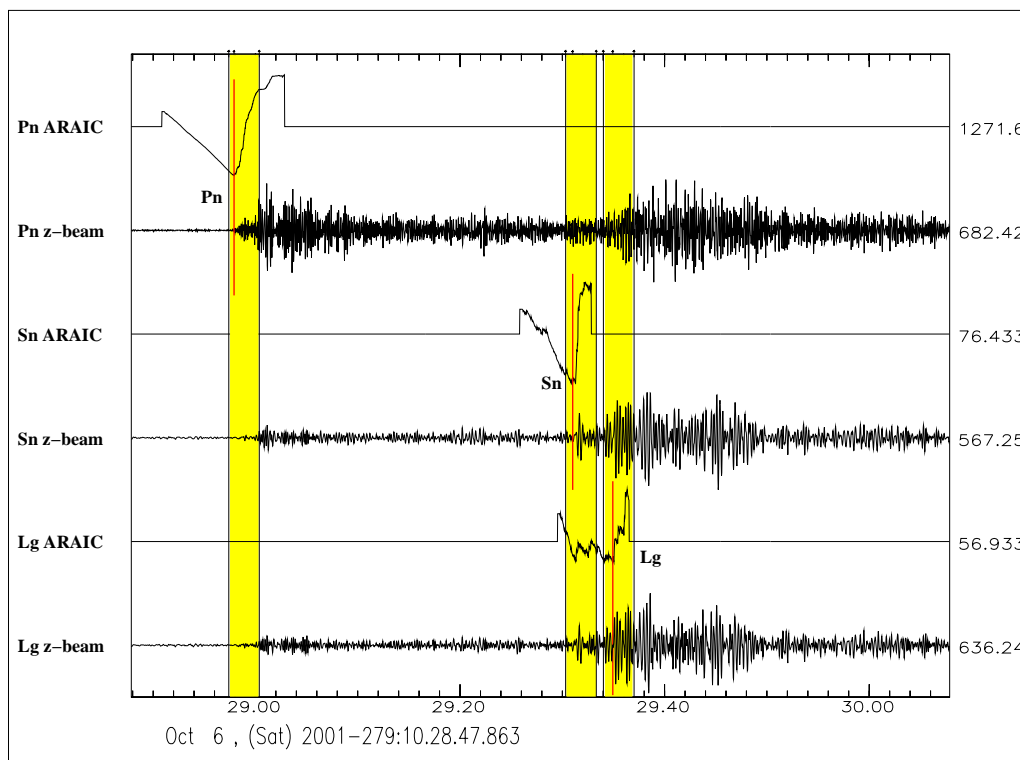


Fig. 6.2.3. Fixed time windows relative to the Pn onset for fk-analysis of phases as indicated displayed with Pn, Sn, and Lg onset picks for the KRSC verified Kovdor event of 2001-279.

The results of this procedure are summarized in Table 6.2.2. For several events, the result of the fk-analysis was demonstrably unrepresentative of the seismic phase being measured. For example, many fk results from the ($t_p+32.5$, $t_p+35.5$) second time window gave far higher apparent velocity values than could be accounted for by an Sn-phase from a Kovdor event. In all of these cases, the cause was identified as a Pn-phase from a secondary event superimposed on the Sn-signal. The Lg fk-analysis results displayed a large spread in azimuth but were more robust, probably due to the larger amplitude of the Lg-signal.

Phase	Filter band (Hz)	Apparent velocity (kms ⁻¹)			Azimuth (°)			Number of events used
		Min	Mean	Max	Min	Mean	Max	
Pn	2-5	6.68	7.15	7.81	132.1	134.9	136.7	39
	3-8	7.03	7.35	7.83	132.2	136.0	139.4	40
	8-16	6.92	8.03	8.94	132.2	138.5	144.1	33
Sn	2-5	3.92	4.63	5.49	132.2	138.0	143.6	33
Lg	2-5	3.43	3.93	4.41	128.6	137.6	144.8	39

Table 6.2.2. Summary of the fk-analysis for the 40 confirmed Kovdor events listed in Table 6.2.1 for which there exists ARCES data.

6.2.3 Classification of detections which correspond to likely Kovdor events

We wish to use the ARCES regional array to be able to identify and locate any seismic event likely to originate from Kovdor. This is achieved by the automatic process displayed in Figure 6.2.4. The following notes provide details for the tests conducted:

- **TEST ONE:** We decide whether a detection in the ARCES FKX list could correspond to an initial Pn-arrival from a Kovdor event. The decision is based upon whether or not both the apparent velocity (*vel*) and azimuth (*azi*) fall within appropriate ranges. The ranges of interest were determined by considering the *vel* and *azi* values obtained for 40 confirmed Kovdor events listed in Table 6.2.1 which were detected by ARCES. These events registered *vel* in the range 6.5 kms⁻¹ to 16.2 kms⁻¹ and *azi* in the range 118° to 143°. In order to catch all potential Kovdor events, the ranges had to be considerably larger and the acceptable *vel* and *azi* ranges were set to [6.1-18.0] kms⁻¹ and [100° - 160°] respectively.
- **TEST TWO:** The Pn-onset time and fk-analysis for the Pn time window were carried out exactly as described for Steps 1 and 2 in Section 6.2.2. It is therefore appropriate to base our acceptance criteria on the minima and maxima obtained for the confirmed events (Table 6.2.2). An event passed the test if *vel* and *azi* were within range for either the 3-8 Hz band, or both of the bands 2-5 Hz and 8-16 Hz.
- **TEST THREE:** The fk-analysis for the Sn and Lg phases was identical to that carried out in Step 3 of Section 6.2.2 and so, based upon the minima and maxima in Table 6.2.2, an Sn fk-result was accepted if *vel* and *azi* fell in the ranges [3.8,5.5] and [131,145] respectively, and an Lg fk-result was accepted if *vel* and *azi* fell in the ranges [3.3,4.5] and [127,146] respectively. This test was passed if either Sn or Lg phases were acceptable.

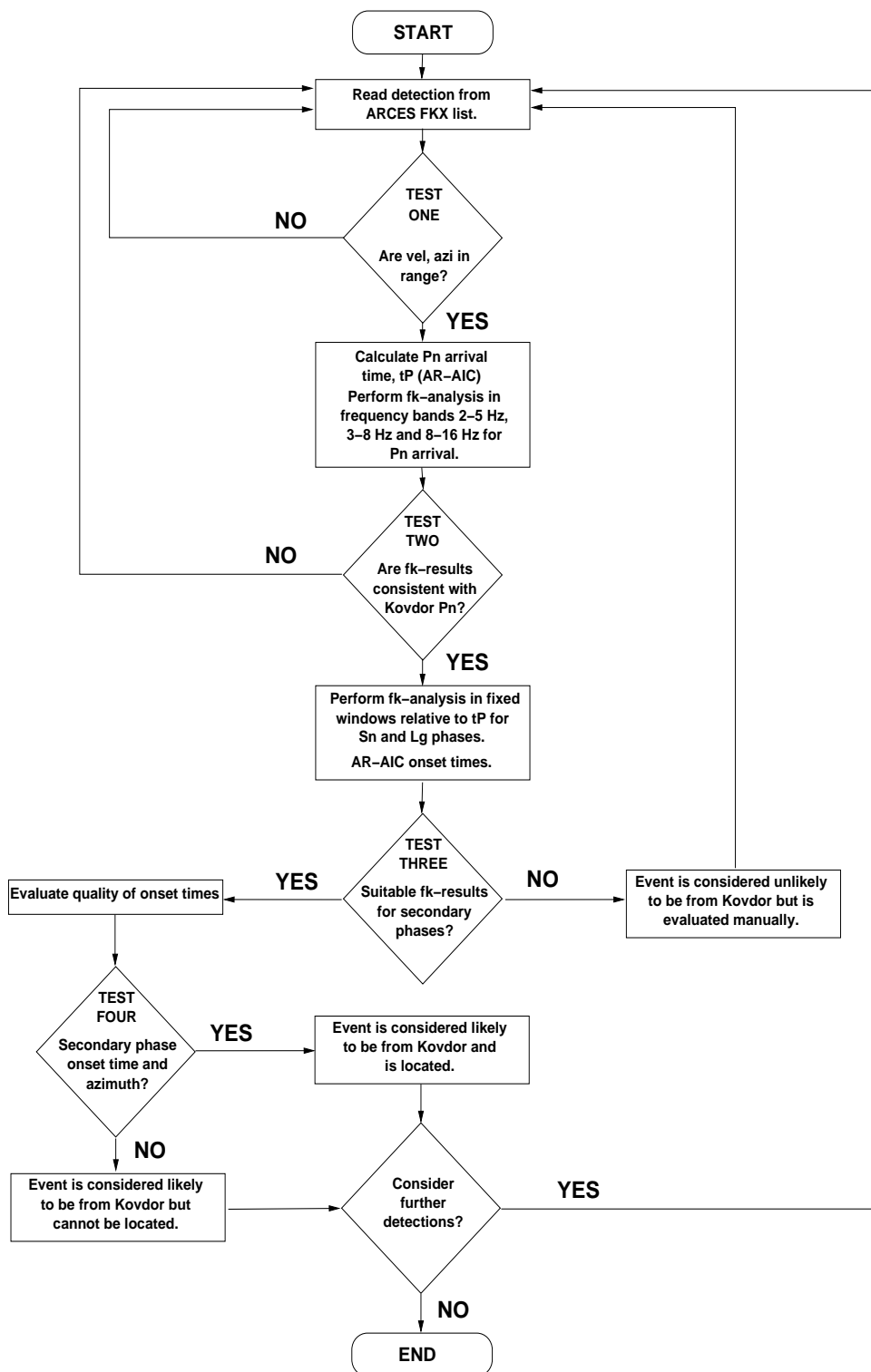


Fig. 6.2.4. Flowchart of steps in the automatic identification of events from the Kovdor mine.

- TEST FOUR: For an onset time for a secondary phase to be valid it had to satisfy a signal to noise ratio condition, be within an anticipated range, and be associated with an fk-result deemed to be acceptable from the previous test. For both Sn and Lg onset determinations, t_{Sn} and t_{Lg} , O_SNR was defined to be the 1 second mean of the envelope immediately following the onset divided by the 3 second mean immediately before the onset. For Sn picks, O_SNR had to be greater than 1.95, and, for Lg picks, O_SNR had to be greater than 2.0. t_{Sn} had to be within 1.2 seconds of $t_p+33.0$ and t_{Lg} had to be within 1.5 seconds of $t_p+37.0$. Any event for which an acceptable onset pick for a secondary phase was made was subsequently located using the HYPOSAT program (Schweitzer, 2001).

A very large number of ARCES detections passed the first test; 6176 between 2002-001 and 2002-208. This is inevitable given the large ranges of velocity and azimuth required to catch all potential events. The slowness and azimuth values from these detections are displayed in the left hand plot of Figure 6.2.5 with KRSC confirmed events highlighted as red triangles. The results from the new fk-analysis are displayed in the right hand plot and the scatter for the confirmed events is demonstrably reduced. All of the detections displayed here were calculated with the old ARCES detection recipes; the new recipes, introduced on 21 November 2002, appear to give more robust and reliable estimates of slowness and azimuth.

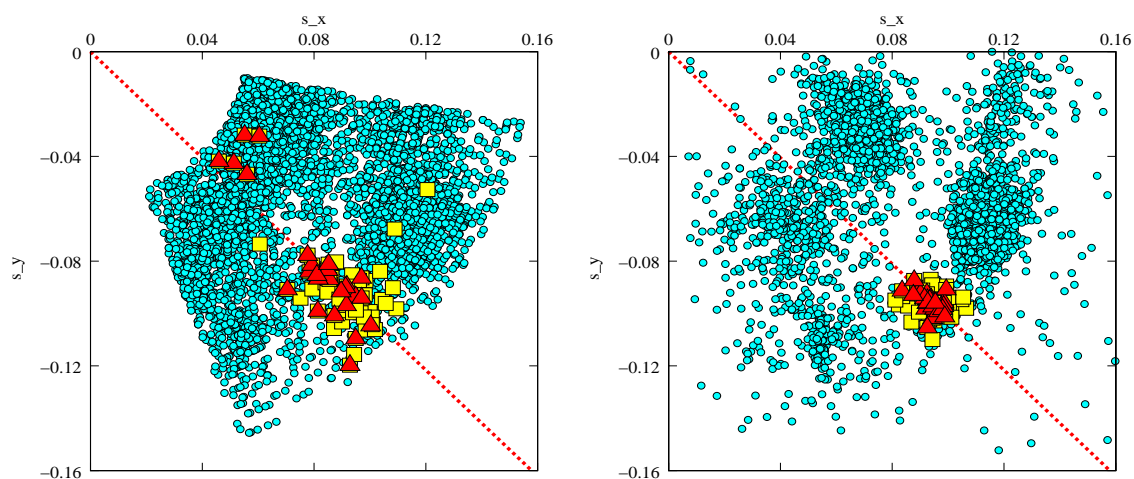


Fig. 6.2.5. The x and y components of horizontal slowness from the automatic ARCES detection list (left hand plot) and as given after autoregressive reestimation of onset time and new f-k analysis in the 3-8 Hz frequency band (right hand plot). P-phases corresponding to KRSC confirmed events are indicated by red triangles, whereas yellow squares correspond to P-phases of secondary Kovdor events and other events subsequently located close to the Kovdor mine

For the second test, in practice, only the result from the 3-8 Hz frequency band was usually required; for cases where both the 2-5 Hz and 8-16 Hz fk-analysis produced vel and azi in the accepted ranges, the velocity and azimuth calculated in the 3-8 Hz band were also within the appropriate limits. A total of 72 detections passed both of the first two tests and thus had been associated with an arrival which had a velocity and azimuth consistent with a Pn-arrival from a Kovdor event.

Of these 72 detections, 24 were discarded after the third test as they showed no indication of either an Sn or Lg phase consistent with a Kovdor event. Figure 6.2.6 shows fk-plots for the Sn

phase for three detections. The first of these, 2002-026, is a confirmed Kovdor event which gives a high-quality fk -plot and a velocity and azimuth within the expected ranges. The second plot in Figure 6.2.6 also displays the results from a confirmed event (2002-012) which recorded an acceptable azimuth, but an apparent velocity which was too high to correspond to an Sn phase. Inspection of the waveforms indicates that this time window is in the coda of the P-arrival from a secondary event which, due to a good fk -result and onset pick for the Lg phase, was able to be located close to Kovdor. The third plot shows analysis of a hypothetical Sn window corresponding to a Pn detection consistent with a Kovdor event. There is no evidence for a signal from the correct azimuth and thus no evidence for a Kovdor-consistent Sn phase. Using data from the ARCES and FINES arrays, the NORSAR GBF (Generalized Beam-forming) system (Kværna et al., 1999) located the event at 62.21°N , 40.54°E , or 1062 km from ARCES with an azimuth of 133° ; the corresponding secondary phases will arrive later than under the Kovdor event hypothesis.

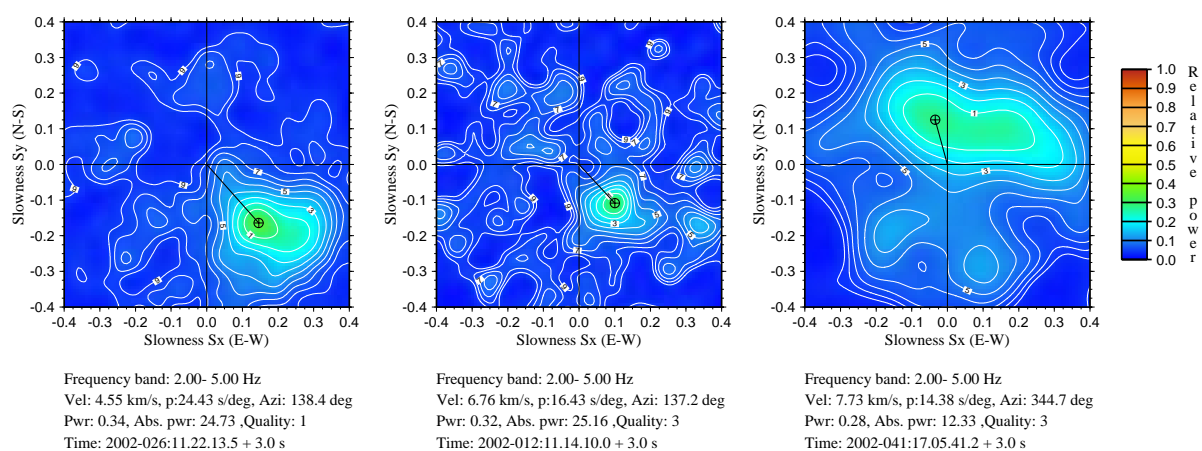


Fig. 6.2.6. Results of fk -analysis for the Sn time window for three events which passed the first two tests as indicated in Figure 6.2.4.

The first three tests resulted in 48 event hypotheses. Of these, only a single one was untrue. This is to say that the detection was the result of an event which did not occur at Kovdor; the NORSAR GBF system located it approximately 80 km south-east of Kovdor, using ARCES and Apatity data.

Of the KRSC confirmed Kovdor events, 29 occurred within the period of study (2002-001 to 2002-208) and 28 were recorded by ARCES. All of these resulted in ARCES detections which passed the first three tests, and 25 of them could be located using HYPOSAT. For the three events which could not be located, this was due to the contamination of the secondary phases with P-phases from secondary events. 19 of the true event hypotheses were the result of events not explicitly reported by KRSC, although 16 of these were secondary events occurring within 3 minutes of a confirmed event. A total of 38 events could be located.

6.2.4 Event location

Locations were determined using HYPOSAT and the 'barey' velocity model. In addition to a variability in the azimuth and differential travel times obtained, there were systematic deviations of azimuth from the geographical azimuth, and secondary phase arrival times from those predicted by the velocity model. Biases relative to the barey model were calculated from the 14

confirmed events which occurred in 2001 (see Table 6.2.1) and are displayed in Table 6.2.3. The events from 2001 were used in order to separate the population for which the biases are calculated from the testing population.

Phase	Á priori errors (uncorrected)		Travel-time biases relative to 'barey' model (s)	Azimuth bias (°)	Á priori errors (with data corrected for bias)	
	Time	Azi			Time	Azi
Pn	0.25	1.7	-	0.193	0.25	1.6
Sn	1.0	4.2	0.083	3.146	1.0	3.2
Lg	1.2	3.4	-2.549	1.425	1.0	3.2

Table 6.2.3. HYPOSAT Parameters

As we did not have absolute origin time information available, we had to use the time differences between the different phases to estimate the travel-time biases relative to the 'barey' model. Pn was set to have no bias. Based on the observed variation in relative travel-time and azimuth estimates of the 2001 events, the á priori estimates of errors of the HYPOSAT input data were set conservatively as listed in Table 6.2.3.

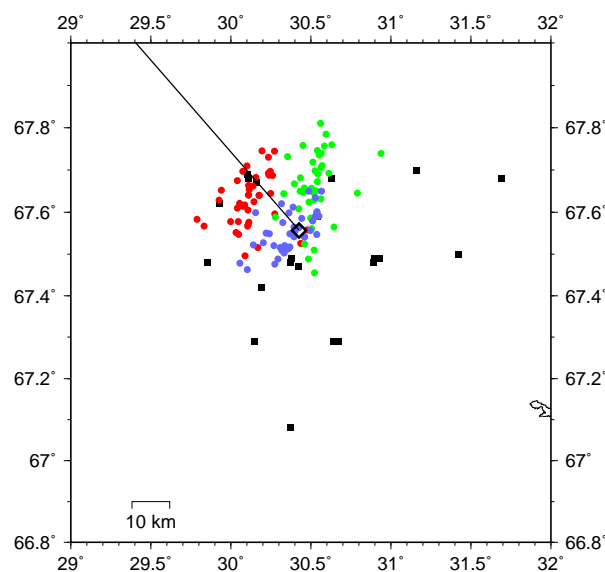


*Fig. 6.2.7. Different types of event locations for Kovdor events.
 Black diamond: Kovdor mine
 Black line: Azimuthal line from the Kovdor mine to ARCES.
 Red: One-array locations without travel-time and azimuth corrections.
 Blue: One-array locations with travel-time and azimuth corrections.
 Green: Manually (analyst) reviewed network locations.
 Black: Automatic network locations (GBF method).*

The event locations are displayed in Figure 6.2.7 and the statistics of these locations are given in Table 6.2.4.

Location type	Number of events	Location difference (km)			
		90%	95%	Median	Maximum
Automatic network locations (GBF method)	36	32.1	42.9	20.3	102.7
ARCES one-array locations without bias corrections	38	22.7	23.3	16.6	27.3
ARCES one-array locations with bias corrections	38	12.0	12.8	5.8	18.0
Analyst reviewed network locations ^a	40	21.7	24.3	11.0	28.9

a. Note that the manual locations did not apply any bias corrections.

Table 6.2.4. Statistics of event locations relative to the Kovdor mine.

6.2.5 Conclusions

We have developed a stepwise, fully automatic algorithm for identifying, processing, and locating events from the Kovdor mine, using only data from the ARCES array. Using results from the analysis of confirmed Kovdor events, we have developed a set of criteria to help determine whether or not detections from ARCES result from events at Kovdor. A detection is considered very likely to result from a Kovdor event if it passes the following three tests:-

1. The automatic ARCES detection list gives velocity and azimuth values within appropriate ranges, determined from confirmed Kovdor events.
2. Velocity and azimuth values obtained from a fixed frequency band fk-analysis are consistent with a Pn-arrival from a Kovdor event.
3. There is evidence of a secondary phase (appropriate velocity and azimuth from fixed frequency band fk-analysis within a time window at a fixed delay after the first P-arrival).

The automatic process was run on ARCES data from January 1, 2002, to July 27, 2002.

- A total of 6176 detections passed test 1.
- 72 detections were still considered likely candidates after test 2.
- 48 detections were still considered likely following test 3, of which only one was found to correspond to an event located at a different site.
- All of the events confirmed by KRSC to have originated at Kovdor were successfully identified by these three tests.

Of the events which are successfully identified as likely Kovdor candidates, those satisfying a fourth condition - that at least one secondary phase has been assigned a satisfactory arrival time - may be located within the automatic process. A total of 38 events were located in this way with an error comparable to that of the manually reviewed network locations.

References

- Akaike, H. (1974): Markovian representation of stochastic processes and its application to the analysis of autoregressive moving average processes. *Ann. Inst. Stat. Math.* **26**, 363-387.
- Fyen, J. (1989): Event processor program package. In NORSAR Semiannual Technical Summary. 1 Oct 1988 - 31 Mar 1989. Scientific Report **2-88/89**. Kjeller, Norway.
- Fyen, J. (2001): NORSAR seismic data processing - user guide and command reference. NORSAR (contribution 731) Kjeller, Norway.
- GSE/JAPAN/40 (1992): A Fully Automated Method for Determining the Arrival Times of Seismic Waves and its Application to an on-line Processing System
- Kremenetskaya, E., Asming, V. and Ringdal, F. (2001): Seismic Location calibration of the European Arctic. *Pure appl. geophys.* **158**, 117-128.
- Kværna, T. (1995): Automatic onset time estimation based on autoregressive processing. Semiannual Technical Summary, 1 April - 30 September 1995, NORSAR Sci. Rep. No. 1 95/96, Kjeller, Norway.
- Kværna, T., Schweitzer, J., Taylor, L. and Ringdal, F. (1999): Monitoring of the European Arctic using Regional Generalized Beamforming. In: NORSAR Semiannual Tech. Summ. 1 October 1998 - 31 March 1999, NORSAR Sci. Rep. 2-98/99, Kjeller, Norway, 78-94.
- Schweitzer, J. (2001): HYPOSAT - An Enhanced Routine to Locate Seismic Events. *Pure appl. geophys.* **158**, 277-289.
- Schweitzer, J. and Kennett, B. L. N. (2002): Comparison of location procedures - The Kara Sea event of 16 August 1997. In: NORSAR Semiannual Tech. Summ. 1 July - 31 December 2001, NORSAR Sci. Rep. **1-2002**, Kjeller, Norway, 97-103.

S. J. Gibbons

T. Kværna

F. Ringdal

6.3 Site-specific GBF monitoring of the Novaya Zemlya test site

Introduction

In the two preceding NORSAR Semiannual Technical Summaries we have reported on our developments concerned with monitoring the Lop Nor test site in China (Lindholm et. al., 2002; Kværna et. al., 2002a). Using data from the global arrays and single stations having the best detection capability for the area, we have developed and tested both an optimized site-specific threshold monitoring (SSTM) and a site-specific Generalized Beamforming (SSGBF) system for the Lop Nor test site.

For the former test site on Novaya Zemlya (NZ), a continuous seismic threshold monitoring scheme has been operational at NORSAR for several years. A comprehensive description and discussion of this processing is given by Kværna et. al., 2002b. In order to improve the experimental monitoring capability, we have now also developed a site-specific Generalized Beamforming (SSGBF) for the NZ test site.

Development of site-specific GBF

The Generalized Beamforming (GBF) technique, originally developed by Ringdal and Kværna (1989), is now widely accepted as the most efficient method for associating seismic phases from a global or regional network. In a typical implementation, a large number of generalized “beams” are steered to the points in a global or regional grid. An automatic detector is applied to each station or array in the network, and a set of “box-car” or “triangular” functions is generated for each station, such that the non-zero parts of these functions correspond to a time interval around a detection. By summing these functions with appropriate weights and with time delays corresponding to the particular phase-station-grid point combination, one obtains a “beam” that may then be subjected to a detector algorithm.

A common feature of such implementations is the need to group the large number of individual beam “detections” in order to eliminate side-lobes and associate the detection group with an event at the correct hypocenter. This grouping, which can become quite complex, is clearly unavoidable when a large geographical region is to be monitored. However, if one is monitoring a particular site, such as a suspected nuclear test site, it is possible to simplify this procedure considerably, and at the same time optimize the parameter settings to ensure the best possible detection probability for the target site. This idea was first tested by Ringdal and Kværna (1993) to monitor the aftershocks of a large earthquake sequence occurring in Western Caucasus during the GSETT-2 experiment. They concluded that the approach showed a superior performance compared with the association procedures being employed at the four experimental international data centers operating during GSETT-2. In the present paper we elaborate further on this site-specific GBF (SSGBF) approach to monitoring the Novaya Zemlya test site.

Array network and analysis procedure

The 4-array network displayed in Fig. 6.3.1 has been shown to provide a monitoring capability for the NZ test site down to m_b 2.0 for most time intervals (Kværna et. al., 2002b). Similarly, we have in the implementation of the SSGBF processing used the same 4-array network, and the processing parameters have been derived from the same events in the Novaya Zemlya region as have been used for the tuning of the SSTM process (Kværna et. al., 2002b). Table 6.3.1 summarizes the station and phase information and also lists the range of the azimuth and

slowness parameters used for forming the beam towards the test site. The limits on arrival time tolerances are not defined in Table 6.3.1, since these tolerances are to a large extent dependent on the desired sharpness of the generalized beam. We have used the formula:

$$dT = S \cdot R$$

where dT is the time tolerance in seconds, R is the desired beam radius in km and S is the P-phase slowness (in s/km) corresponding to the distance from the target site to the station being processed. We have chosen to use fairly large tolerances, to ensure that there is only a small probability of missing real detections corresponding to an event at the site. Specifically, for NZ we used a radius of 100 km. The expected Pn-wave phase velocity at ARCES and SPITS is about 8 km/s, so the assumed range of the time tolerance is approximately +/- 12 seconds.

The beamforming procedure follows the GBF standard, except that only one generalized beam is formed in the site-specific case. The main steps are:

- Applying an automatic detector at each of the stations/arrays in the network
- Summing “boxcar” or “triangular” weight functions representing the detector outputs with the appropriate restrictions on travel time, azimuth and slowness
- Applying a thresholding procedure on the resulting generalized beam

We have used “triangular” functions centered at the expected arrival time for the beamforming in our NZ analysis. Experiments have shown that the effect of sidelobes is reduced compared with when using “boxcar” functions, while still retaining high sensitivity for detecting events in the target area.

Example 1: 23 February 2002

Our first example, shown in the left part of Fig. 6.3.2, is the day 23 February 2002. At 01:21:12.1 GMT on that day there was an event with a magnitude of about 3.2, located about 100 km north-east of the former nuclear test site. The SSGBF traces for each phase considered are shown, together with the network trace on top. The peaks of the panels for each phase represent detections that fall within the NZ azimuth and slowness ranges given in Table 6.3.1. To align the detections we have subtracted the phase travel-time from NZ to the respective arrays. The network trace on top is calculated by adding “triangular” functions surrounding each detection, using the six phases given in Table 6.3.1.

Alerts (red diamonds) are declared when the network trace (the full network) has a value of at least 2. To obtain a value of 2 using “triangular” weight functions, we would need at least two matching phases with perfect time fit. However, but more realistically, three matching detections would be required. From the SSGBF traces of Fig. 6.3.2 we find that during 23 February 2002 there is only one event trigger. By summing the “triangular” weight functions of the six detected phases, we obtained a network SSGBF value of about 4.7 for the NZ event.

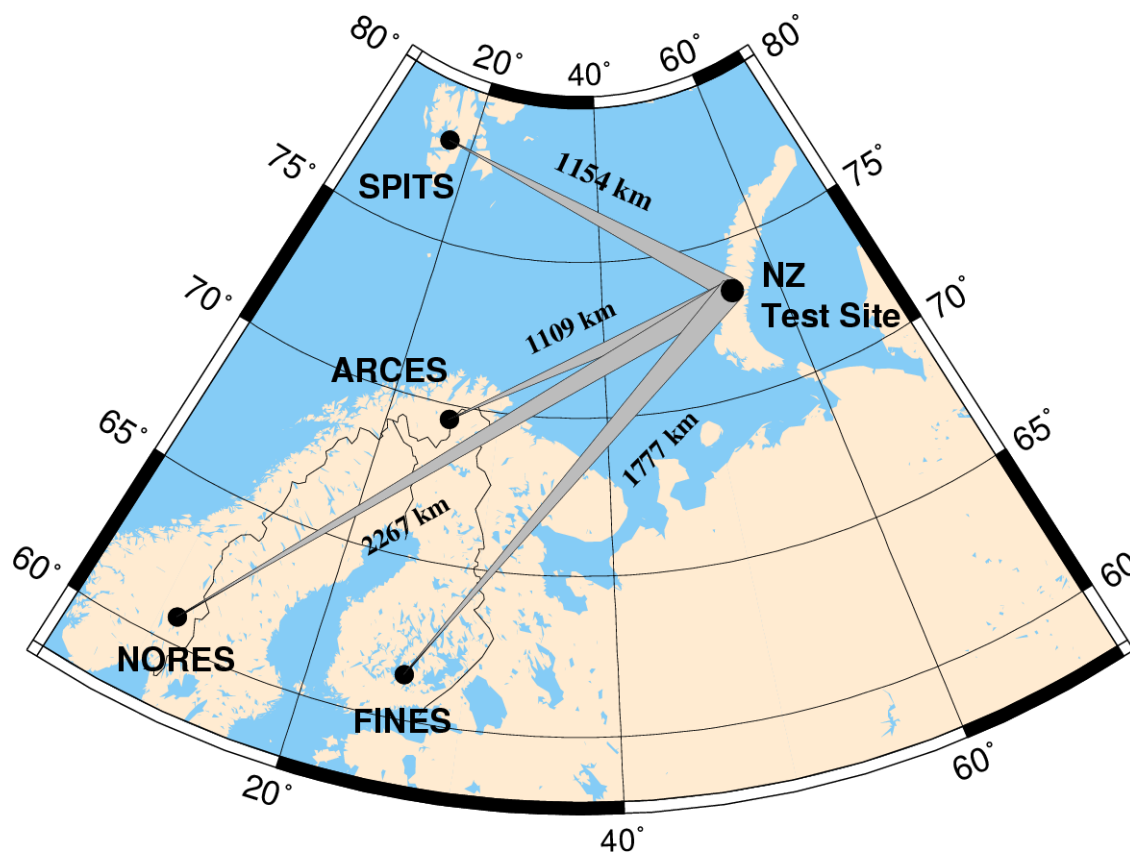


Fig. 6.3.1. Map showing the arrays used for both site-specific Threshold Monitoring and site-specific Generalized Beamforming of the former Novaya Zemlya test site.

Table 6.3.1. The stations used for Site-Specific Generalized Beamforming processing of the former Novaya Zemlya test site. In order for a signal detection to be used as a candidate for an event at the NZ test site, its azimuth and slowness estimates have to be within the ranges given in the table.

Station	Type	Phase	Distance (km)	Travel time (s)	Azimuth Range (deg)	Slowness Range (sec/deg)
ARCES	Array	Pn	1108.6	147.5	47.2-77.2	10.6-17.1
ARCES	Array	Sn	1108.6	254.2	49.3-79.3	19.8-31.8
SPITS	Array	Pn	1154.2	152.6	77.6-227.6	10.6-17.1
SPITS	Array	Sn	1154.2	263.0	77.6-227.6	19.9-34.8
FINES	Array	P	1776.9	224.2	11.6-47.6	10.6-14.8
NORES	Array	P	2267.3	281.4	18.6-48.6	9.3-14.3

For comparison, the corresponding SSTM traces are shown in the right part of Fig. 6.3.2. From the SSTM traces we see that the magnitude threshold is below mb 2.0 for most of the day except for a few time intervals, including the NZ event at 01:21:12.1 GMT.

SSGBF and SSTM traces for a one-hour interval surrounding the NZ event is shown in Fig. 6.3.3.

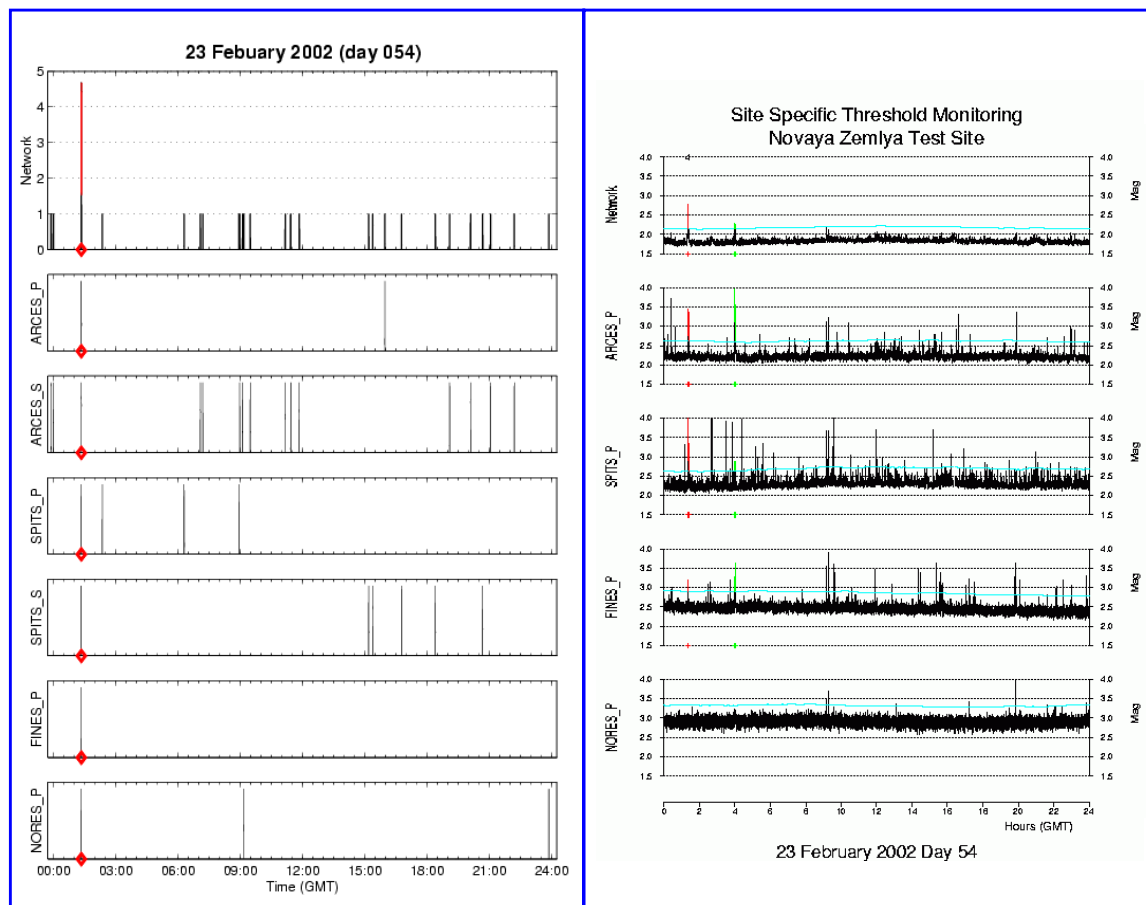


Fig. 6.3.2. SSGBF traces for 23 February 2002 are shown in the left part of the figure. The peaks of the panels for each phase represent detections that fall within the NZ azimuth and slowness ranges given in Table 6.3.1. To align the detections we have subtracted the phase travel-time from NZ to the respective arrays. The network trace on top is calculated by adding “triangular” functions surrounding each detection, using the six phases given in Table 6.3.1. Alerts (red diamonds) are declared when the network trace (the full network) has a value of at least two. The corresponding SSTM traces are shown in the right part of the figure. For detailed information on SSTM we refer to Kværna et. al., 2002b.

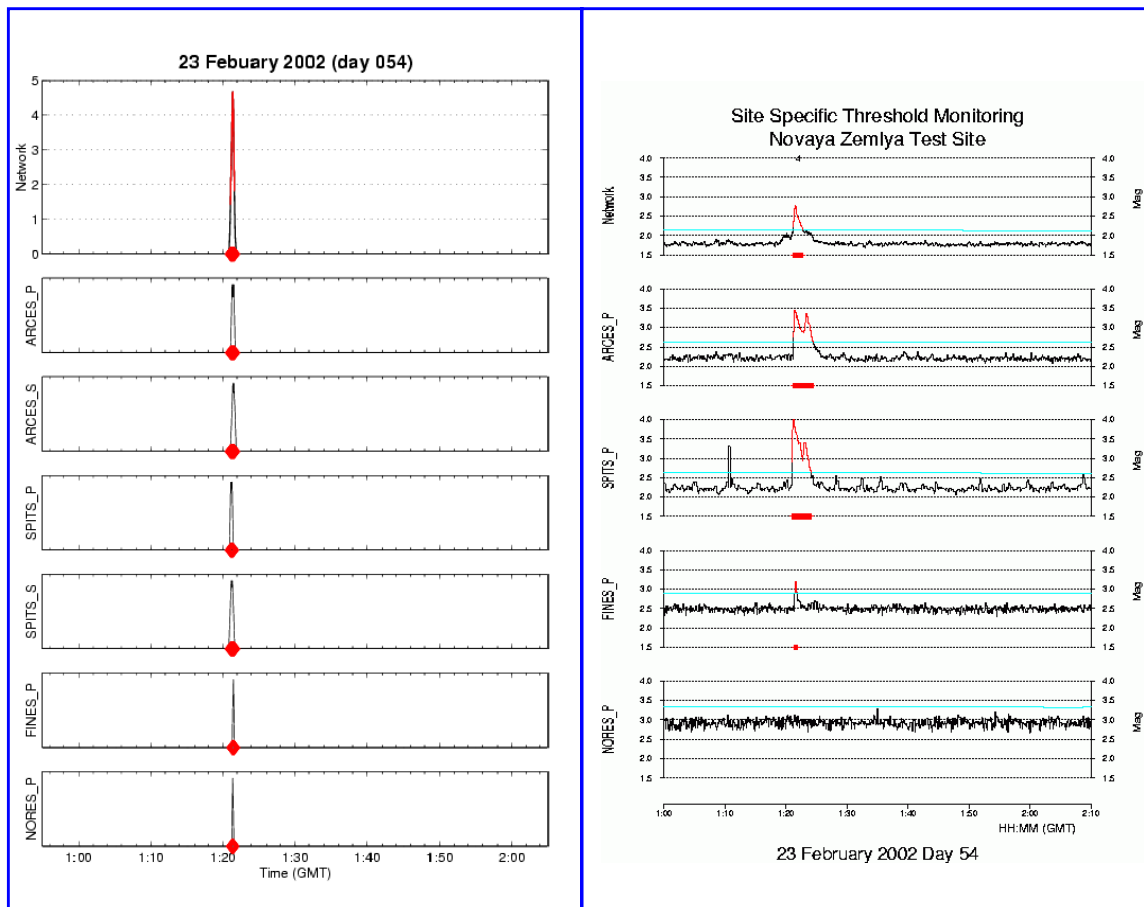


Fig. 6.3.3. SSGBF and SSTM for 23 February 2002, 01:00 - 02:00 GMT. See Fig. 6.3.2 for details. Notice the triangular shape of the SSGBF weight functions.

Example 2: 11 January 2002

For most days the SSGBF plots have no triggers, like for 11 January 2002, shown in Fig. 6.3.4. For the two-month time period January-February 2002, there were only two additional instances where alerts were declared, i.e., when the network trace (the full network) has a value of at least 2. Both these alerts were false alarms that could be ruled out as being NZ events by analyzing the corresponding array data. We have also experimented with lower alert thresholds, which of course provided higher false alarm rates. For example an alert threshold of 1.7 provided 10 false alarms during January and February 2002

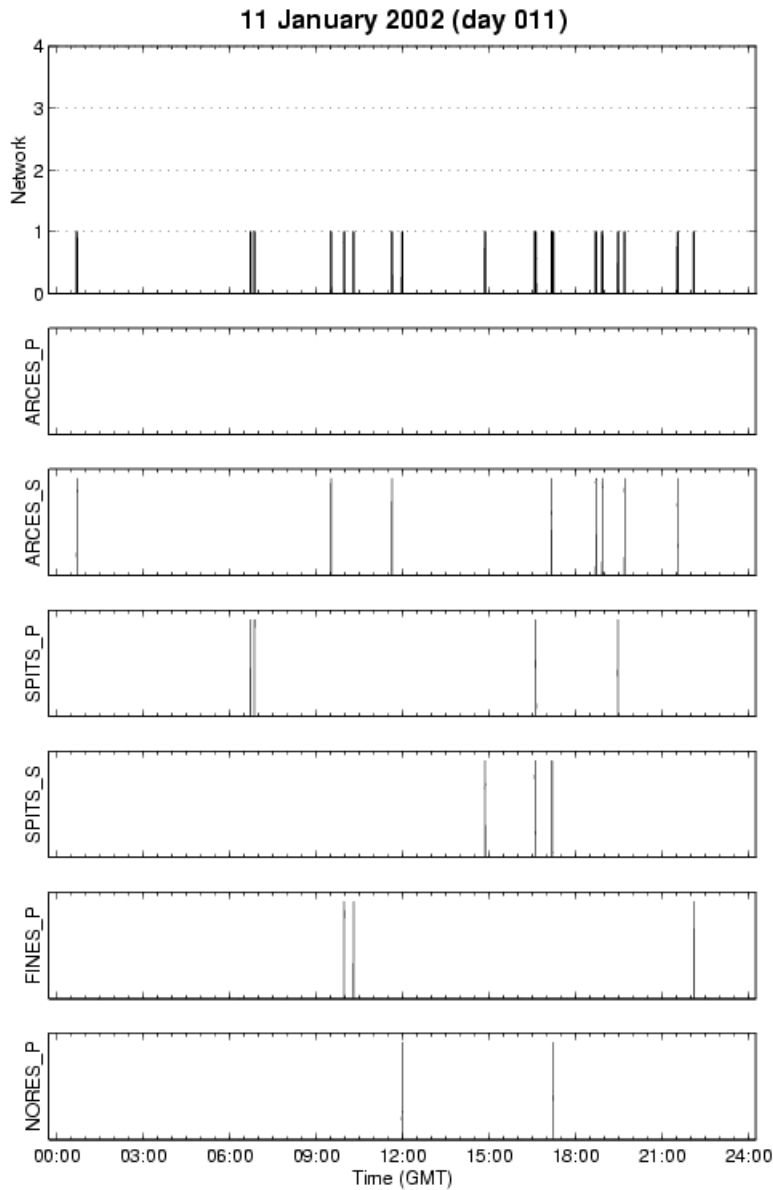


Fig. 6.3.4. SSGBF traces for 11 January 2002. See Fig.6.3.2 for details

Regional GBF processing for the Barents Sea region

In order to investigate the sensitivity of the SSGBF approach for monitoring, we have developed a regional implementation of the method covering the Barents Sea region. The grid system, having a spacing of about 28 km, is shown in Fig. 6.3.5. The ‘barey’ travel-time model of Schweitzer and Kennett (2002) was used for predicting the P- and S-phase arrival times and slownesses at the four arrays ARCES, SPITS, FINES and NORES. For FINES and NORES

only P-type phases are considered, whereas for ARCES and SPITS we use Pn and Sn. Azimuth tolerances of ± 30 degrees and a slowness tolerance of ± 4 sec/degree around the predicted slowness are applied. The time tolerances, calculated from the grid spacing, were about ± 3 seconds for Pn and about ± 5 seconds for Sn.

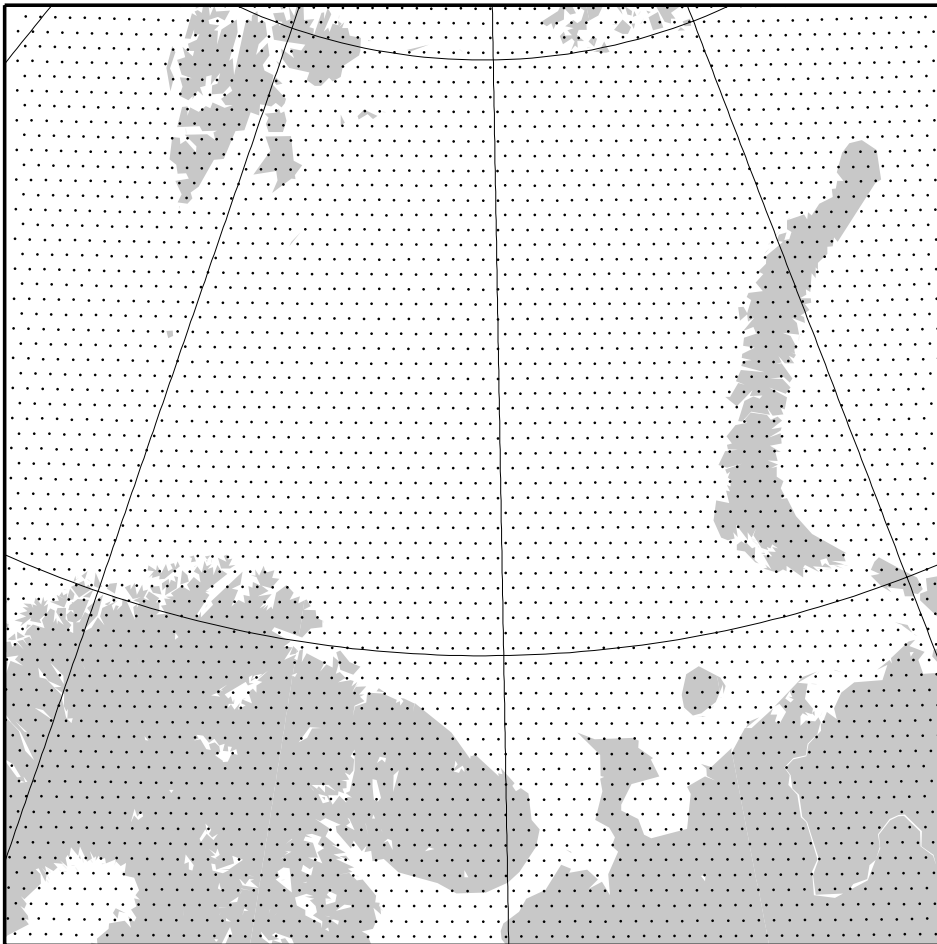


Fig. 6.3.5. Regional GBF grid system covering the Barents Sea Region, having a grid spacing of about 28 km.

An illustration of the regional GBF results for 23 February 2002 is given in Fig. 6.3.6. The upper trace shows the time-wise maxima of the network GBF traces for all targets of the grid system. Notice that there are several instances where the network GBF values exceed the alert threshold of 2 used for the SSGBF of the NZ test site. The color coding of the map below represents the point-wise maxima of the network GBF traces during the 24 hour time interval. Notice the high values on Novaya Zemlya, on the Kola Peninsula and in Northern Sweden, all corresponding to seismic events in these regions. See Fig. 6.3.2 for a comparison with SSGBF and SSTM.

Regional GBF results for the one-hour time interval 01:00 - 02:00 on 23 February 2002 are shown in Fig. 6.3.7. During this time interval there was only one event, located in the vicinity

of Novaya Zemlya, such that the areal extent of the topmost part of the GBF peak reflects the sensitivity of the SSGBF method with respect to events in the NZ region.

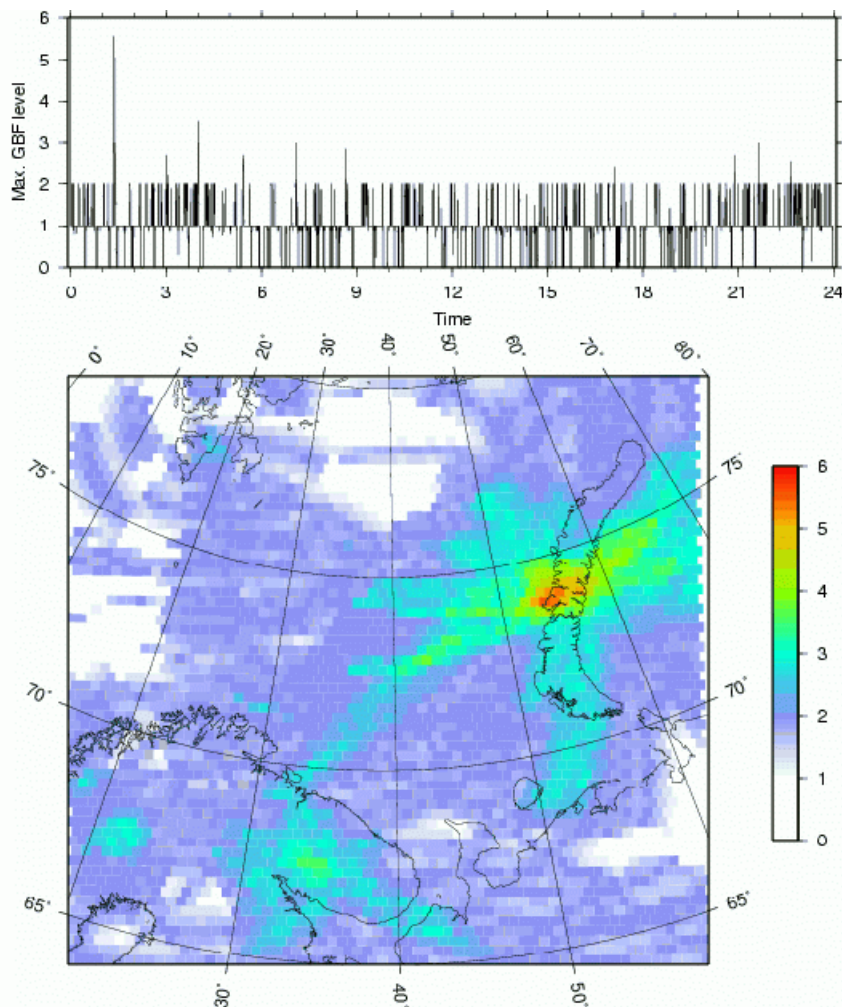


Fig. 6.3.6. Regional GBF results for 23 February 2002. The upper trace shows time-wise maximum of the network GBF traces for all targets of the grid system. The map below represents the point-wise maxima of the network GBF traces during the 24 hour time period. Triangular weight functions are used.

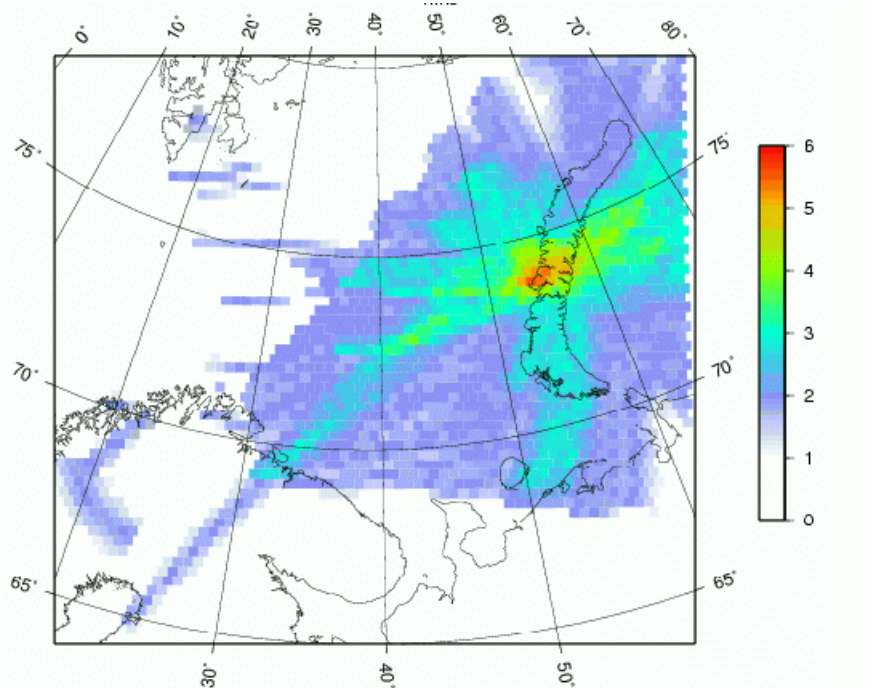


Fig. 6.3.7. Regional GBF results for 23 February 2002, 01:00-02:00 GMT. See Fig. 6.3.3 for comparison with the SSGBF and SSTM results.

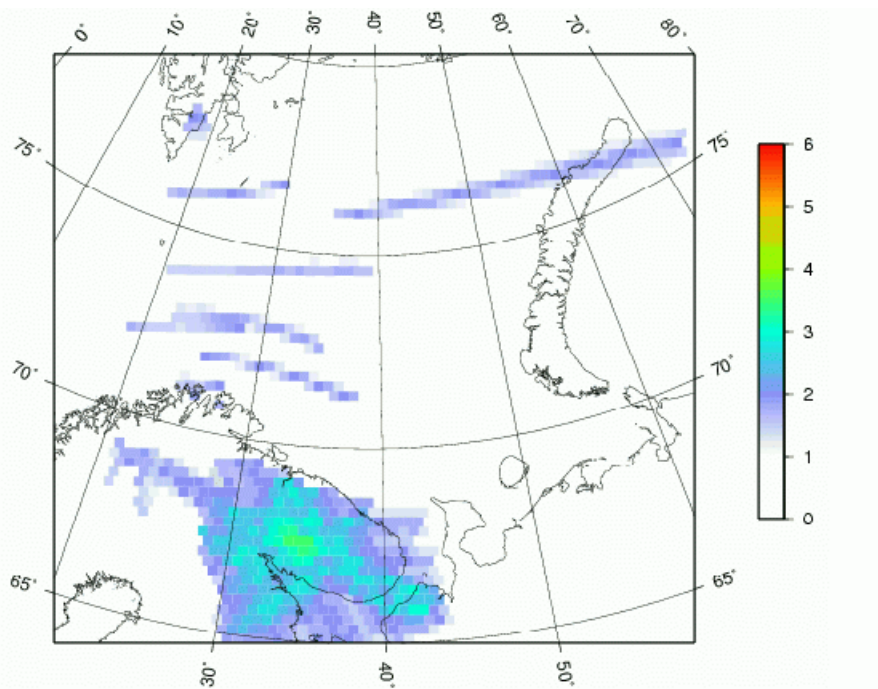


Fig. 6.3.8. Regional GBF results for the one-hour time interval 04:00-05:00 GMT on 23 February 2002. At 04:00:37 there was an 76 ton underground explosion in one of the mines in the Khibiny Massif on Kola.

Regional GBF results for the one-hour time interval 04:00 - 05:00 on 23 February 2002 are shown in Fig. 6.3.8. During this time interval there was one event occurring in the Khibiny Massif on the Kola peninsula. As seen from the figure, there is an area of at least 100x100 km for which the network GBF levels are very close to the peak value.

As a final example we show in Fig. 6.3.9 the regional GBF results for 11 January 2002. As seen from Fig. 6.3.4 there were no SSGBF alerts for the NZ test site during this day. This is also seen on the regional GBF map where there are no indications of increased levels near NZ. The peak are south of Svalbard correspond to signals from a magnitude 3 earthquake at 17:14 GMT.

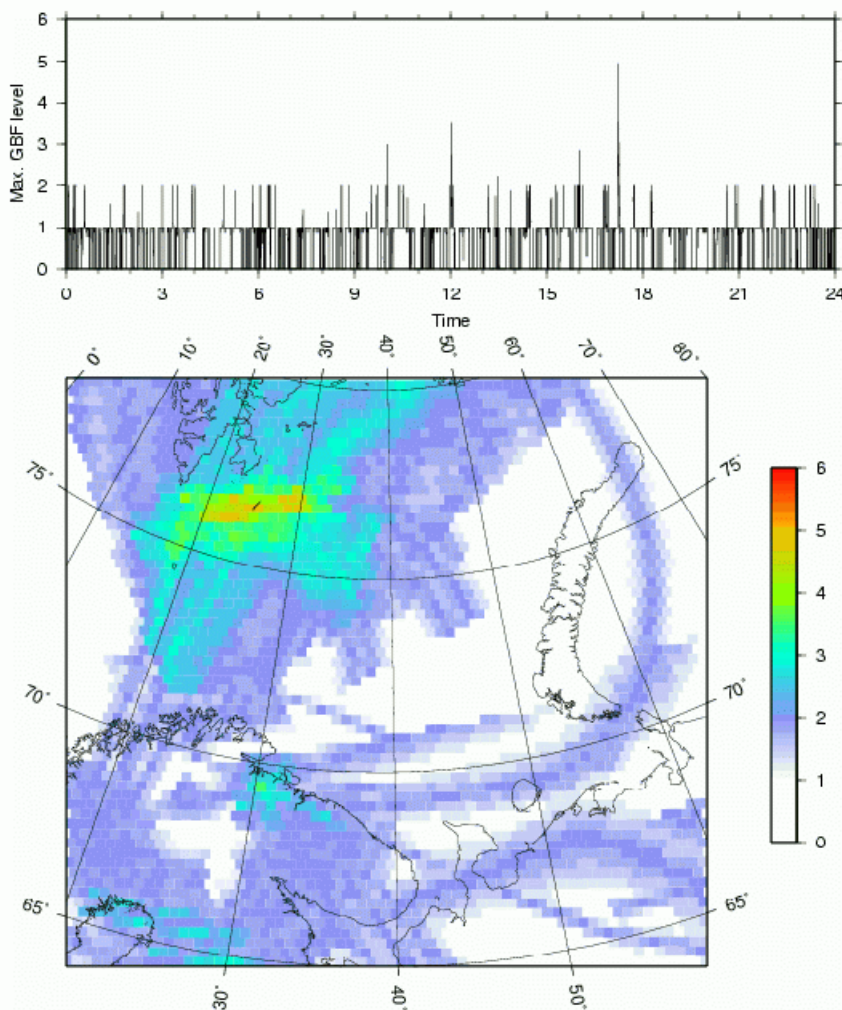


Fig. 6.3.9. Regional GBF results for 11 January 2002. The main peak area is caused by a magnitude 3 earthquake south of Svalbard at 17:14 GMT.

Conclusions

The combination of the SSTM and the SSGBF methods has been shown to provide a very convenient tool for day-to-day monitoring of the Novaya Zemlya test site. The SSTM technique has as its main strength the ability to display the real seismic field, regardless of “station detector performance”. On the other hand, the SSGBF technique takes advantage of the individual station detector outputs, and uses this combined information to narrow down the number of possible candidates for events in the target area.

These two monitoring tools have now been running in parallel on a daily basis at NORSAR since the beginning of 2002, and calendars with standard displays are made available via a Web application. Based on the accumulated processing results we plan to investigate the threshold settings for declaring alerts, false alarm rates, and possibly also the introduction of more sensitive detectors aimed at capturing signals from the Novaya Zemlya Region.

A regional GBF implementation has also been made for the Barents Sea Region, and the graphical output from this processing provides a visual overview of major events in the region. The spatial and temporal pattern from the regional GBF provides information on the resolution of a site-specific GBF, e.g., steered towards the Novaya Zemlya test site. We find that using the four-array network ARCES, SPITS, FINES and NORES, all events within 100 km of the test site are efficiently captured by the site-specific approach. If larger areas are to be monitored, site-specific GBF distributed with a spacing of 100 - 150 km would be preferable.

We finally provide some comments on the selection of station networks for optimized site-specific monitoring. In this regard, there is a fundamental difference between the SSGBF and the SSTM procedures. With SSGBF, it is very important to include only those stations with the best monitoring capability for the target site. Including additional, poorer, stations in the network will cause no increase in the monitoring capability, but may well cause a significant increase in the number of false alarms. On the other hand, for SSTM, inclusion of such additional, poorer stations will cause no significant change in the monitoring results.

In this paper, we have used the same four-array network for SSGBF and SSTM of the Novaya Zemlya test site. Since two of the arrays (ARCES and SPITS) have significantly better capability than the other two, it would be interesting to consider only these two “best” arrays in the SSGBF procedure. This might contribute to an even lower false alarm rate than seen for the current process (2 false alarms during two months, given a GBF threshold of 2.0). Admittedly, if one (or both) of these arrays are inoperational, the inclusion of additional arrays would indeed be important, so the picture is not clear-cut. Nevertheless, the idea of reducing the array coverage and assessing the impact on the false alarm rate should be investigated in the future. In such a scenario, the SNR thresholds for the individual array detection processing as well as the GBF threshold could be reduced to increase the sensitivity while maintaining an acceptable false alarm rate.

References

- Hicks, E.C., Kværna, T., Mykkeltveit, S., Schweitzer, J. and Ringdal, F. (in press), Travel-times and attenuation relations for regional phases in the Barents Sea region, *Pure and Applied Geophysics*, in press.
- Ringdal, F. and T. Kværna (1993): Generalized Beamforming as a tool in IDC processing of large earthquake sequences, *Semiannual Technical Summary, 1 April - 30 September 1993*, NORSAR Sci. Rep. 1-93/94, Norway.
- Kværna, T., E. Hicks and F. Ringdal (2002a): Site-Specific Generalized Beamforming (SSGBF) applied to the Lop Nor test site. *Semiannual Technical Summary 1 January - 30 June 2002*, NORSAR Sci. Rep. 2-2002, Kjeller, Norway.
- Kværna, T., F. Ringdal, J. Schweitzer, and L. Taylor (2002b): Optimized Seismic Threshold Monitoring – Part 1: Regional Processing. *Pure Appl. Geophys.*, **159**, 969-987.
- Lindholm, C., T. Kværna and J. Schweitzer(2002): Site-Specific Threshold Monitoring (SSTM) applied to the Lop Nor test site. *Semiannual Technical Summary 1 July - 31 December 2001*, NORSAR Sci. Rep. 1-2002, Kjeller, Norway.
- Ringdal, F. and T. Kværna (1989). A multichannel processing approach to real time network detection, phase association and threshold monitoring, *Bull. Seism. Soc. Am.*, **79**, 1927-1940.
- Schweitzer, J., and Kennett, B.L.N. (2002), Comparison of location procedures - the Kara Sea event 16 August 1997, *Semiannual Technical Summary, 1 July - 31 December 2001*, NORSAR Sci. Rep. 2-2001/2002, Kjeller, Norway.

T. Kværna

E. Hicks

F. Ringdal

6.4 Analysis of infrasound data recorded at the Apatity array

6.4.1 Introduction

Kola Regional Seismological Centre (KRSC) of the Russian Academy of Sciences has for many years cooperated with NORSAR in the continuous monitoring of seismic events in North-West Russia and adjacent sea areas. This work has been based on a network of sensitive regional arrays which has been installed in northern Europe during the last decade in preparation for the global monitoring network under a comprehensive nuclear test ban treaty (CTBT).

As part of a project aimed at improving seismic and infrasound monitoring capabilities for the Arctic region, KRSC has installed a small-aperture infrasound array within the existing seismic array in Apatity. The Apatity infrasound array will in the future become an important complement to the planned infrasound array in northern Norway near the ARCES seismic array. This paper gives a brief description of the Apatity infrasound system and presents initial results from the infrasound array operation.

6.4.2 The Apatity seismic/infrasound array

Since 1996, Kola Regional Seismological Center (KRSC) has been engaged in infrasonic research and development. As part of this effort, a small-aperture microbarographic array was installed in conjunction with the seismic array near lake Imandra in the Kola Peninsula, with data digitized at the array site and transmitted in real time to a processing center in Apatity. A total of three infrasound sensors are installed in the innermost ring of the array, forming a triangle of approximately 500 m diameter. The sensors are differential microbarographs of model K-304-AM. The frequency range is 0.01-10Hz, and the sensitivity is 37.5 mV/Pa. The geometry of the combined seismic/infrasound array is shown in Fig. 6.4.1. Figure 6.4.2 shows the location of the Apatity and ARCES arrays, as well as some nearby mines from which explosion data have been analyzed in this study.

6.4.3 Data analysis

We have studied the background infrasonic noise level over extended periods (2-3 months), and have found, not unexpectedly, that the variation is considerable. During high-wind conditions the typical level is a factor of 100 (two orders of magnitude) greater than during quiet conditions. In the future, the performance during windy conditions could be improved by installation of additional noise-reducing porous hoses, and this will be considered. Figure 6.4.3 shows an example of noise (and signals) during 4 hours of "quiet" conditions. Infrasonic signals from four nearby mining explosions are clearly seen on these recordings. A combined view of the seismic and infrasound recordings from two of these explosions (both in Khibiny) are shown in Figure 6.4.4.

We have analyzed a number of infrasonic recordings of selected events in the Kola Peninsula and adjacent regions. Several large mines in this region generate explosions that are routinely detected by the seismic systems installed in northern Fennoscandia and NW Russia. Some of these explosions are also recorded by the infrasound sensors. We present analysis results from 19 such mining explosions, with a distance range from 38 to 220 km. The analysis includes frequency-wavenumber analysis of the array recordings, estimation of phase velocity and azimuth, and estimation of group velocity based on travel time calculations. We have analyzed 3-6

events from each of the following mines: Khibiny, Zapolarnyi, Kovdor and Olenegorsk (see Table 6.4.1 for details). We find that the azimuth estimates are quite stable, typically within a range of 5 degrees or less for events from the same mine. This is very satisfactory taking into account the small array aperture.

Another source of data has been a set of ammunition demolition explosions in Northern Finland, at a distance of 300 km from the array. In these cases, we have been able to identify three separate phase arrivals for each of the five analyzed events. Following the phase conventions used at the prototype IDC (Brown et. al., 2002, see also Armstrong, 1998 and Hagerty et. al., 2002), these phases are identified as the tropospheric arrival (Iw), the stratospheric arrival (Is) and the thermospheric arrival (It). An example illustrating these three phases for one of the explosions is shown in Figure 6.4.5. We note that the amplitudes of these phases are very different, and in fact (as can be seen from the table) the relative amplitudes of the phases vary also from one explosion to the next. Even the smallest phase (It) can be easily seen in an enlarged plot, as shown in Figure 6.4.6.

Figure 6.4.6 shows that the moveout of the signals are quite clear and the signal coherency is excellent. Similar features are seen for the other phases (although not shown here). As a result, reliable f-k analysis can be performed on each phase. Figure 6.4.7 illustrates the results of f-k analysis applied to the three phases for the event shown in Figure 6.4.5.

Table 6.4.2 shows details of the processing results for the entire set of Northern Finland explosions. Again, we find that the azimuth estimates from the (in this case) 15 total phases are very consistent, ranging from 278 to 288 degrees (true azimuth is 284 degrees). The observed group velocities (average travel velocities) range between 326-336 m/s for the Iw arrival, 300-305 m/s for the Is arrival and 244-254 m/s for the It arrival. The phase velocities (apparent velocities) range between 330-400 m/s, with the lowest values for the Iw phases and the highest values for the It phases. However, with this very small array (aperture only 500 m) the estimates of phase velocity are not quite stable enough to provide a confident indication of the phase type.

6.4.4 Future plans

We note that the detection of infrasonic phases is very dependent on the background atmospheric conditions, and that such phases are usually observed only during relatively quiet wind conditions. Our future plans include the installation of additional noise-reducing porous hoses to improve the detectability during windy conditions. After the projected infrasonic array in Karasjok, northern Norway, is installed, we plan to carry out joint processing of data from these two arrays. Further perspectives include cooperation with colleagues in Sweden, the Netherlands and Germany for more extensive joint processing.

An important task which we have not yet addressed is the development of an infrasonic real time signal detector. Several such detectors are available at various institutions, and we intend to build on this experience when designing the detector. Among the topics to be considered are which detection algorithm to select (e.g. Fisher detector, correlation detector, STA/LTA). We also need to find one or more filter bands for optimum processing, and define time windows for processing and f-k analysis.

The detector output will be similar to what is produced today for the seismic detectors. A phase association procedure will be implemented, attempting to associate the detected phases to seismic events detected by the regional network (Generalized Beamforming algorithm). We expect

to have a number of unassociated detections, (i.e. detections by infrasound data only), and it will be a challenging task to associate these detections so as to define new events.

Finally, it will be important to establish an interactive analysis tool and integrate the analysis with that currently done for the seismic data. Our preliminary aim is to augment the existing NORSAR regional seismic bulletin (analyst reviewed) with infrasound observations.

Yu. Vinogradov

F. Ringdal

References

- Armstrong, W.T. (1998), Comparison of infrasound correlation over different array baseline, Proc. 20th Annual Seismic Research Symposium, September 21-23, 1998.
- Brown, D.J., C.N. Katz, R. Le Bras, M.P. Flanagan, J. Wang and A.K. Gault (2002): Infrasonic Signal Detection and Source Location ant the Prototype International Data Center, PAGEOPH 159, 1081-1126
- Hagerty, M.T., Won-Young Kim and P. Martysevich (2002) Infrasound detection of large mining blasts in Kazakhstan, PAGEOPH 159, 1063-1079.

Table 6.4.1 List of 19 mining explosions from four separate mines analyzed in this study.

Location	Date 2002	Explo- sion time	Acoustic phase/arrival	Travel time, s	Dis- tance km	Gr. vel m/s	App. vel. m/s	Azi- muth, degrees	Amplitude, counts	Wind m/s	Wind dir. deg			
68.06	33.16	07.06	11.49.53	Iw/11.52.21	148	51.3	347	350	6	1200	11340	7570	4	SE 160
68.06	33.16	12.07	11.03.34	Iw/11.06.08	154	51.3	333	334	6	34100	28500	17300	1	E 90
68.08	33.38	05.06	09.45.12	Iw/09.47.59	167	55.4	332	340	15	44100	48580	42450	2	SE 150
68.08	33.38	20.06	07.53.04	Iw/07.55.45	161	55.4	344	350	18	33500	21400	15200	2	N 360
68.08	33.38	26.06	08.42.28	Iw/08.45.13	165	55.4	336	335	14	2360	1200	950	3	W 280
68.15	33.20	11.07	12.30.18	Iw/12.33.21	183	61.4	336	350	6	15580	13680	10900	1	SE 130
67.62	33.90	14.05	11.54.53	Iw/11.56.47	114	38.4	336	337	85	417**	321**	253**	3	S 180
67.62	33.90	13.07	11.33.09	Iw/11.35.00	111	38.4	346	350	86	560	580	350	2	Sw 240
67.62	33.90	19.07	11.51.26	Iw/11.53.15	109	38.4	352	354	86	5120	5200	4590	4	SE 150
67.62	33.90	11.09	11.40.17	Iw/11.42.15	118	38.4	325	341	91	9650	8700	5960	3	Nw 340
67.62	33.93	13.09	11.41.52	Iw/11.43.55	123	39.7	323	337	86	1225	940	800	2	S 170
67.62	33.90	20.09	11.52.27	Iw/11.54.22	115	38.4	334	333	90	2621	1690	1500	3	NE 30
69.40	30.69	24.04	11.27.43	Is/11.40.12	749	220.6	295	342	338	2170	1570	1632	2	SE 160
69.40	30.69	24.04	11.34.38	Is/11.47.18	760	220.6	290	334	337	2615*	1890*	1518*	2	SE 160
69.40	30.69	30.10	12.07.06	Is/12.20.14	788	220.6	280	379	334	2450	1560	1690	2	Nw 330
69.40	30.69	01.11	12.10.48	Is/12.23.27	759	220.6	290	338	336	7400	5950	5000	3	N 350
67.56	30.43	20.07	10.18.15	Iw/10.24.04	351	109	311	334	268	5120	5200	4590	4	SE 160
67.56	30.43	28.09	10.51.38	Iw/10.57.17	339	109	322	340	273	2950*	2820*	2700*	3	S 180
67.56	30.43	12.10	10.09.17	Iw/10.14.48	331	109	329	334	272	560**	515**	521**	1	Nw 300

*) - filtered in 1-4 Hz band, **) - filtered in 2-6 Hz band. Is phases are marked with green color.

Table 6.4.2 List of 5 explosions from the ammunition demolition site in northern Finland analyzed in this study. Note that three infrasonic phases have been detected for each explosion.

Location	Date	Explo- sion time	Acoustic phase/ arrival	Travel time, s	Dist. km	Gr. vel. m/s	App. vel. m/s	Azi- muth, degrees	Amplitude, counts	Wind m/s	Wind dir. deg.		
Lat.	Lon								Bar1	Bar2	Bar3		
68.00	25.96	04.09	12.59.58	Iw/13.14.46	298	336	348	281	44800	33000	38300	2	Nw 300
			s-signal	980		304	357	282	2000	1530	1850		
			t-signal	1175		254	390	286	2850	2500	2100		
68.00	25.96	05.09	13.30.00	Iw/13.44.44	298	337	360	281	4100	3600	3700	2	Sw 220
			s-signal	976		305	365	284	6350	5200	5600		
			t-signal	1190		250	404	283	1500	1250	1300		
68.00	25.96	07.09	13.00.00	Iw/13.15.15	298	326	335	279	43450	35000	39800	3	N 360
			s-signal	980		304	365	283	7000	6400	6800		
			t-signal	1220		244	399	288	1630	1310	1370		
68.00	25.96	08.09	13.30.05	Iw/13.45.02	298	332	350	281	29550	20900	23350	3	Nw 310
			s-signal	977		305	357	282	11600	8800	11100		
			t-signal	1197		248	372	286	2750	2070	2260		
68.00	25.96	09.09	12.00.02	Iw/12.14.48	298	336	343	278	13170	10680	10700	3	Sw 210
			s-signal	992		300	342	280	7350	5320	5480		
			t-signal	1184		251	364	285	670	490	470		

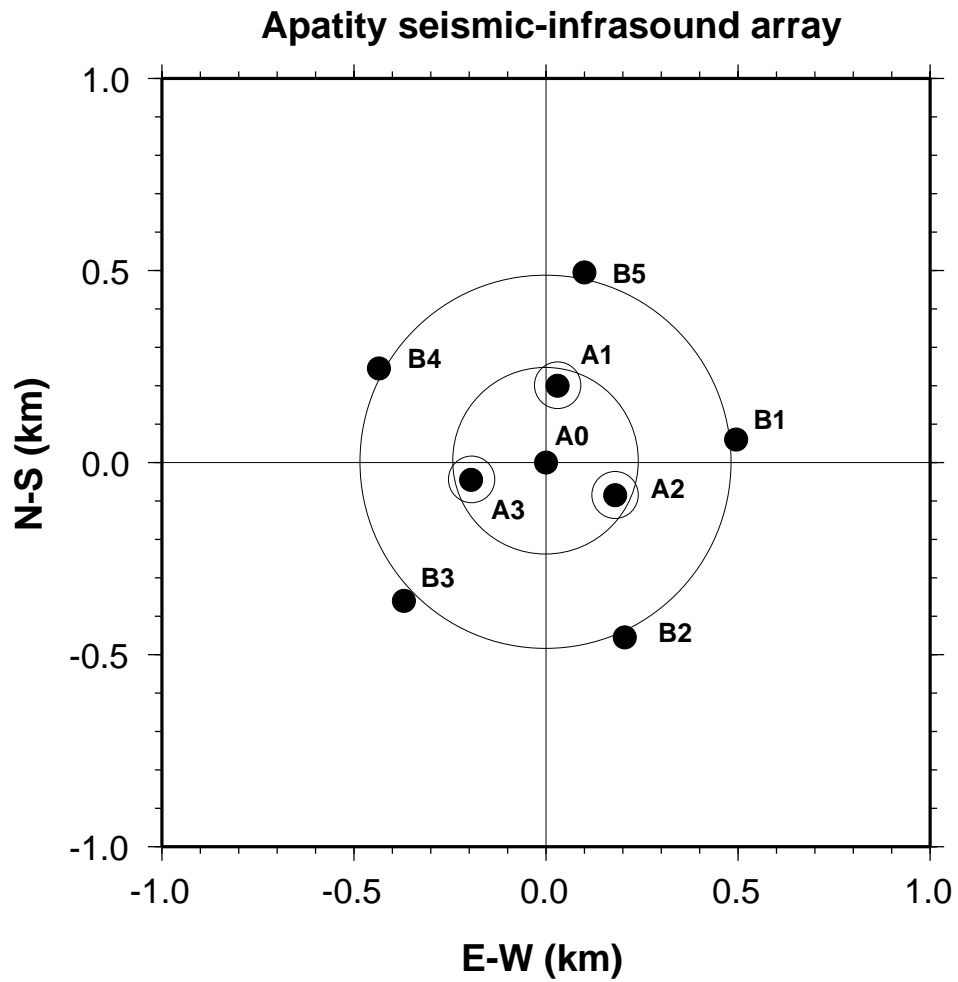


Fig. 6.4.1. Configuration of the Apatity seismic-infrasound array. Seismometers are shown as filled circles, with the location of the three infrasonic sensors (A1, A2 and A3) marked as small circles. The two concentric circles have diameter of 500m and 1000m respectively.

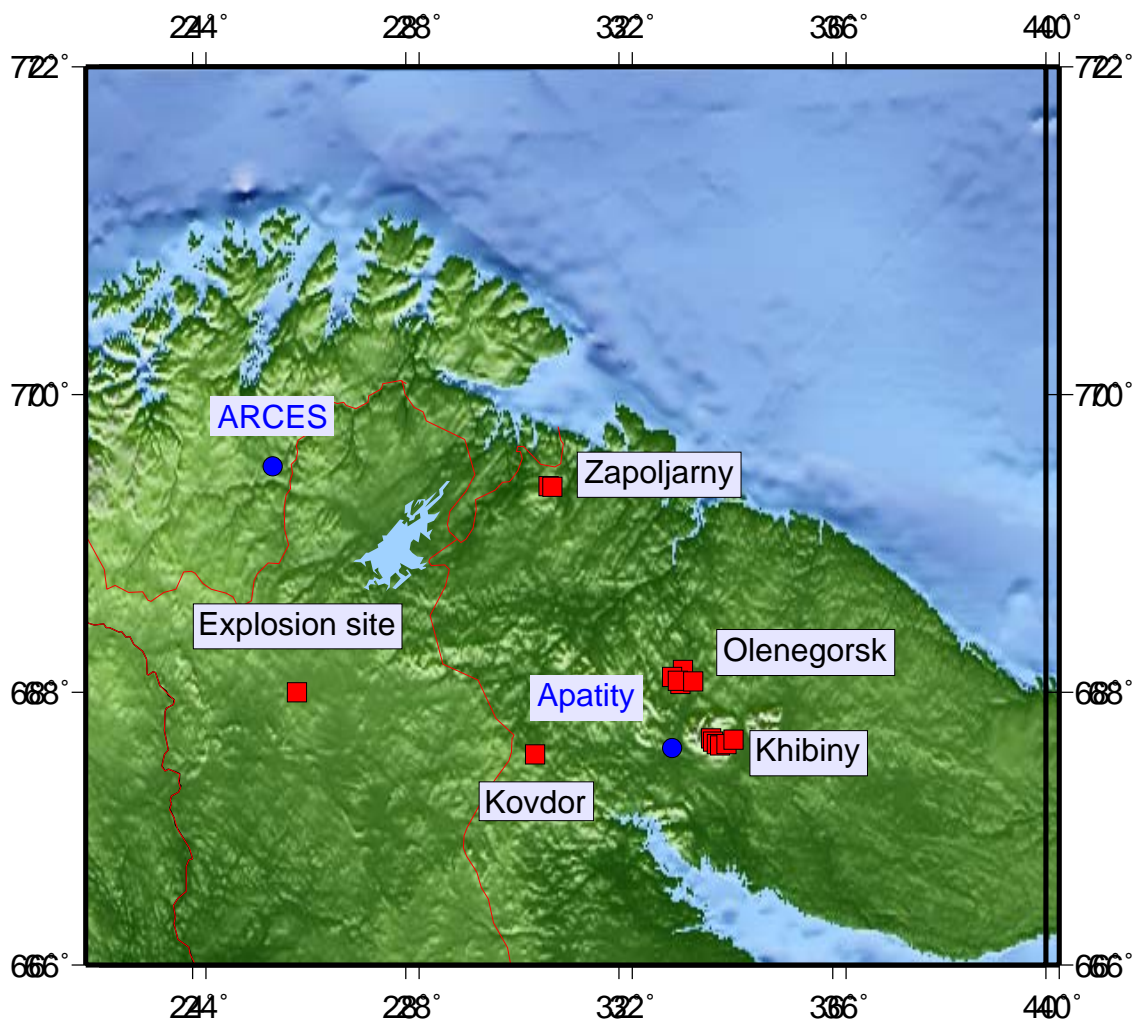


Fig. 6.4.2. Map showing the location of the Apatity and ARCES arrays (marked as blue), together with selected mines and the northern Finland site for ammunition demolition (red squares).

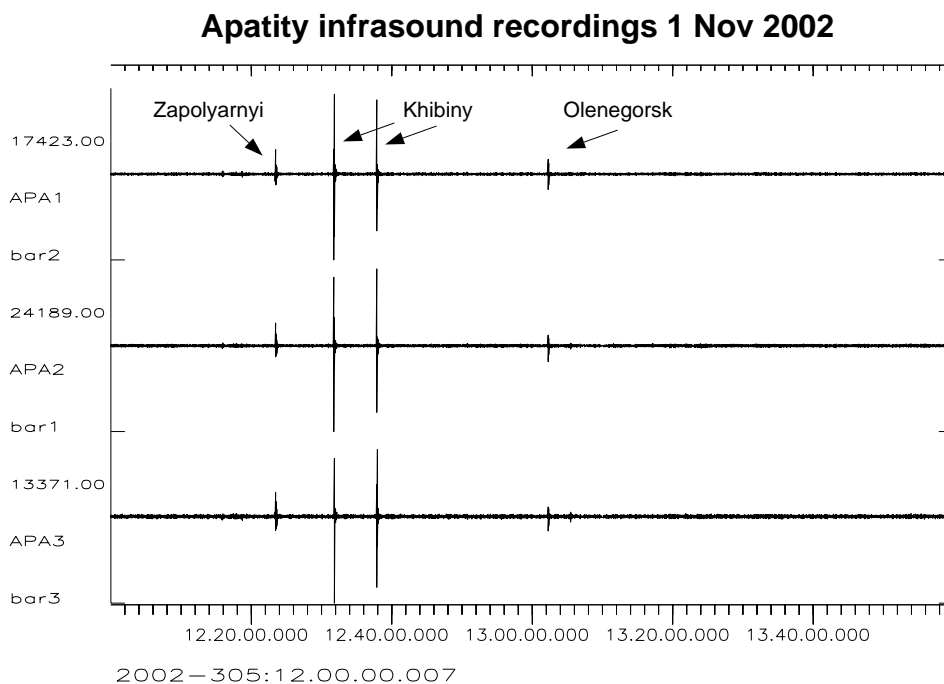


Fig. 6.4.3. Example of infrasound recordings at Apatity for a 4-hour interval on 1 November 2002. Infrasound signals from four mining explosions are marked.

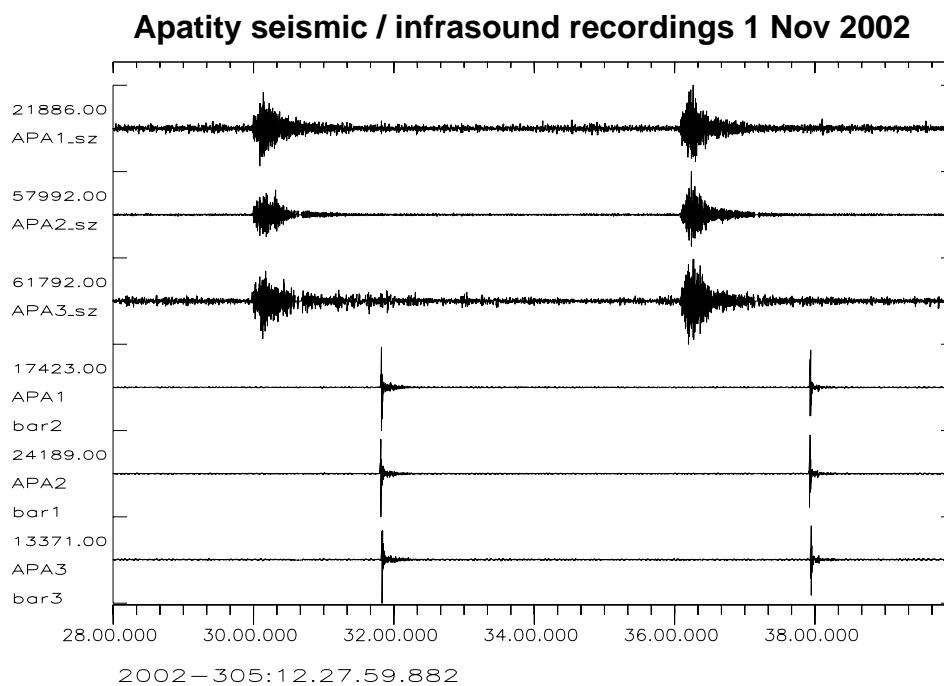


Fig. 6.4.4. Seismic and infrasound data for the two Khibiny explosions shown in Figure 6.4.3.

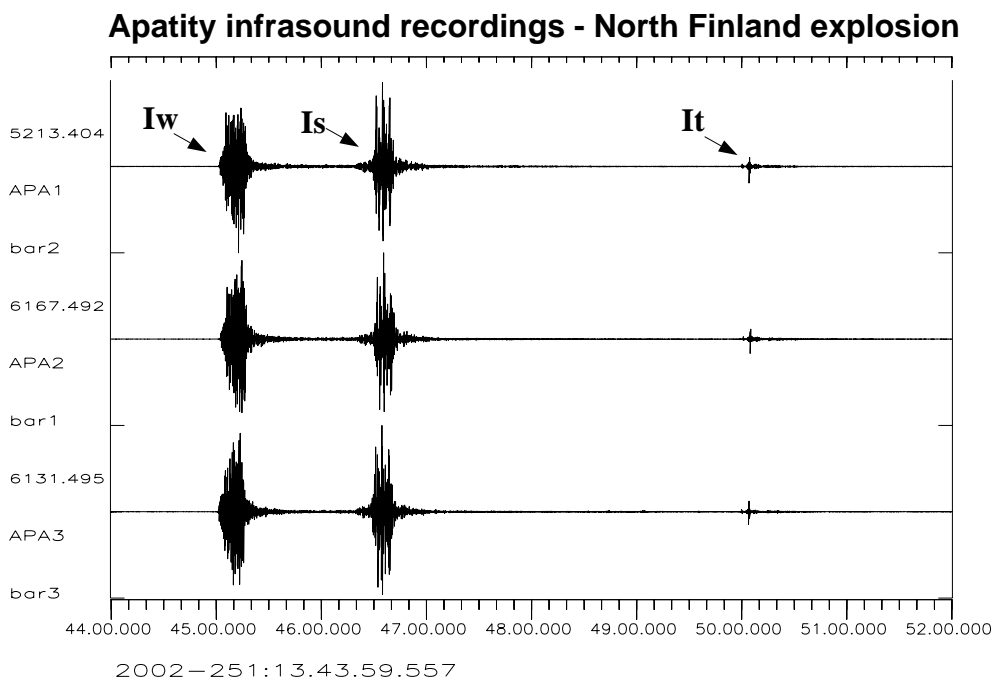


Fig. 6.4.5. *Infrasound recordings of an ammunition demolition explosion in northern Finland at 300 km distance. Data are filtered 2-6 Hz. Three distinct infrasonic phases are indicated.*

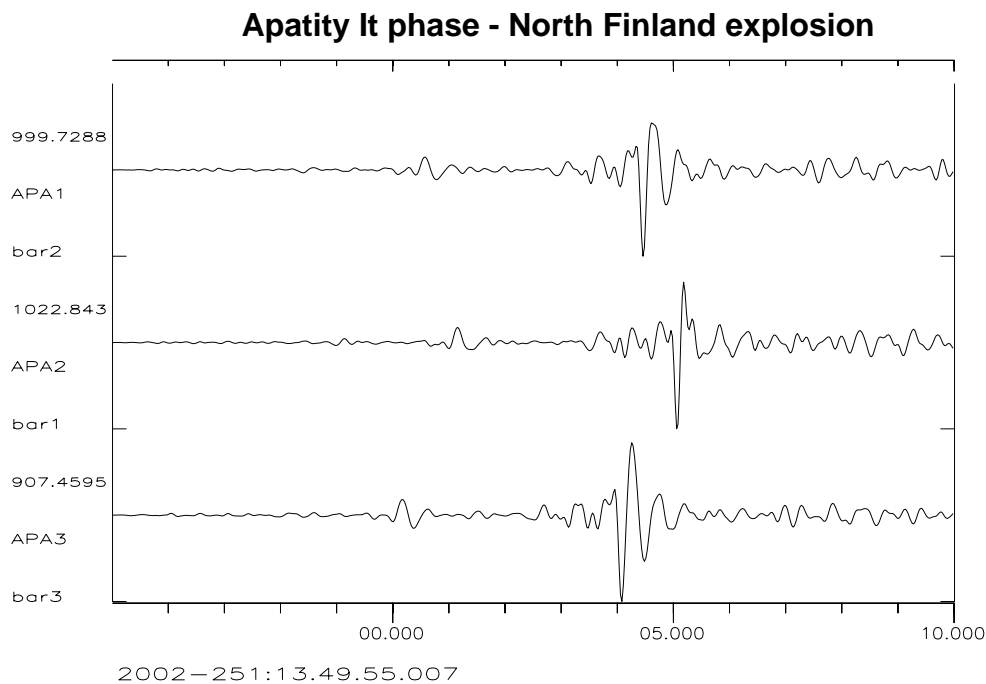


Fig. 6.4.6. *Enlarged plot of the third (It) phase shown in Figure 6.4.5. Note the clear moveout as well as the good signal coherency. The It phase appears to have two distinct arrivals.*

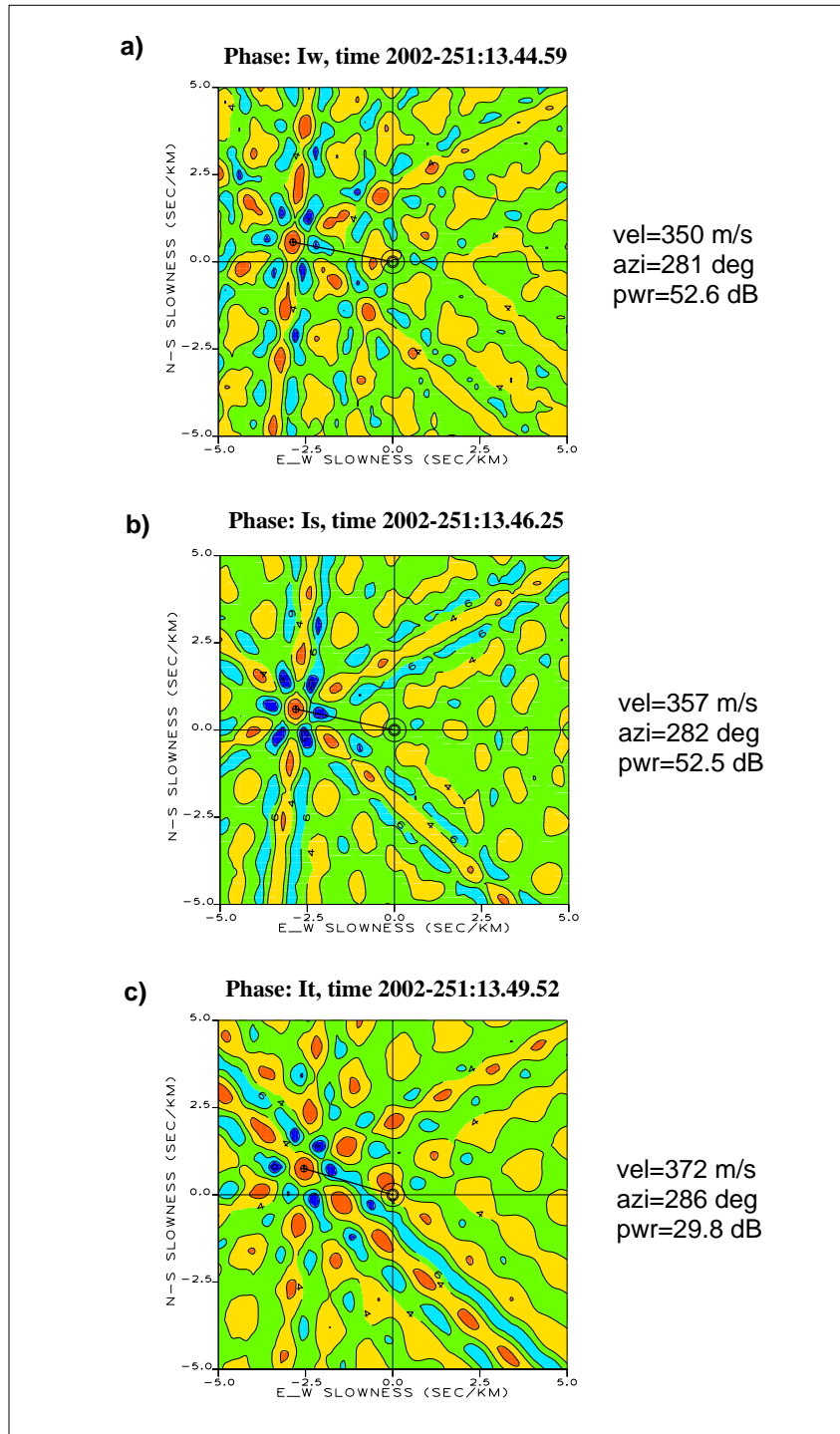


Fig. 6.4.7. F-K analysis results of the three phases shown in Fig. 6.4.5.

6.5 Threshold Monitoring of the Mines in the Kola Region

Sponsored by Defence Threat Reduction Agency, Contract No. DTRA01-00-C-0107

Introduction

We have evaluated the utility of a regional threshold monitoring scheme for the mining areas on the Kola Peninsula, Russia. Fig. 6.5.1 shows the location of the major mines in this area, together with the location of the two seismic arrays ARC and APA. Both the primary IMS array ARC and the non-IMS station APA record high-SNR observations of all important regional phases at a range up to at least 500 km, which is the maximum distance range being considered in this case study. Furthermore, for the more distant recordings, these phases are well-separated in time.



Fig. 6.5.1. Map of the Kola Peninsula with the main mining areas. Also shown are the locations of the ARCES and Apatity arrays.

We have access to ground truth information, and explosion and rockburst observations for mines of the Kola peninsula. Such information is regularly collected from the mine operators by Kola Regional Seismological Center (KRSC), and will serve as a reference set for our studies. The mining areas comprise Khibiny, Olenegorsk, Kovdor and Zapoljarnyi.

In particular, the mines of the Khibiny Massif provide a natural laboratory for examining and contrasting the signals generated by different types of mining explosions and rockbursts. Of the five mines in the Massif, three have both underground operations and surface pits. Shots underground range in size from very small (~2 tons) with only a few delays and durations on the order of a few hundred milliseconds, to very large (400 tons) with many delays and durations approaching a half second (Ringdal et al., 1996). Shots above ground range from 0.5 tons to 400 tons with a wide range of delays and durations. Induced seismicity is frequent and triggered rockbursts accompany a significant fraction of the underground explosions (Kremenetskaya and Trjapitsin, 1995).

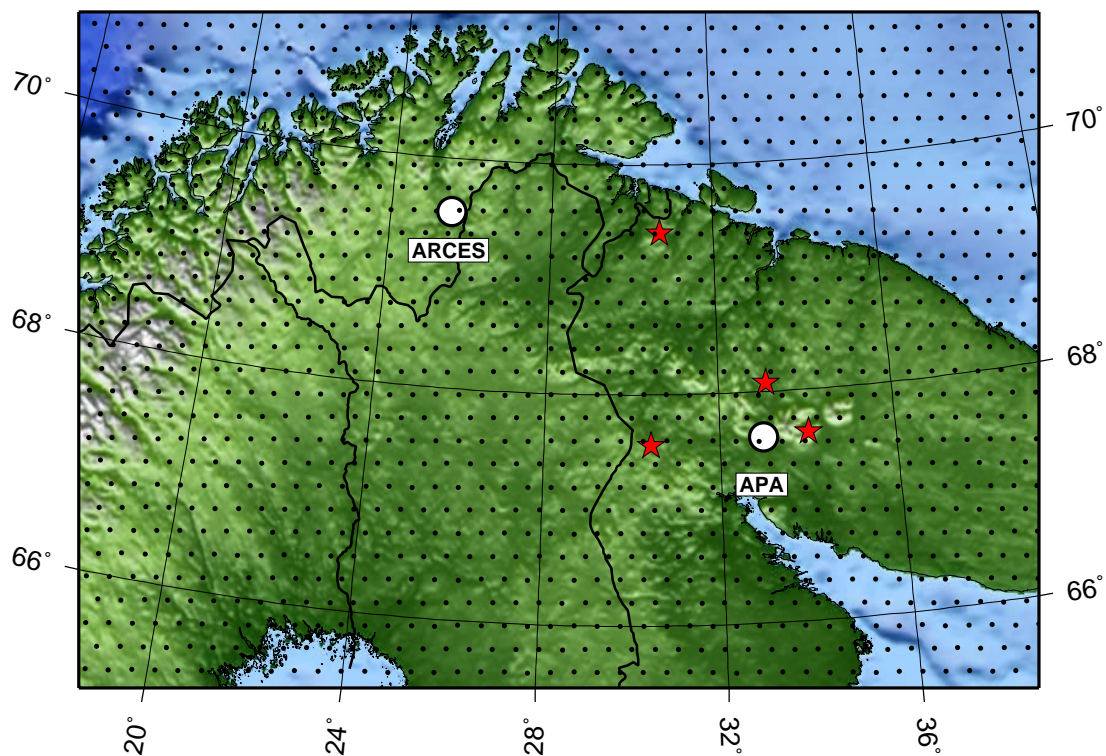


Fig. 6.5.2. Grid points used for regional threshold monitoring of the Kola Peninsula. The grid spacing is 0.2 degrees.

The grid system used for this study is shown in Fig. 6.5.2, and is based on a dense grid spacing of 0.2 degrees. In computing the threshold traces, magnitudes based on the attenuation of Pg and Lg amplitudes were used for grid point to station distances within 2 degrees, while magnitudes for distances above 2 degrees are based on Pn and Sn attenuation (see Table 6.5.1). This is in accordance with the distances at which these phases are observable in the actual region. The frequency band used in the study was 3-6 Hz for all phases, except for Lg for which we used 2-4 Hz. Software to extract peak and mean threshold magnitudes for each grid point within a given time segment was used to analyze the TM results.

Table 6.5.1. Parameters used for Regional Threshold Monitoring of the Kola mining areas

Travel time model	'barey' - Schweitzer and Kennett, 2002
Attenuation model	Hicks et al., 2002
Grid Spacing	0.2 degrees
Pg distance range	0 - 2 degrees
Pn distance range	2 - 20 degrees
Lg distance range	0 - 2 degrees
Sn distance range	2 - 20 degrees
Pg frequency band	3 - 6 Hz
Pn frequency band	3 - 6 Hz
Lg frequency band	2 - 4 Hz
Sn frequency band	3 - 6 Hz

Processing example 1

Fig. 6.5.3 shows mean threshold magnitudes for each grid point for a 1-hour time segment starting at 2002-102:06.30. Even if this time interval is not without seismic events, this figure is representative of the combined TM capabilities of ARC and APA during typical noise conditions. In this and other similar plots, the individual TM grid points have been resampled onto a continuous grid using a minimum curvature surface fitting algorithm. As seen from the figure, the monitoring capability is between 0.5 and 1.0 m_b units for the mining sites (marked as black squares).

Fig. 6.5.4 shows the threshold time traces for a two hour interval surrounding the interval described previously. We have plotted the threshold trace of the grid point closest to the actual mine for each of the four major mining sites. There is one large mining explosion (mine 5 of the Khibiny group) during this time interval, and this explosion causes a peak for each beam. Otherwise, the typical background threshold is between 0.5 and 1.0 m_b units, consistent with Fig. 6.5.3.

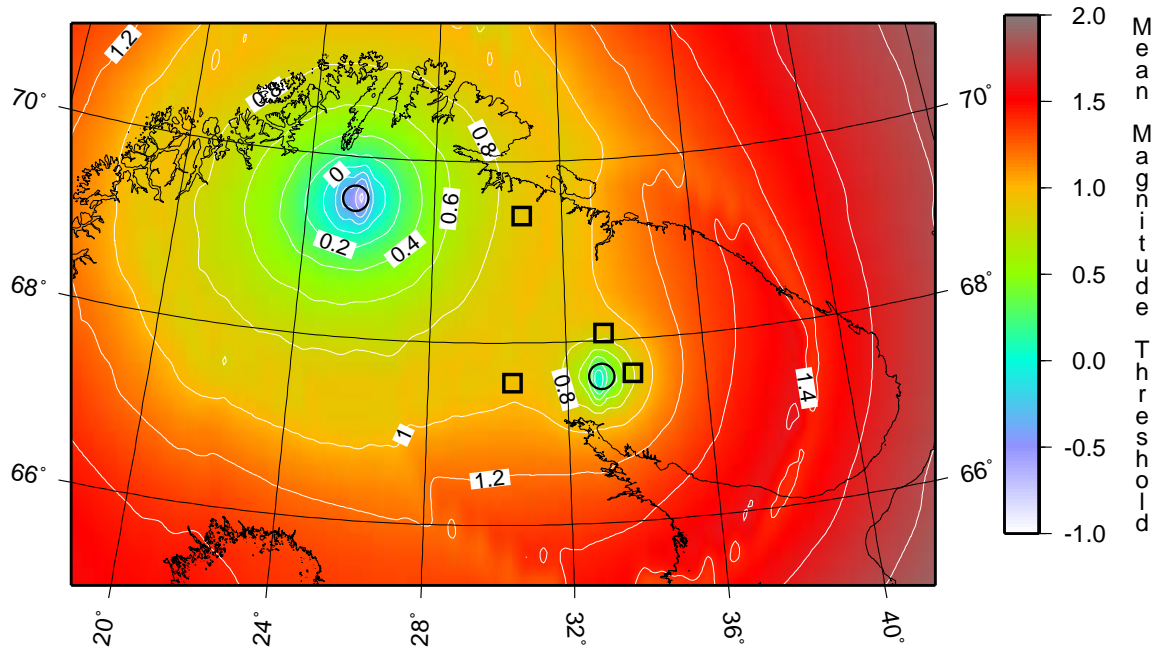
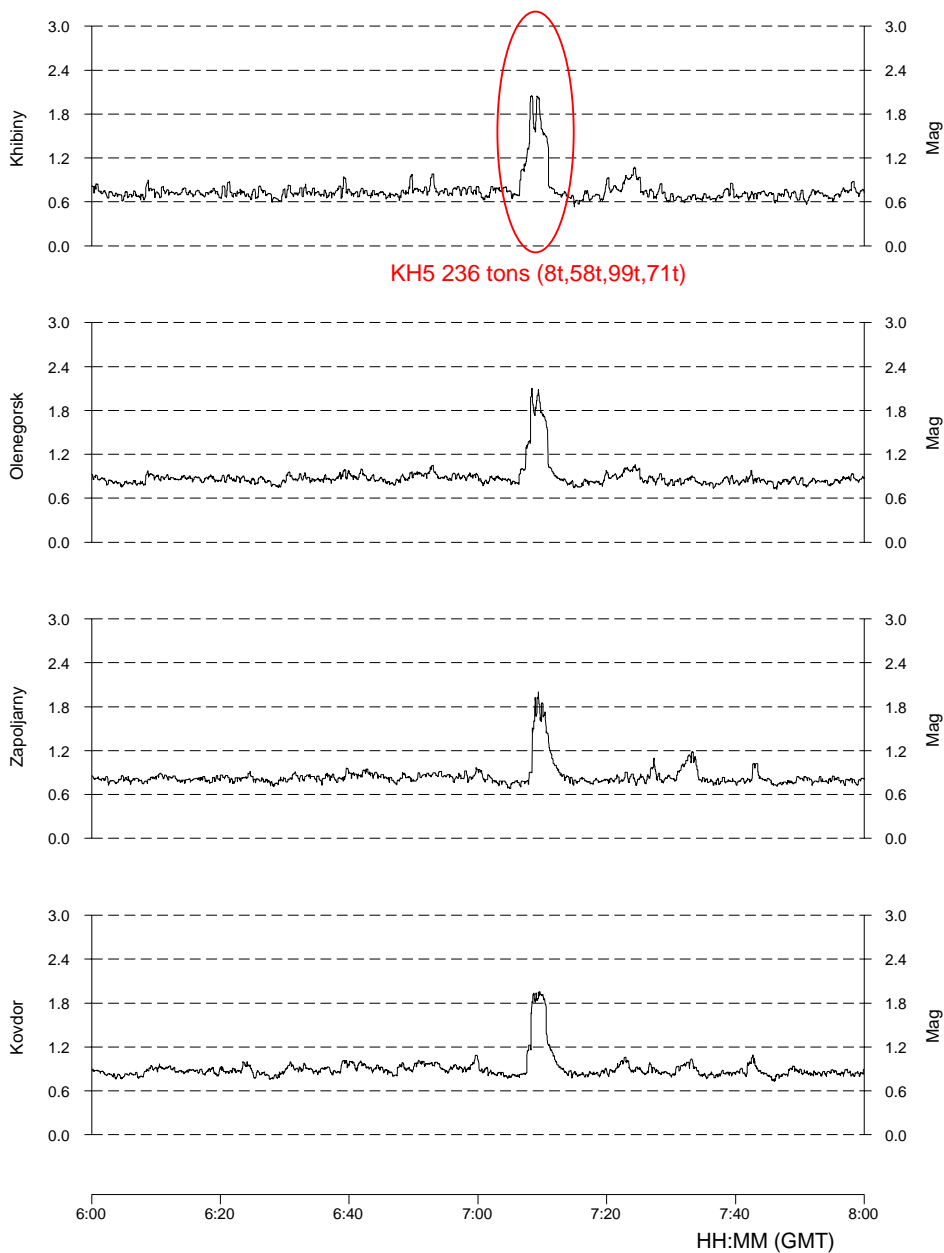


Fig. 6.5.3. Mean network magnitude thresholds for a 1-hour time interval starting 2002-102:06.30, using the ARCES and Apatity arrays (black circles). The locations of the mining areas Khibiny, Olenegorsk, Kovdor and Zapoljarny (see Fig. 6.5.1) are shown by black squares.

Regional Threshold Monitoring of the Kola mining areas



12 April 2002 Day 102

Fig. 6.5.4. Network magnitude thresholds for the grid points closest to the four mining areas shown in Fig. 6.5.1, for the 2-hour time interval starting 2002-102:06.00. The threshold peak corresponds to an explosion in the open mine Koashva (KH5) located in the Khibiny area. The total yield of the ripple-fired explosion was reported to 236 tons, and consisted of 4 smaller explosions with yields of 8, 58, 99 and 71 tons, respectively.

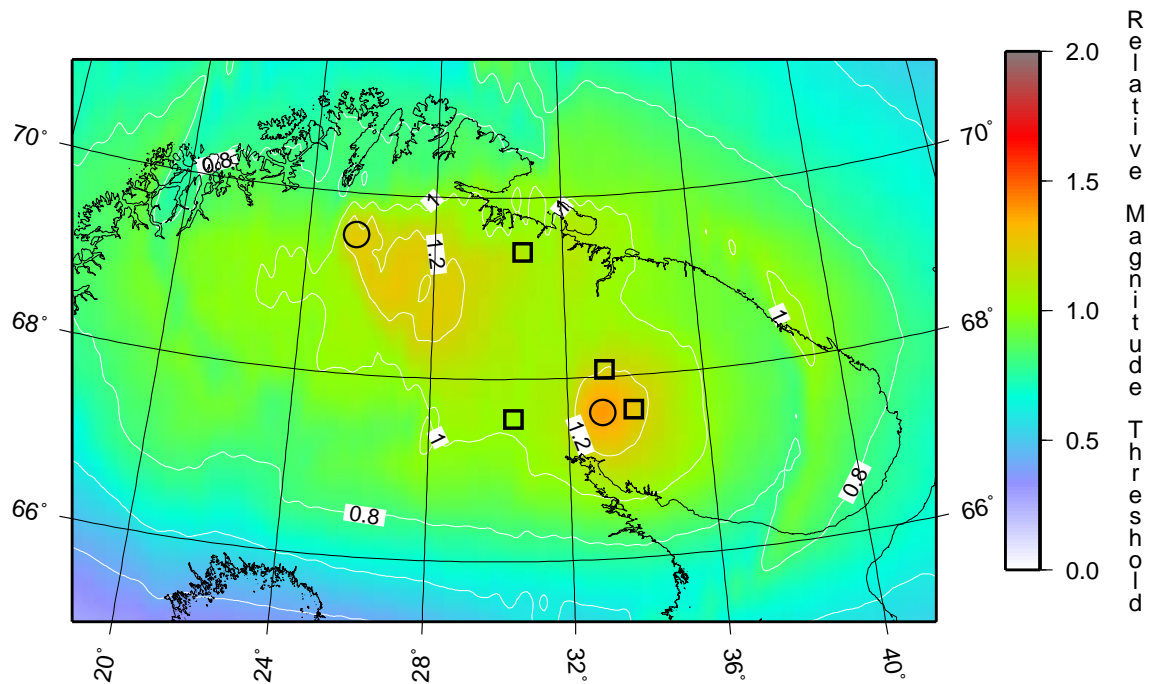


Fig. 6.5.5. Peak network magnitude thresholds with mean subtracted for the same 1-hour time interval as shown in Fig. 6.5.3.

Fig. 6.5.5 shows the peak network magnitude thresholds with mean subtracted for the same 1-hour time interval as shown in Fig. 6.5.3. This essentially shows the height of the highest peak above the background level within the time interval for each grid point. Note that the event in the Khibiny mine KH5 (see Fig. 6.5.4) creates a significant threshold peak in almost the entire region.

Processing example 2

Figs. 6.5.6- 6.5.8 show a second example of threshold plots, similar to the plots shown in Figs. 6.5.3-6.5.5. In this second case, the time interval processed is a two-hour interval starting at 2002-102:10.00, i.e. some hours later during the same day. The mean magnitude thresholds (Fig. 6.5.6) are almost identical to the mean thresholds for the first interval (Fig. 6.5.3), which shows that the background noise level is stable. The individual time traces for each of the four mining sites (Fig. 6.5.7) show quite significant activity during these two hours, with confirmed mining explosions both at Khibiny, Olenegorsk and Zapolyarnyi. As expected, there is a corresponding threshold increase on all the traces for each mine explosion, but in each case the increase in threshold level is greatest for the actual site of the explosion. There is also an unknown event (perhaps a small earthquake) that is located outside of the mining areas. The peak network threshold magnitudes with mean subtracted (Fig. 6.5.8) are quite similar to those in Fig. 6.5.5.

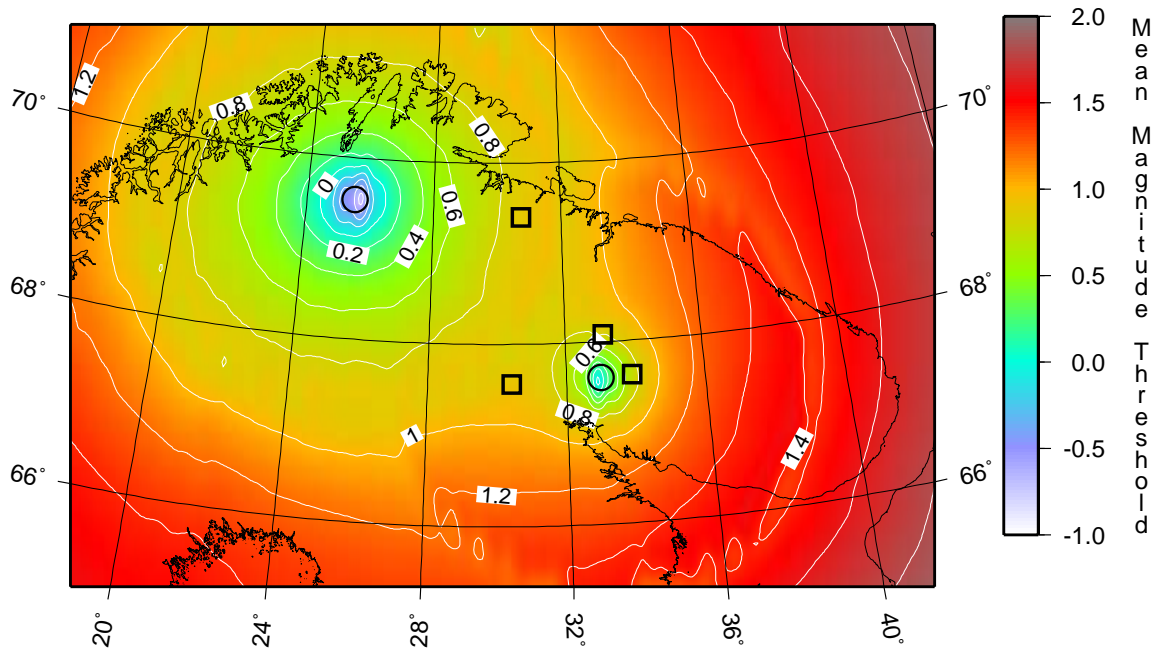


Fig. 6.5.6. Mean network magnitude thresholds for a 2-hour time interval starting 2002-102:10:00.

Processing a 24 hour interval

Fig. 6.5.9 shows network magnitude thresholds for the grid points closest to the four mining areas Khibiny, Olenegorsk, Zapoljarny and Kovdor for the entire day 12 April 2002. This is the same day from which the two previous time segments were extracted. During this day 10 events are found which are located in three of these mining areas, of which 6 are confirmed by KRSC. The corresponding mines and threshold peaks are indicated by red arrows.

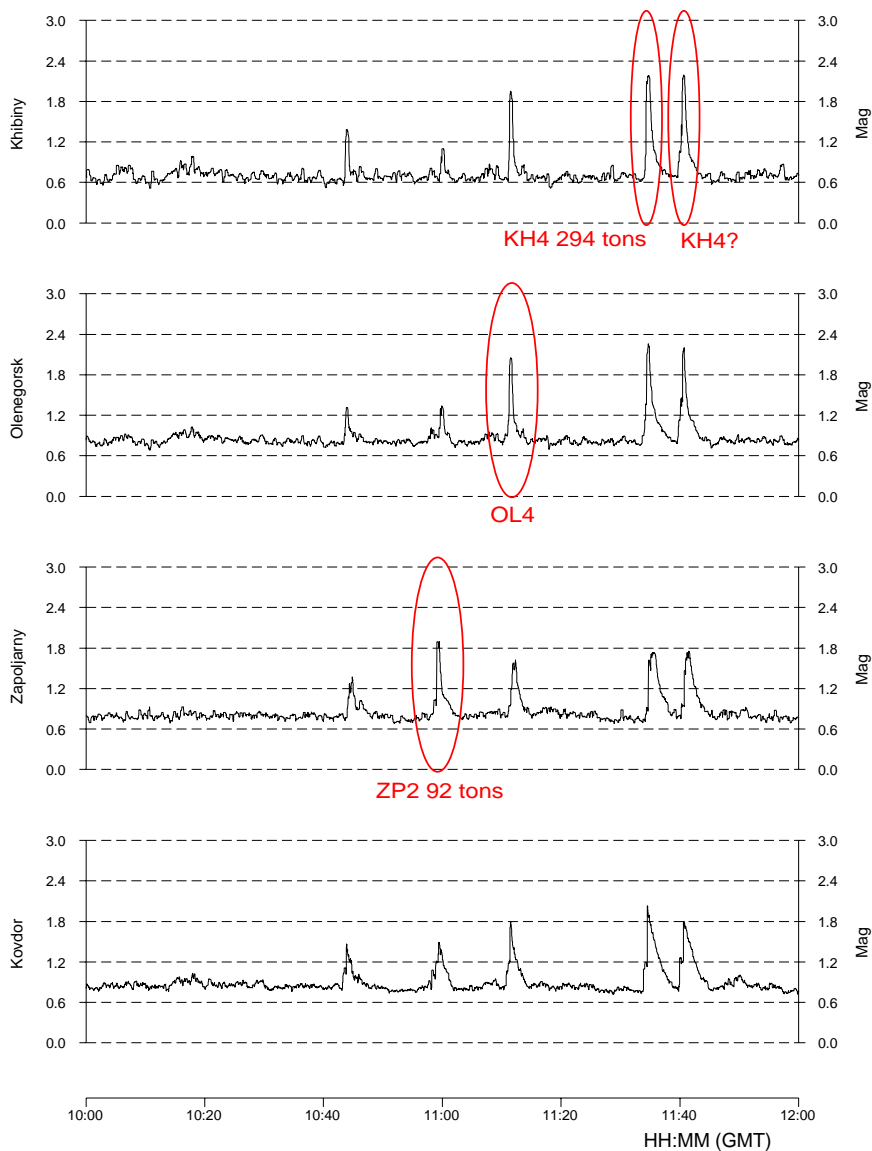
Conclusions

Using data from the ARCES and Apatity arrays, we have implemented a regional threshold monitoring scheme for northern Fennoscandia, including the Kola Peninsula. For the most active mining areas in this region (Khibiny, Olenegorsk, Zapoljarny and Kovdor), the magnitude thresholds during “normal” noise conditions vary between 0.7 and 1.0 magnitude units. During the studied time interval (12 April 2002), 10 out of 18 peaks exceeding threshold magnitude 1.2 at any of the mining areas were caused by events in the actual mining areas. However, the spatial resolution of the threshold magnitudes when using the ARCES and Apatity arrays is quite low, such that the mining events also created significant threshold peaks for the other mining areas.

This implies that for a regional threshold monitoring scheme for the Kola Peninsula it will be sufficient to deploy a set of targets for the most active mining areas. When a threshold peak is found at any of these targets, the peaks have to be associated to seismic events by correlating the threshold plots to seismic detection lists or bulletins.

T. Kværna

Regional Threshold Monitoring of the Kola mining areas



12 April 2002 Day 102

Fig. 6.5.7. Network magnitude thresholds for the grid points closest to the four mining areas shown in Fig. 6.5.1, for the 2-hour time interval starting 2002-102:10.00. Five significant threshold peaks are seen during this time interval, of which three are mining explosions reported by the KRSC. The last peak at 11:40 is believed to be an additional explosion at the Central Khibiny mine KH4. The first peak at 10:44 is caused by an event located approximately 70 km south-west of the Apatity array.

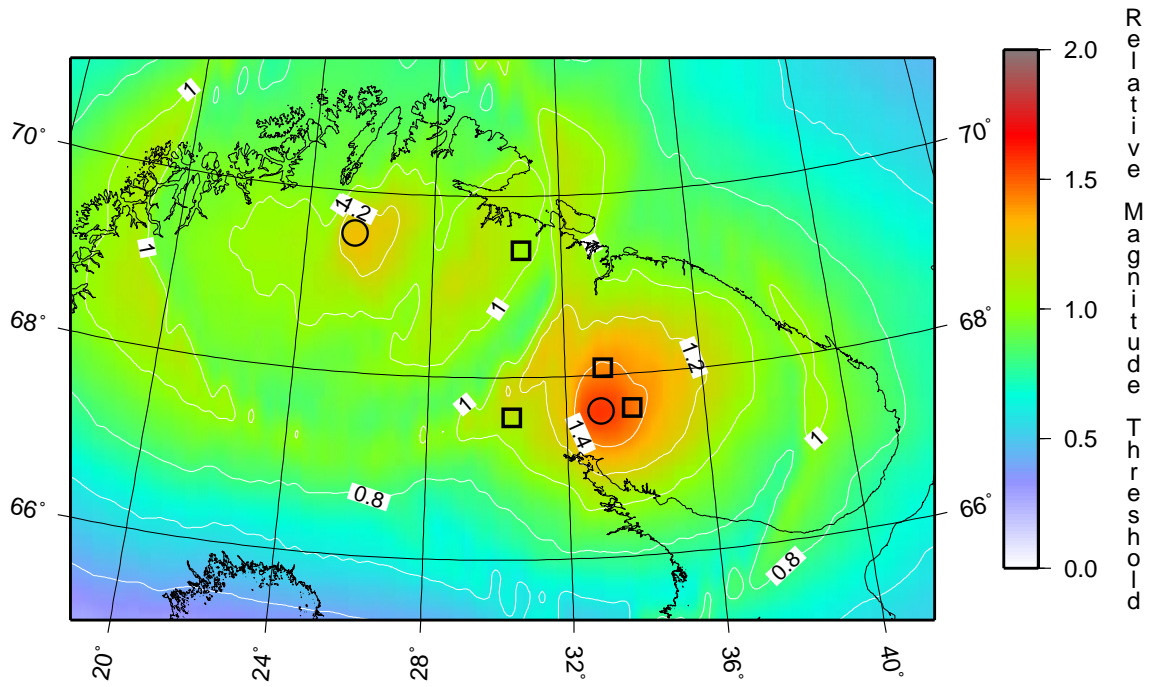
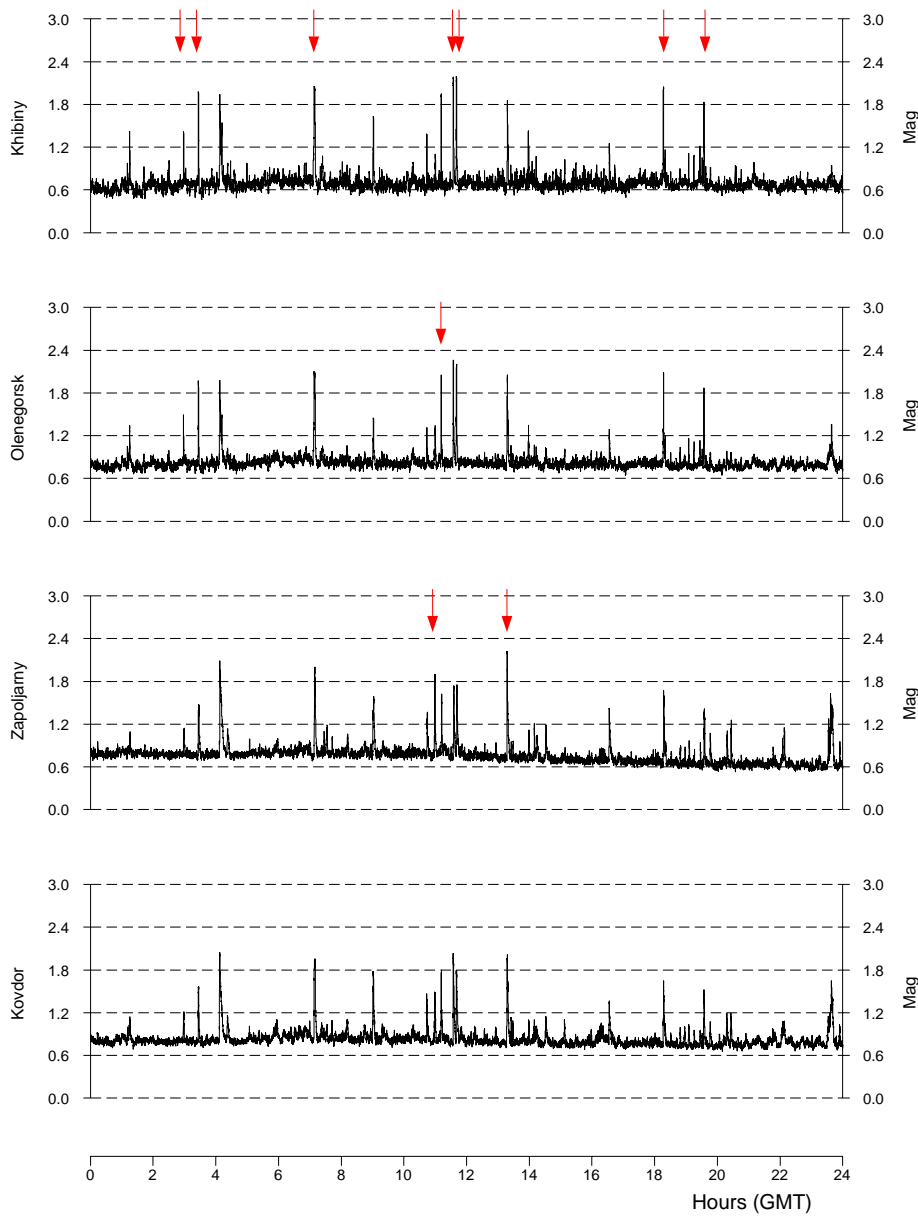


Fig. 6.5.8. Peak network magnitude thresholds with mean subtracted for the same 2-hour time interval as shown in Fig. 6.5.6. This essentially shows the height of the highest peak above the background level within the time interval for each grid point. The five events occurring in the region during this time interval create significant threshold peaks in the entire region.

Regional Threshold Monitoring of the Kola mining areas



12 April 2002 Day 102

Fig. 6.5.9. Network magnitude thresholds for the grid points closest to the four mining areas Khibiny, Olenegorsk, Zapoljarny and Kovdor for 12 April 2002. During this day 10 events are found which are located in three of these mining areas, of which 6 are confirmed by KRSC. The corresponding mines and threshold peaks are indicated by red arrows.

References

- Hicks, E.C., Kværna, T., Mykkeltveit, S., Schweitzer, J. and Ringdal, F. (in press), Travel-times and attenuation relations for regional phases in the Barents Sea region, *Pure and Applied Geophysics*, in press.
- Kremenetskaya, E.O. and V.M.Trjapitsin (1995): Induced seismicity in the Khibiny Massif (Kola Peninsula), *Pure and Applied Geophysics*, 145(1), 29-37.
- Ringdal F., E.Kremenetskaya, V.Asming, I.Kuzmin, S.Evtuhin, V.Kovalenko (1996): Study of the calibration explosion on 29 September 1996 in the Khibiny Massif, Kola Peninsula. Semiannual Technical Summary 1 April - 30 September 1996, *NORSAR Sci. Rep. 1-96/97*, Kjeller, Norway.
- Schweitzer, J., and Kennett, B.L.N. (2002), Comparison of location procedures - the Kara Sea event 16 August 1997, Semiannual Technical Summary, 1 July - 31 December 2001, *NORSAR Sci. Rep. 2-2001/2002*, Kjeller, Norway, 97-114.